TUHH
Hamburg University of Technology

Konstruktion
und Festigkeit
von Schiffen

TUHH · M-10 · Am Schwarzenberg Campus 4C · D-21073 Hamburg

BACHELOR THESIS

Statistical assessment of post-weld treated welded joints by burr grinding

Submitted by: Xiru Wang

Student ID Number: 21596942

Supervisors: Prof. DSc. (Tech.) Sören Ehlers

M.Sc. Moritz Braun

Submission Date: May 25,2020

Abstract

Burr grinding is one of the post-weld improvement methods that are widely used in various industries to improve the fatigue strength of welds: bridges, offshore structures, ships and land-based structures. In this paper, main influencing parameters and effect of burr grinding technique on the fatigue strength for butt-welded, longitudinal welded, doubling plates, load-carrying transverse, non-load carrying transverse welded and T-joints as well as I-section with cope hole and out-of-plane longitudinal welds has been evaluated, based on the extracted 395 fatigue data points from 34 existing publications. The specimens used in these studies with yield strength 175 MPa < σ_{YS} <1100 MPa, which were tested with stress ratio -1 < R < 0.5, are analyzed and assessed with statistical methods. The assumed value of S-N slope m = 4 and proposed FAT classes seem to be applicable for the extracted data. More experimental testing is needed to draw the conclusion more exactly.

Keywords: Burr grinding, Fatigue strength, Fatigue strength improvement, Post-weld improvement methods

Declaration of Academic Honesty

I assure that I prepared the thesis single-handed without external help.

For the composition of the work only the referenced sources have been used. Literally or analogously taken parts are marked as such.

Hamburg, 25.05.2020

Signature

I agree that my thesis can be published, especially that my thesis can be handed out to other parties for inspection or that copies of the thesis may be handed out to other parties.

Hamburg, 25.05.2020

Signature

TUHH
Hamburg University of Technology

Konstruktion
und Festigkeit
von Schiffen

TUHH · M-10 · Am Schwarzenberg Campus 4C · D-21073 Hamburg

BACHELOR THESIS 2020

für

Xiru Wang

Statistische Untersuchung der Schwingfestigkeit ausgeschliffener Schweißnähte

Statistical assessment of post-weld treated welded joints by burr grinding

Die Kiele von High-Performance-Segelyachten werden zunehmend aus hochfesten Stählen mit Streckgrenzen von über 900 MPa gefertigt. Dabei bestehen die Konstruktionen dieser Kiele sowohl aus gefrästen Profilen als auch aus geschweißten Hohlkammerprofilen. Wie alle meerestechnischen Konstruktionen und Seeschiffe unterliegen auch Yachten zyklischen Belastungen. In vielen Regelwerken berücksichtigt die Abschätzung der Betriebsfestigkeit von nachbehandelten Schweißverbindungen die höhere Streckgrenze und damit verbundene bessere Betriebsfestigkeit noch nicht, obwohl damit konstruktive Nachteile verbunden sind.

Im Rahmen dieser Arbeit soll das Schwingfestigkeitsverhalten hochfester Stähle näher untersucht und bewertet werden. Hierzu sollen Literaturdaten und Testergebnisse aus früheren Arbeiten statistisch ausgewertet werden.

Das Ziel dieser Arbeit ist es, die Konstruktion von nachbehandelten Schweißverbindungen zu verbessern, indem der Effekt der Nahtnachbehandlung unter Berücksichtigung der Materialfestigkeit herausgestellt wird. Im Weiteren soll damit die internationale Normgebung verbessert werden. Für die statistische Auswertung sollen international anerkannte Normen und Standards Anwendung finden. Im Rahmen der Arbeit sollen die folgenden Punkte bearbeitet werden:

1. Literaturstudie zu Studien bezüglich der Verbesserung der Schwingfestigkeit mittels Ausschleifen
2. Statistische Auswertung der gefundenen Ergebnisse und früherer Testergebnisse am Institut nach international anerkannten Normen und Standards
3. Herausstellen des Effekts der Materialfestigkeit bzw. anderer wichtiger Parameter auf die Schwingfestigkeit ausgeschliffener Schweißnähte

Thesis format

The thesis should be organised in a rational manner to give a clear exposition of results, assessments, and conclusions. The text should be brief and to the point, with a clear language and the objective to be published in a conference article and/or scientific journal. It is thus desirable that the thesis is written in English. Telegraphic language should be avoided.

The thesis shall contain the following elements: An executive summary, list of symbols and acronyms, followed by the main body of the thesis consisting of a brief background introduction, a state of the art defining the knowledge gaps defining the scope or work and limitations, the actual contribution chapters, conclusions with recommendations for further work, references and (optional) appendices. All figures, tables and equations shall be numerated.

The supervisors require that the candidate, in an early stage of the work, presents a written plan for the completion of the work. The plan may include a budget for the use of computer and laboratory resources if applicable. Overruns shall be reported to the supervisors.

The original contribution of the candidate and material taken from other sources shall be clearly defined following basic academic principles and an acknowledged referencing system, which includes the name of the referred authors followed by the publication year in the text. The subsequent reference list can thus be alphabetical.

The report shall be submitted in two copies:
- Signed by the candidate
- The text defining the scope included
- In bound volume(s)
- Drawings and/or computer prints, which cannot be bound should be organised in a separate folder.
- The report shall also be submitted in PDF along with essential input files for computer analysis, spread sheets, MATLAB files etc. in digital format.

Ownership
According to the current rules, the candidate has the ownership of the thesis. However, he hereby accepts to transfer the ownership to TUHH M-10. Any use of the thesis has to be approved by TUHH M-10 (or external partner when this applies). TUHH M-10 has the right to use the thesis as if a TUHH M-10 employee carried out the work, if nothing else has been agreed in advance.

Thesis supervisors
Sören Ehlers
Moritz Braun

Deadline: 25.05.2020

Hamburg, 15.02.2020

Content

List of Figures VII
List of Tables IX
Nomenclature X
Abbreviations XII
1.Introduction 1
2. Methodology 4
2.1 Definition of Burr grinding 4
2.1.1 Introduction 4
2.1.2 Equipment 4
2.1.3 Procedure 4
2.1.4 Effect of burr grinding on fatigue strength of joints 5
3. Statistical methods 7
3.1 Statistical analysis 7
3.2 Design S-N curves 7
3.3 DVS Recommendation 12
3.4 ASTM Practice 15
3.5 IIW Recommendation 21
4. Results 25
4.1 Extracted fatigue data and analysis with IIW 25
4.2 S-N slope calculation 31
4.3 Results of analysis 31
5. Discussion 34
5.1 *S-N* curve slopes 34
5.2 The degree of improvements 36
5.3 Proposed FAT values 40
6. Conclusion 43
Reference XVI
Appendix XVI

List of Figures

Fig. 1. Weld geometry improvement methods (taken from Maddox and Haagensen, 2007 [1]) 2
Fig. 2. Residual stress modification improvement methods (taken from Maddox and Haagensen, 2007 [1]) 2
Fig. 3. The burr grinding technique (taken from Maddox and Haagensen, 2007 [1])...5
Fig. 4. Specimens with micrographs for as-welded and burr grinding joints (taken from study by Pedersen et al. [11]) 6
Fig. 5. Fatigue *S-N* curves for steel (taken from IIW Recommendation by Hobbacher [8]) 6
Fig. 6. Designed *S-N* curve for example 1 7
Fig. 7. Designed *S-N* curve for example 2 8
Fig. 8. Stress cycle and related stress ratios [40] 11
Fig. 9. Normal distribution with survival probability [41] 11
Fig. 10. Fatigue data from example 1 with DVS practice, as-welded and ground joints with fixed slope m = 3 13
Fig. 11. Fatigue data from example 1 with DVS practice, ground joints with best-fit slope 13
Fig. 12. Fatigue data from example 2 with DVS practice, as-welded and ground joints with fixed slope m = 3 14
Fig. 13. Fatigue data from example 2 with DVS practice, ground joints with best-fit slope 14
Fig. 14. F distribution [43] 17
Fig. 15. Fatigue data from example 1 with ASTM practice, as-welded joints with fixed slope m = 3 17
Fig. 16. Fatigue data from example 1 with ASTM practice, ground joints with best-fit slope 18
Fig. 17. Fatigue data from example 2 with ASTM practice, as-welded joints with fixed slope m = 3 19
Fig. 18. Fatigue data from example 2 with ASTM practice, ground joints with best-fit slope 19
Fig. 19. Fatigue data from example 1 with IIW practice, as-welded joints with fixed slope m = 3 22
Fig. 20. Fatigue data from example 1 with IIW practice, ground joints with fixed slope m = 3 22
Fig. 21. Fatigue data from example 1 with IIW practice, ground joints with best-fit slope 23
Fig. 22. Fatigue data from example 2 with IIW practice, as-welded joints with fixed slope m = 3 23
Fig. 23. Fatigue data from example 2 with IIW practice, ground joints with fixed slope m = 3 24
Fig. 24. Fatigue data from example 2 with IIW practice, ground joints with best-fit slope 24
Fig. 25. Slope calculation based on number of specimens for the extracted fatigue data improved by burr grinding 32
Fig. 26. Slope calculation based on steel grades for T-joints and transverse non-load-carrying welds improved by burr grinding 33
Fig. 27. Slope calculation based on number of specimens for the doubling plates in large size improved by burr grinding 33

Fig. 28. Fatigue data from example 1 with IIW practice, ground joints with fixed slope $m_1 = 4$ 35
Fig. 29. Fatigue data from example 2 with IIW practice, ground joints with fixed slope $m_1 = 4$ 35
Fig. 30. Analysis of fatigue data with assumed slope $m_1 = 4$ 38
Fig. 31. Enhancement factor f(R) (taken from IIW Recommendation [8]) 39
Fig. 32. Improved fatigue data for each type of welds 42

List of Tables

Table 1. Details with FAT classes for as-welded steel joints recommended by IIW (figures taken from IIW recommendation [8] and study by Braun et al. [20]) 3
Table 2. Fatigue data for example 1, as-welded Specimen C, cruciform welded joint.8
Table 3. Fatigue data for example 1, ground Specimen C, cruciform welded joint......9
Table 4. Fatigue data for example 2, as-welded Specimen B, cruciform welded joint.9
Table 5. Fatigue data for example 2, ground Specimen B, cruciform welded joint....10
Table 6. Values of t_p (taken from ASTM [4])..16
Table 7. Values of F_p (taken from ASTM [4])...16
Table 8. Extracted fatigue data for butt joints improved by Burr grinding 27
Table 9. Extracted fatigue data for longitudinal attachments improved by Burr grinding 27
Table 10. Extracted fatigue data for doubling plates improved by Burr grinding........28
Table 11. Extracted fatigue data for transverse load-carrying welds improved by Burr grinding...28
Table 12. Extracted fatigue data for T-joints improved by Burr grinding....................28
Table 13. Extracted fatigue data for transverse non-load-carrying welds improved by Burr grinding 29
Table 14. Extracted fatigue data for I - section with cope hole improved by Burr grinding 30
Table 15. Extracted fatigue data for out-of-plane longitudinal gusset welded to plate improved by Burr grinding..30
Table 16. FAT classes and calculated $\Delta\sigma_{50\%}$ for each specimen type 30
Table 17. Analysis of extracted data using a slope of $m_1 = 4$ 40

Nomenclature

A		$logC$ in S-N curve in linear model
B		slope m in linear model
d	mm	depth of grinding
$f(R)$		the fatigue enhancement factor depends on R
F_p		value in F distribution depends on degrees of freedom and probability in ASTM practice
k		number of test specimens
K		value depends on number of test specimens in IIW recommendation
l		level of stress range used in the test
L	mm	length of gusset of longitudinal attachments
$log\ C$		logarithm of constant value in S-N curve
$log\ N$		logarithm of fatigue life
$log\ \Delta\sigma$		logarithm of stress range
m		slope of S-N curve
m_1		slope of S-N curve for $N < 10^7$
m_2		slope of S-N curve for $N > 10^7$
n		degree of freedom of value t_p in ASTM practice
n_1		1. degree of freedom of value F_P in ASTM practice
n_2		2. degree of freedom of value F_P in ASTM practice
N		number of cycles
P		survival probability
$P_{10\%}$		10% probability of failure P in strength
$P_{90\%}$		90% probability of failure P in strength
R		stress ratio
stdv(logC)		standard deviation of *logC* in DVS recommendation
stdv_logC		standard deviation of *logC* in IIW recommendation
stdv(m)		standard deviation of m in DVS recommendation
r	mm	toe radii
t	mm	thickness of welded joints
t_P		value depends on survival probability P in ASTM practice

T_σ		scatter ratio in strength in DVS recommendation
x_i		the expression of *logC* in IIW recommendation
x_k		the expression of characteristic value of *logC* in IIW recommendation
x_m		the expression of mean value of *logC* in IIW recommendation
X		$log\Delta\sigma$ in linear model
$\overline{X}$		Average of X
Y		*logN* in linear model
$\widehat{A}$		estimator of A in ASTM practice
$\widehat{B}$		estimator of B in ASTM practice
dY		residual square in DVS recommendation
$\sigma_{\max}$	MPa	maximum stress
$\sigma_{\min}$	MPa	minimum stress
σ_{YS}	MPa	yield stress of steel grades
$\widehat{\sigma}$		standard deviation of the normal distribution for *logN* in ASTM practice
$\widehat{\sigma}_{\widehat{A}}$		confidence interval for $\widehat{A}$
$\widehat{\sigma}_{\widehat{B}}$		confidence interval for $\widehat{B}$
σ_N		standard deviation in life
$\Delta\sigma$	MPa	stress range
$\Delta\sigma_{50\%}$	MPa	mean value corresponding to 50 survival probability at 2×10^6 to failure
$\Delta\sigma_{97.5\%}$	MPa	characteristic value corresponding to 97.5 survival probability at 2×10^6 to failure

Abbreviations

AS	As-welded joints
ASTM	American Society for Testing and Materials
BG	Burr grinding
DVS	Deutscher Verband für Schweißen und verwandte Verfahren
HSS	high strength steel
IIW	International Institute of Welding

1.Introduction

Welding is a commonly used method to connect engineering parts such as steel in ship industry. However, it is also well known that welded joints have a lower fatigue strength than the base material. The main reason is that local stress concentration occurs because of tensile residual stress in weld toe, which is the main source of fatigue cracks. Therefore, enhancement of the fatigue strength of welded attachments applying different post-weld improvement techniques receives much attention. These improvement methods can be divided into two main groups [2]: weld geometry techniques and residual stress techniques. Methods from IIW recommendations (Haagensen and Maddox, 2007 [1]) are shown in Figs. 1-2.

The weld geometry methods remove the weld toe defects and reduce the stress concentration. The residual stress methods remove the harmful tensile welding residual stresses or introduce compressive stresses.

Among all the post-weld improvement methods, toe grinding is one of the methods, that is currently widely used and recommended for reducing the weld toe defects to increase the fatigue strength. Many of the literature have published that burr grinding had a great influence on the fatigue strength. Studies from Clegg et al. [17], Mecséri et al. [30], Booth [31] and Knight [37] had also shown the benefit of disc grinding and weld profiling compared with burr grinding. In addition, there are many parameters that may influence the effect of burr grinding, which should be considered in the application. Kirkhope et al. [18], [19] and Baptiata et al. [27] had studied the increase of burr grinding in seawater. In the publications from Uchida et al. [33], it was concluded that the fatigue strength improvement was related to radius of groove. Moreover, it was found by Mecséri et al. [30] and Hanzawa et al. [35] that the plate thickness would affect the results of fatigue strength by burr grinding. Furthermore, the tests were completed by Huther et al. [3], Kirkhope et al. [19], as well as Knight [37] with different types of steel to explore the influence of base material strength on the effect of burr grinding.

In order to investigate the effect of burr grinding techniques on the fatigue strength and the main influencing parameters in more detail, 395 test results from the 34 publications for butt-welded, longitudinal welded, doubling plates, load-carrying transverse, non-load carrying transverse welded and T-joints as well as I-section with cope hole and out-of-plane longitudinal welds are extracted. The specimens with various yield strength and stress ratio are analyzed and evaluated. FAT classes according to IIW Recommendation [8] for all these specimen geometries are given in Table 1.

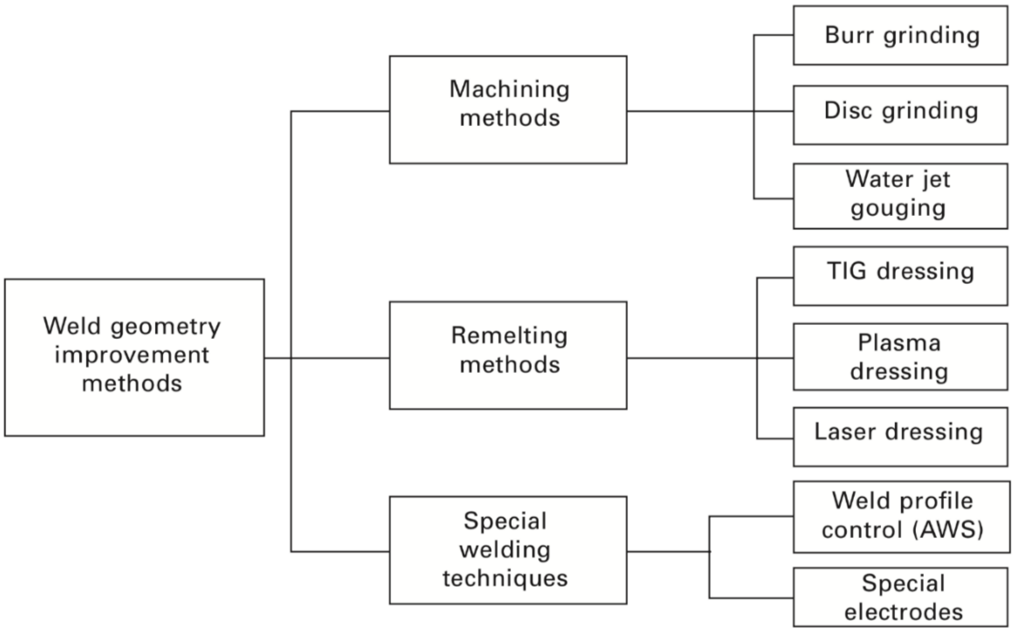

Fig. 1. Weld geometry improvement methods (taken from Maddox and Haagensen, 2007 [1])

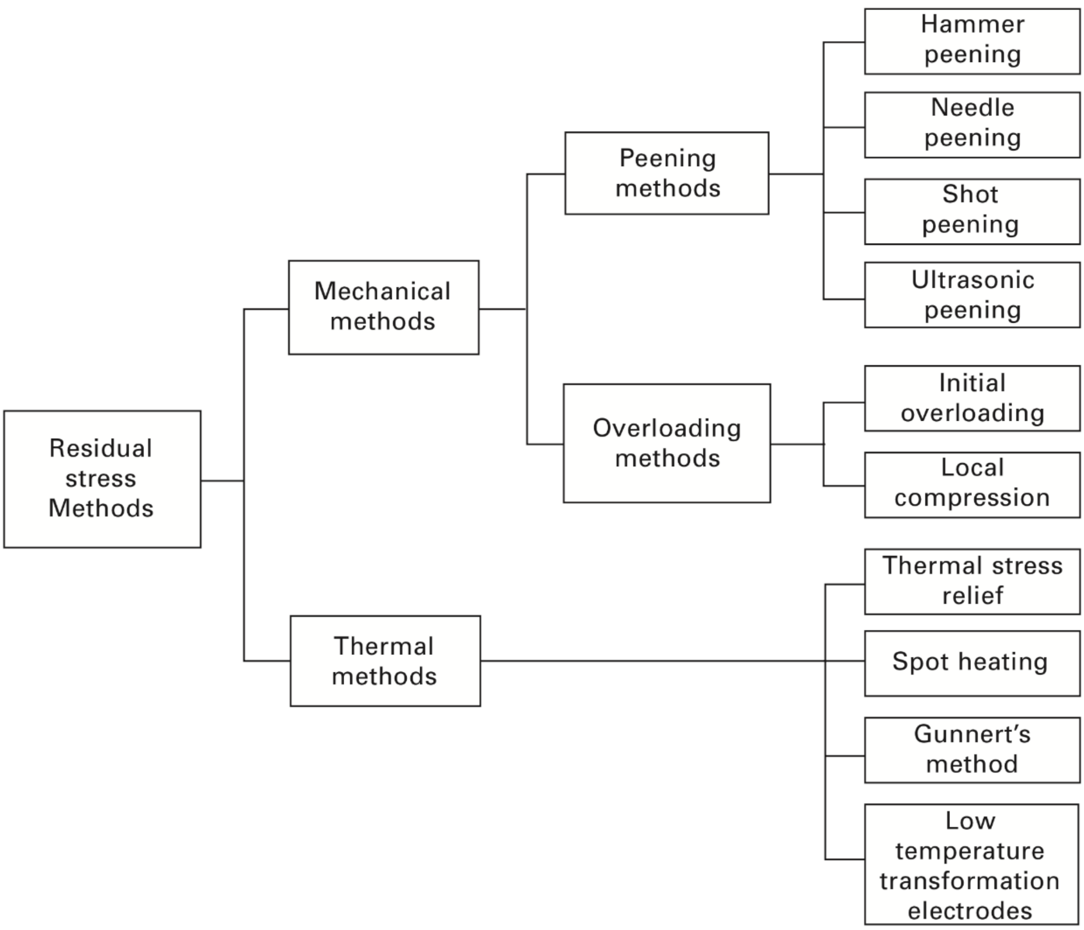

Fig. 2. Residual stress modification improvement methods (taken from Maddox and Haagensen, 2007 [1])

Type of welds	Description	FAT class for as-welded recommended by IIW [8]
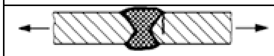	Transverse butt welds	90
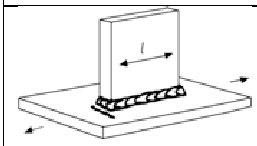	Longitudinal fillet welded gusset of length L *L* < 150 mm *L* < 300 mm	 71 63
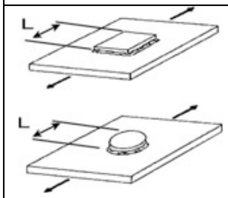	Doubling plates 50 mm < *L* ≤ 150 mm	 71
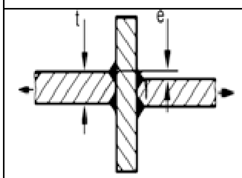	Transverse load-carrying welds	71
	Single sided T-joints	90
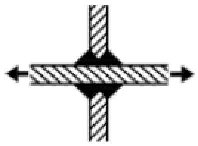	Transverse non-load-carrying welds	80
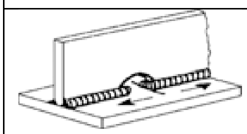	Longitudinal butt weld, fillet weld or intermittent weld (I - section) with cope holes	50
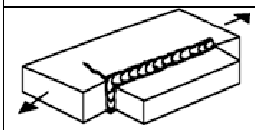	Out-of-plane longitudinal gusset welded to plate with gusset length *L* < 150 mm	 50

Table 1. Details with FAT classes for as-welded steel joints recommended by IIW (figures taken from IIW recommendation [8] and study by Braun et al. [20])

2. Methodology

To analyze the effect of burr grinding on the welds, the following methodology was adopted in the current study:
In the first place, in order to determine the design *S-N* curves, all the extracted data sets were analyzed with 3 approaches: DVS [7], ASTM [4], IIW [8]. Meanwhile, the mean value $\Delta\sigma_{50\%}$ corresponding to 50 survival probability at $N = 2 \times 10^6$ to failure and the characteristic value $\Delta\sigma_{97.5\%}$ corresponding to 97.5 survival probability for as-welded joints with slope $m = 3$ and ground joints with slope $m = 3$ as well as best-fit slope are obtained and represented.

Secondary, a new slope for all ground data for types of welds should be found out based on the best-fit slope. Then, in order to validate the applicability of the new slope, the mean value $\Delta\sigma_{50\%}$ and the characteristic value $\Delta\sigma_{97.5\%}$ for ground data would be calculated, using IIW recommendation with the new slope, and be compared with FAT classes produced by IIW for specimens in the as-welded condition.

Finally, a comparison between the ground characteristic value $\Delta\sigma_{97.5\%}$ and FAT class for ground welds would be made to present the actual improvement of burr grinding based on the new slope to IIW recommendation.

2.1 Definition of Burr grinding

2.1.1 Introduction

The aim of burr grinding are to remove crack-like defects at the weld toe, from which fatigue cracks propagate, and increase the weld toe radii by smoothly bending the transition between the plate and weld face, which leads to lower the stress concentration at the weld and improvement of fatigue performance.

2.1.2 Equipment

According to IIW recommendation [1], to carry out burr grinding, a high speed pneumatic or electric grinder with rotational speed from 15000 to 40000 rpm is required. It is recommended that the air pressure might be from 5 to 7 bar. The tool bit is normally a tungsten carbide burr (or rotating file) with a hemispherical end [1]. The needed burr diameter should be in the range of 10 to 25 mm with plate thickness from 10 to 50 mm.

2.1.3 Procedure

The burr grinding treatment is indicated in Fig. 3. Before burr grinding, the weld should be de-slagged and cleaned by wire brushing [1]. It is advised by Haagensen and Maddox [1] that the burr is positioned over the welded toe and the angle between tool and horizonal main plate should be 45 - 60°. Additionally, the tool should be placed approximately 30 - 45° to the direction of movement. The grinder will be usually pushed along the weld in order to produce a straight groove. Generally, the grinding must reach to minimum depth of 0.5 mm, maximum of 2 mm or 7% of plate thickness t below undercut with a radius of $r > 0.25 \cdot t$ and $r > 4 \cdot d$ [1], as indicated in Fig. 3. In addition, photos and micrographs for as-welded and burr ground specimens are shown in Fig. 4.

2.1.4 Effect of burr grinding on fatigue strength of joints

At first, it is worth mentioning that the quality of grinding depends on the skill of the operator. Thus, only general advice can be given by IIW.
The improvement of weld toe burr grinding can only be realized for the attachments in FAT 90 class or lower in accordance with IIW recommendation [1]. For higher classes details, including non-welded details, the fatigue lives are not decided by weld toe failure, or they have already been improved.

For those details, with FAT 90 class or lower, the increase factor for ground welds is 1.3 on stress range, corresponding to 2.2 on life, basing on the *S-N* slope $m = 3$. The maximum class that can be reached is the closest classification below the FAT value obtained by 1.3 times of multiplication of as-welded FAT value, corresponding to an increase of two fatigue classes. For steel welds, the maximum class that can be claimed by burr grinding is FAT 112, which corresponds to the two fatigue class increase relative to the highest detail class FAT 90 in which the improvement can be realized, as indicated in Fig. 5. All the *S-N* curves shown in Fig. 5 are limited in the low cycle region by the design *S-N* curve for the parent material, corresponding to FAT 160 curve with a slope of $m = 5$ for steel details. [1]

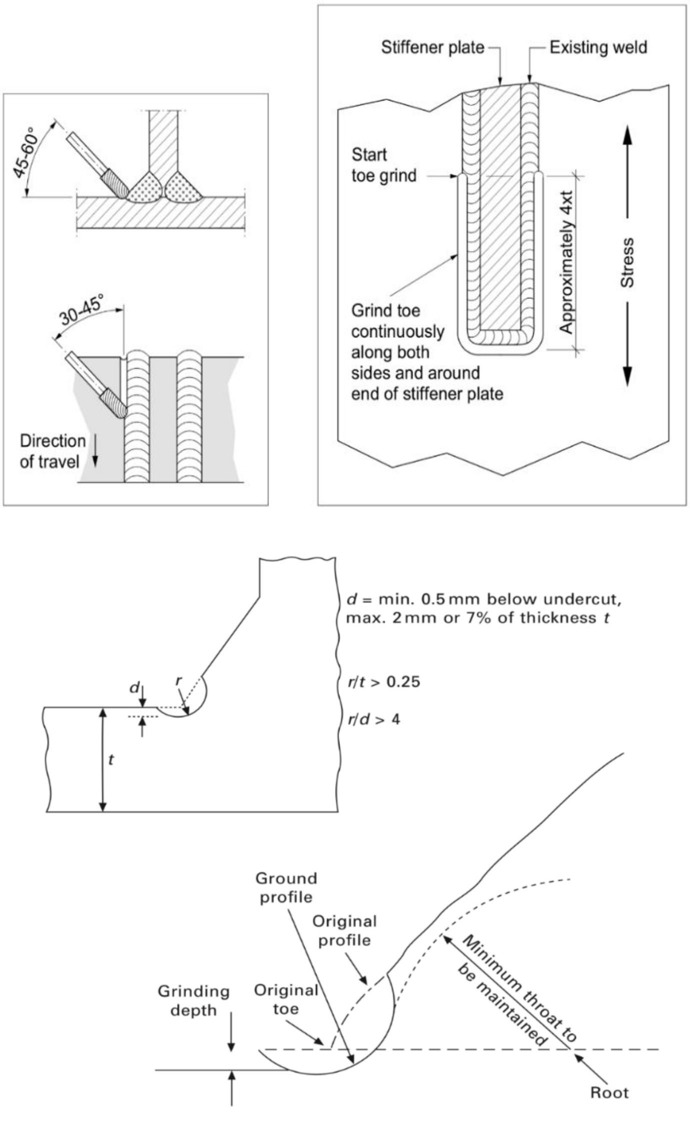

Fig. 3. The burr grinding technique (taken from Maddox and Haagensen, 2007 [1])

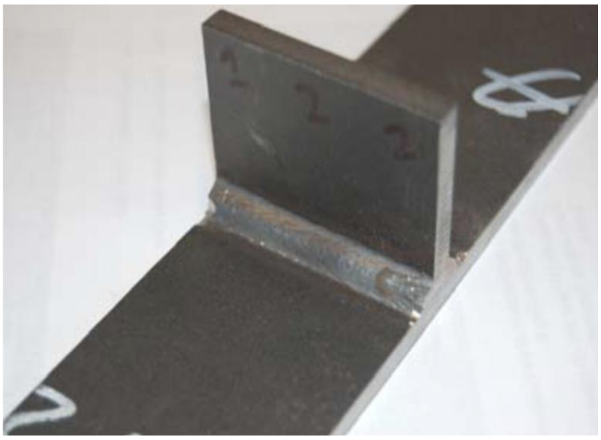

(a) As-welded T-joint

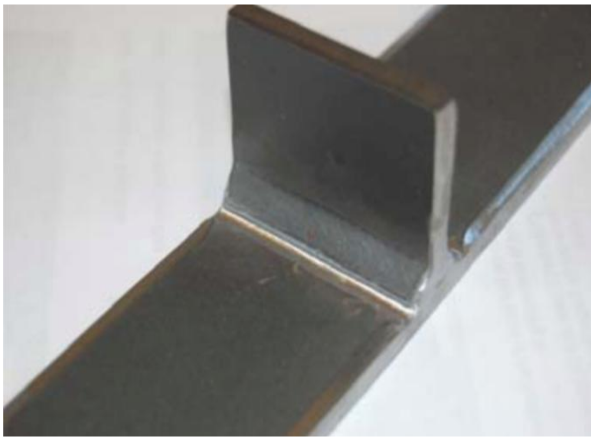

(b) Burr ground T-joint

(c) Micrograph for as-welded

(d) Micrograph for burr grinding

Fig. 4. Specimens with micrographs for as-welded and burr grinding joints (taken from study by Pedersen et al. [11])

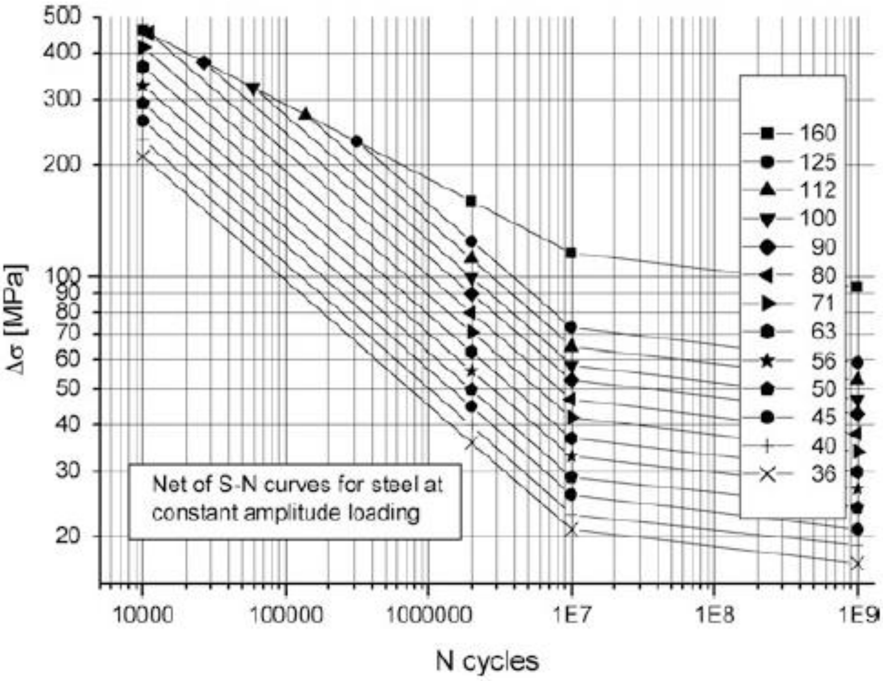

Fig. 5. Fatigue S-N curves for steel (taken from IIW Recommendation by Hobbacher [8])

3. Statistical methods

3.1 Statistical analysis

Statistical methods are used to evaluate the experimental fatigue data in order to characterize the material and predict the performance of other random samples in the future. For different use region of welded attachments, such as bridges, offshore structures and ships, the best efficient post-weld improvement method should be selected, considering the realizability and the fabrication costs. For this purpose, the statistical analysis of available fatigue data has a great significance.

3.2 Design S-N curves

The relationship between stress range $\Delta\sigma$ and the number of cycles N will be presented in *S-N curves* (Figs. 6-7) with the fatigue data example 1 and 2 gathered from Huther et al. [2], listed in Tables 2-5. The stress range $\Delta\sigma$ are plotted along the ordinate and the life N along the abscissa. Additionally, the *S-N* curve is valid only for a constant stress ratio R.

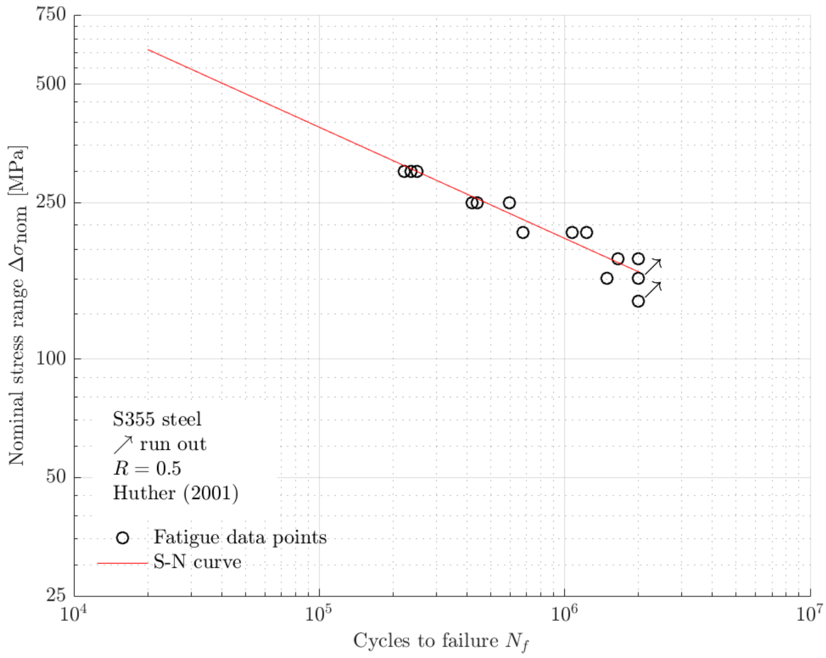

Fig. 6. Designed *S-N* curve for example 1

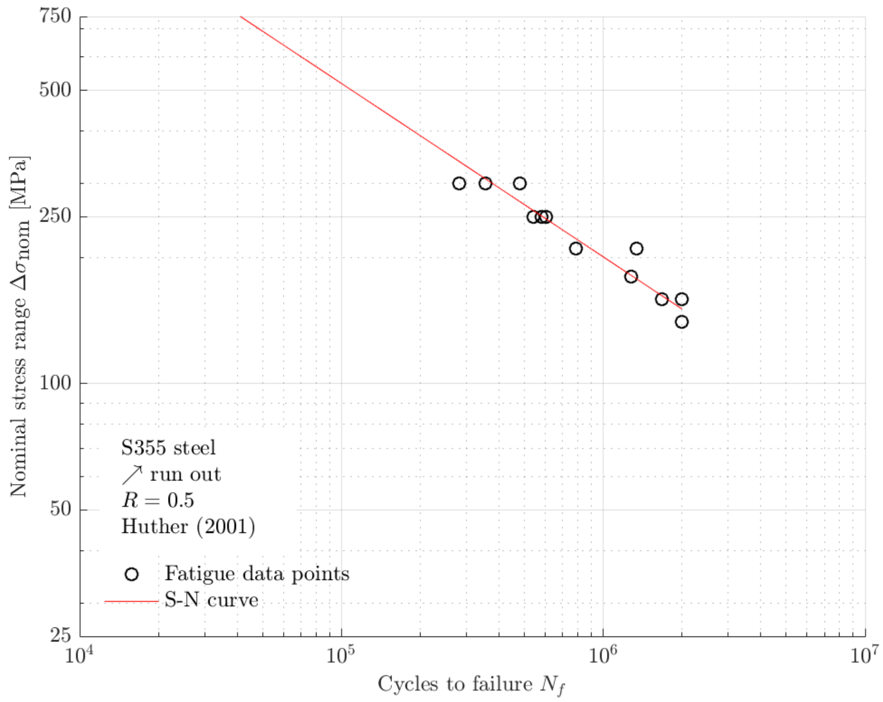

Fig. 7. Designed *S-N* curve for example 2

As-welded	
Stress range *Δσ* (MPa)	Fatigue life *N*
248.37	145795
248.37	215443
179.99	433937
179.99	774264
159.51	795399
159.51	1006760
149.56	1091470
159.51	1248800
140.23	2000640 (run out)

Table 2. Fatigue data for example 1, as-welded Specimen C, cruciform welded joint

Toe ground	
Stress range $\Delta\sigma$ (MPa)	Fatigue life N
300.13	222540
300.13	236222
300.13	249088
249.72	420533
249.72	440508
249.72	593625
209.52	677788
209.52	1070900
209.52	1230870
180.26	1647750
180.26	1997030
160.36	1491780
160.36	1997030 (run out)
140.28	1997030 (run out)

Table 3. Fatigue data for example 1, ground Specimen C, cruciform welded joint

As-welded	
Stress range $\Delta\sigma$ (MPa)	Fatigue life N
250.38	270862
159.51	583555
179.99	603534
140.23	1353880
159.51	1091470
159.51	1591310
179.99	1808460

Table 4. Fatigue data for example 2, as-welded Specimen B, cruciform welded joint

Toe ground	
Stress range $\Delta\sigma$ (MPa)	Fatigue life N
300.13	282524
300.13	356306
300.13	480156
249.72	541010
249.72	591936
249.72	605550
209.52	489429
209.52	1341650
180.26	1280810
159.02	1669740
159.02	1997030 (run out)
140.28	1997030 (run out)

Table 5. Fatigue data for example 2, ground Specimen B, cruciform welded joint

The equation of the *S-N* curve for each type of joint is determined by linear regression on a log-log basis:

$$\log N = \log C - m \cdot \log \Delta\sigma \qquad (1)$$

where m stands for the slope of the straight line in the log-log diagram and $logC$ can be calculated from N and $\Delta\sigma$.

For the derivation of designed *S-N* curve, main influencing parameters should also be taken into consideration such as yield strength of base material, thickness of plate, weld and joint geometry, load method as well as grinding depth and radius.

The stress range $\Delta\sigma$ used in this study is defined as the difference between maximum stress σ_{max} and minimum stress σ_{min}:

$$\Delta\sigma = \sigma_{max} - \sigma_{min} \qquad (2)$$

with stress ratio R to describe the elevation of stress cycle [5], shown in Fig. 8:

$$R = \frac{\sigma_{min}}{\sigma_{max}} \qquad (3)$$

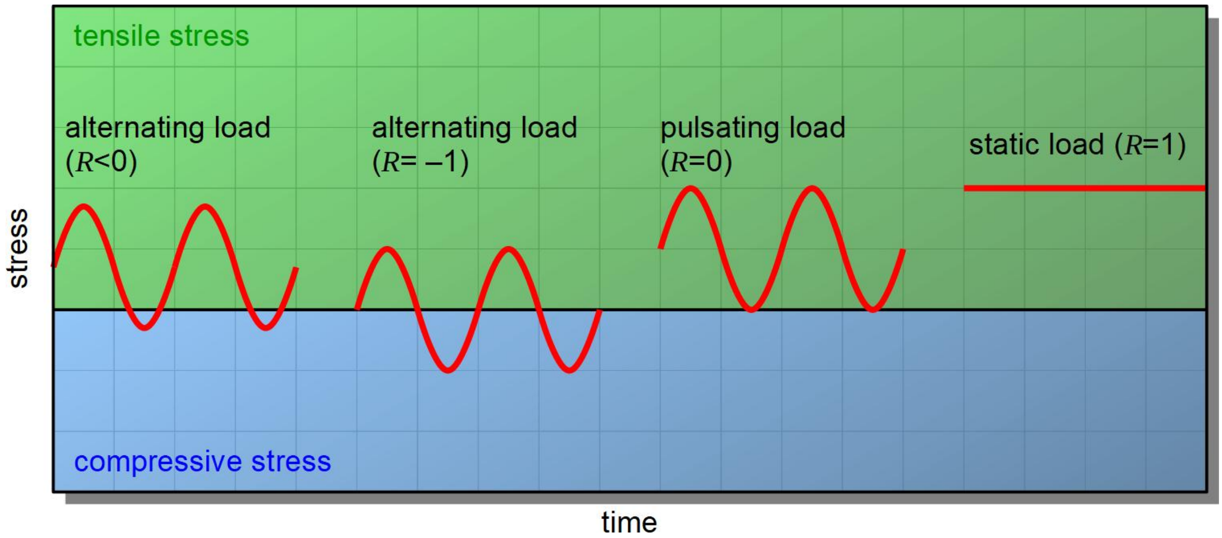

Fig. 8. Stress cycle and related stress ratios [40]

The distribution of life at one load level is assumed to be a log-normal distribution, which stated differently is a normal or Gauss distribution of the logarithm of the fatigue life, same as for the fatigue strength at a definite number of cycles. With this assumption, test results can be statistically evaluated. *S-N* curve would be computed with a definite level of survival probability *P*, corresponding to mean curves (*P* = 50%) and design curves (*P* = 95% and 95.4%) in this paper. The normal distribution with survival probability (% Certainty of Survival) is indicated in Fig. 9.

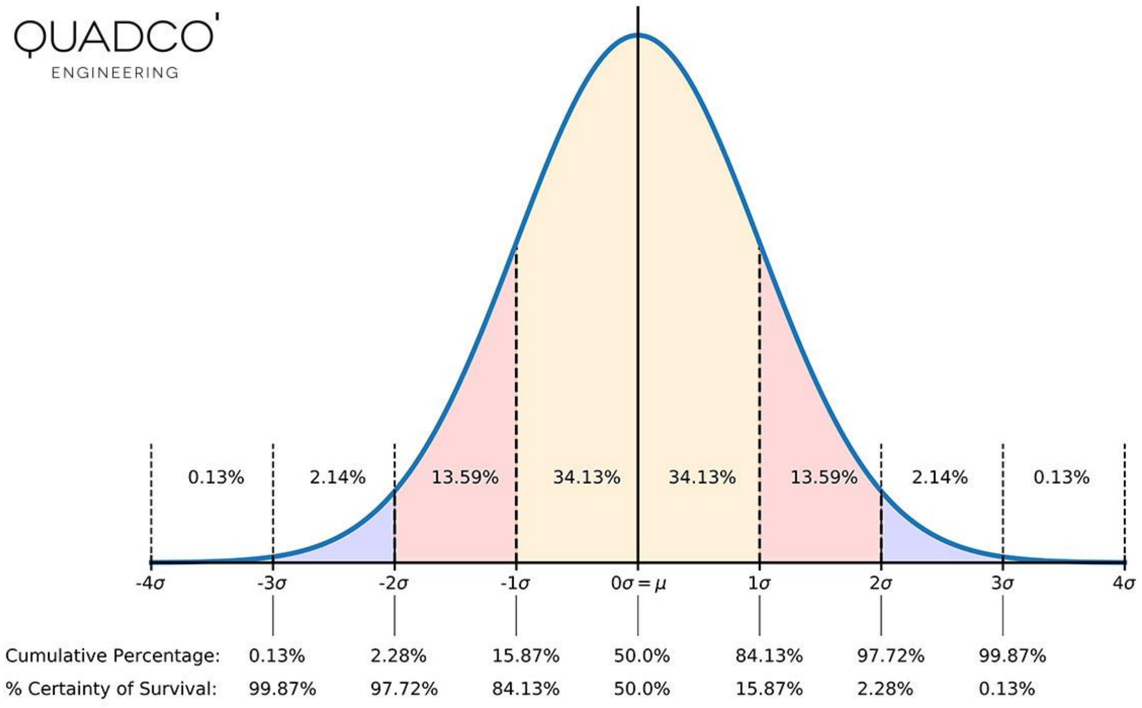

Fig. 9. Normal distribution with survival probability [41]

3.3 DVS Recommendation

The first method that be used to evaluate the test results is recommended by DVS (Deutscher Verband für Schweißen und verwandte Verfahren e.V) [7]. The best-fit *S-N* curve can be determined using linear regression. The stress range $\Delta\sigma$ is the independent variable, while cycles to failure *N* is the dependent variable. Eq. (1) can be transformed in regression form:

$$Y = A + B \cdot X \qquad (4)$$

where *Y* presents the logarithm of the fatigue life *log N* and *X* the *log* $\Delta\sigma$.

Then the summations ΣX, ΣX^2, ΣY, ΣY^2, $\Sigma X \cdot Y$ can be calculated. With the number of specimens *k*, the slope of the median *S-N* curve *m* and the constant intercept *log C* are obtained by using Eq. (5) and Eq. (6):

$$m = \frac{\sum XY - \frac{\sum X \cdot \sum Y}{k}}{\sum X^2 - \frac{(\sum X)^2}{k}} \qquad (5)$$

$$log\ C = \frac{\sum Y}{k} - m \cdot \frac{\sum X}{k} \qquad (6)$$

Here *log C* represents the allowable number of cycles with a stress range of $\Delta\sigma = 1$.

With the residual square *dY*

$$\sum dY^2 = \sum (log\ C + m \cdot X - Y)^2 \qquad (7)$$

the standard deviation of *log C* and *m* can be established by using the following equations:

$$stdv(logC) = \sqrt{\frac{\sum dY^2}{k-2}} \qquad (8)$$

$$stdv(m) = \frac{stdv(logC)}{\sqrt{\sum X^2 - \frac{(\sum x)^2}{k}}} \qquad (9)$$

It is worth mentioning that the denominator of *stdv*(*logC*) is *k*-2 instead of *k*-1, when the population of the data sample is unknown, which leads *stdv*(*logC)* to be an unbiased estimator of the normal population variance.

The scatter ratio in strength T_σ, which also expresses the scatter on the load level, is determined as Eq. (10) and is obtained by Eq. (11):

$$T_\sigma = \frac{P_{90\%}}{P_{10\%}} \qquad (10)$$

$$1: T_\sigma = 10^{-2.56 \cdot \frac{stdv(logC)}{m}} \qquad (11)$$

As Eq. (10) shows, T_σ defines the scatter band between 10% and 90% probability of failure *P* in strength.

In this study, the *S-N* curve for all fatigue data sets will be firstly computed with fixed slope *m* = 3, compared with fatigue class FAT 80 and FAT 100, which recommended by Haagensen [1] for IIW. Usually the design *S-N* curves are defined for 95% survival probability. For ease of computation, fatigue data are evaluated with the mean minus two standard deviations (*stdv(logC)*), corresponding to a survival probability of 97.7%

and the 95.4% confidence bands in this approach. On the other hand, the ground data are also evaluated with best-fit slope with Eq. (5). It is worth mentioning that the run-outs are marked with arrows and are excluded in analysis. They should be viewed as specimens that have been intentionally terminated in the test. In fact, run-outs can be used in maximum likelihood estimation. However, this is not the purpose of this paper. The results of assessment from example 1 and 2 are indicated in Figs. 10-13.

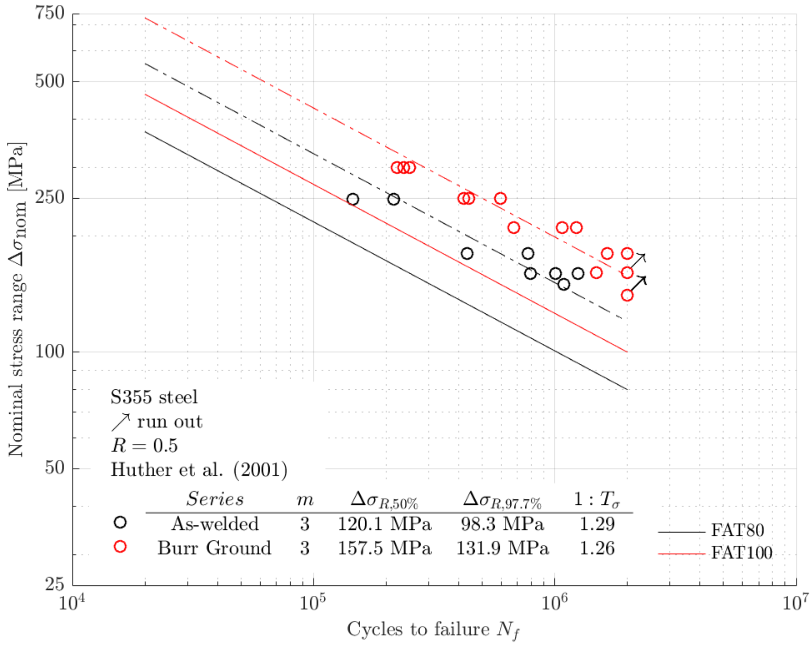

Fig. 10. Fatigue data from example 1 with DVS practice, as-welded and ground joints with fixed slope *m* = 3

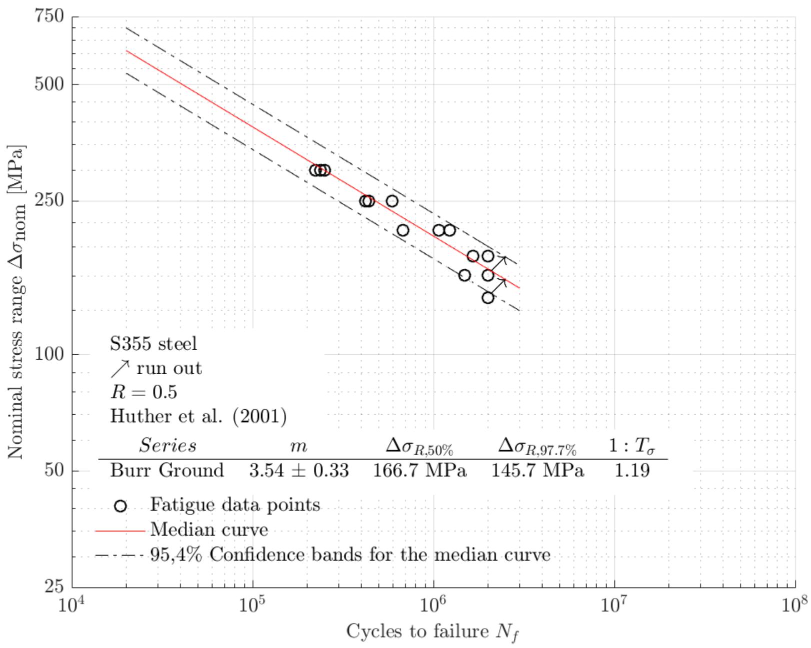

Fig. 11. Fatigue data from example 1 with DVS practice, ground joints with best-fit slope

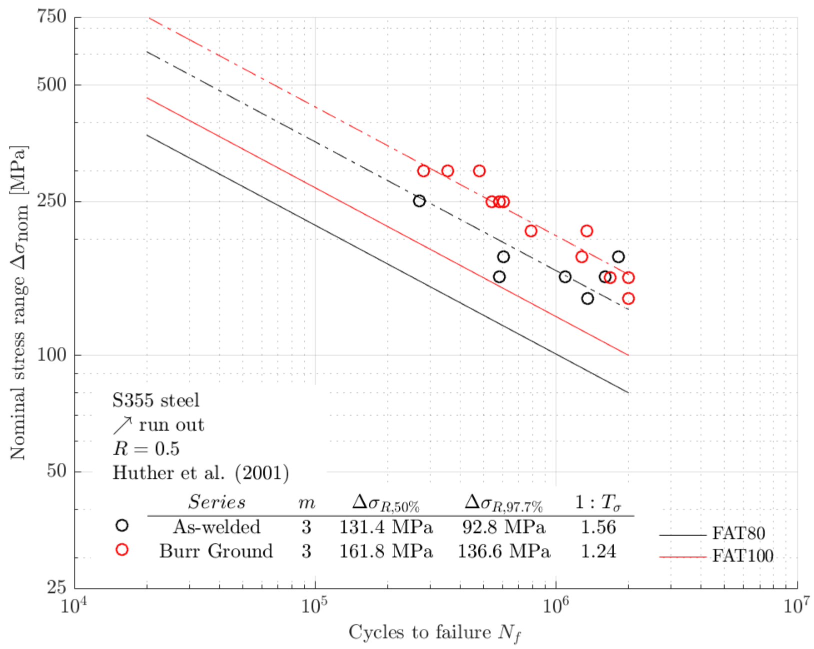

Fig. 12. Fatigue data from example 2 with DVS practice, as-welded and ground joints with fixed slope m = 3

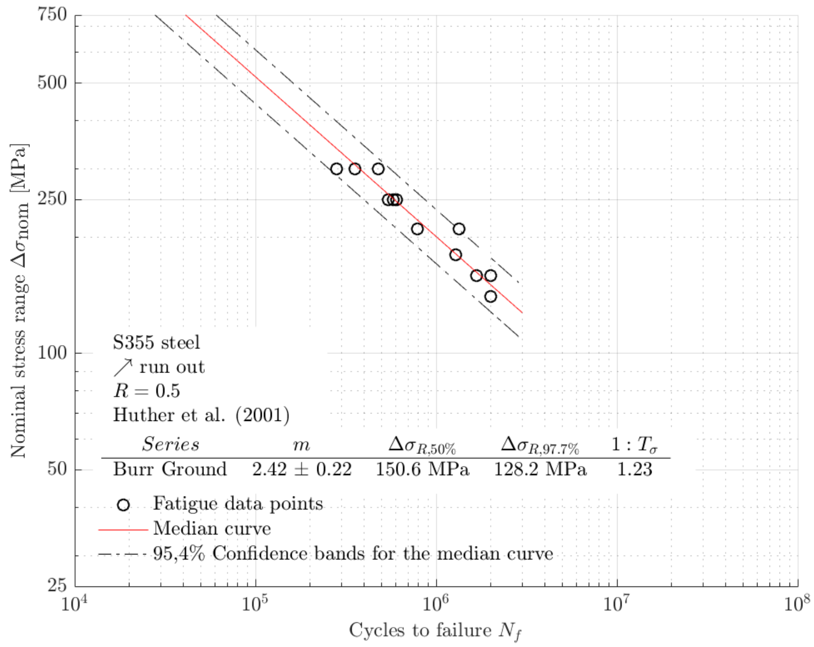

Fig. 13. Fatigue data from example 2 with DVS practice, ground joints with best-fit slope

3.4 ASTM Practice

It is well known that the relationship between stress range and fatigue life may be approximated by a straight line. ASTM standard practice [4] describes not only the evaluation method of best-fit *S-N* slopes but also its confidence interval via regression analysis. It is to be mentioned that run-outs are also excluded.

Linear Model expressed by Eq. (4) is also used in this practice, in which Y refer to the logarithm of the fatigue life *log N* and X the *log* $\Delta\sigma$. The estimators of A and B are calculated by using Eqs. (12)-(13):

$$\hat{A} = \bar{Y} - \hat{B} \cdot \bar{X} \tag{12}$$

$$\hat{B} = \frac{\sum_{i=1}^{k}(X_i - \bar{X})(Y_i - \bar{Y})}{\sum_{i=1}^{k}(X_i - \bar{X})^2} \tag{13}$$

where the symbol “caret” (ˆ) is estimate, the symbol “overbar” (¯) denotes average and k is the number of specimens.

The recommended expression for estimating the variance of the normal distribution for log N is given by

$$\hat{\sigma}^2 = \frac{\sum_{i=1}^{k}(Y_i - \hat{Y}_i)^2}{k-2} \tag{14}$$

in which $\hat{Y}_i = \hat{A} + \hat{B}X_i$ and the term k - 2 is used instead of k to make $\hat{\sigma}^2$ an unbiased estimator of the normal population variance.

The confidence intervals for parameter A is obtained by $\hat{A} \pm t_p \hat{\sigma}_{\hat{A}}$ or using Eq. (15):

$$\hat{A} \pm t_p \hat{\sigma} \left[\frac{1}{k} + \frac{\bar{X}^2}{\sum_{i=1}^{k}(X_i - \bar{X})^2}\right]^{1/2} \tag{15}$$

and for B is given by $\hat{B} \pm t_p \hat{\sigma}_{\hat{B}}$, or

$$\hat{B} \pm t_p \hat{\sigma} \left[\sum_{i=1}^{k}(X_i - \bar{X})^2\right]^{-1/2} \tag{16}$$

where t_p is directly read from Table 6 [4]. In this study, the value of survival probability P is 95%. It must be noted that n is the statistical degrees of freedom of t_p and is an entry parameter in this table: $n = k - 2$.

The confidence bands for the median *S-N* curve can be evaluated by using Eq. (17):

$$\hat{A} + \hat{B}X \pm \sqrt{2F_p}\,\hat{\sigma} \left[\frac{1}{k} + \frac{(X - \bar{X})^2}{\sum_{i=1}^{k}(X_i - \bar{X})^2}\right]^{1/2} \tag{17}$$

where F_p is the value in the F distribution and is read from Table 7 [4]. The F distribution is the most used right-skewed distribution with probability P at right side in the variance analysis, which depends on two degrees of freedom, shown in Fig. 14. In the Table 7, the top values of each row are values of F corresponding to survival probability P = 95%, the bottom values corresponding P = 99%. n_1 and n_2 are two entry parameters: $n_1 = l - 2$, $n_2 = k - l$. Additionally, l represents the number of different levels of X.

n^A	P, %^{B}	
	90	95
4	2.1318	2.7764
5	2.0150	2.5706
6	1.9432	2.4469
7	1.8946	2.3646
8	1.8595	2.3060
9	1.8331	2.2622
10	1.8125	2.2281
11	1.7959	2.2010
12	1.7823	2.1788
13	1.7709	2.1604
14	1.7613	2.1448
15	1.7530	2.1315
16	1.7459	2.1199
17	1.7396	2.1098
18	1.7341	2.1009
19	1.7291	2.0930
20	1.7247	2.0860
21	1.7207	2.0796
22	1.7171	2.0739

^{A} n is not sample size, but the degrees of freedom of t, that is, $n = k - 2$.
^{B} P is the probability in percent that the random variable t lies in the interval from $-t_p$ to $+t_p$.

Table 6. Values of t_p (taken from ASTM [4])

		Degrees of Freedom, n_1			
		1	2	3	4
Degrees of Freedom, n_2	1 {	161.45	199.50	215.71	224.58
		4052.2	4999.5	5403.3	5624.6
	2 {	18.513	19.000	19.164	19.247
		8.503	99.000	99.166	99.249
	3 {	10.128	9.5521	9.2766	9.1172
		34.116	30.817	29.457	28.710
	4 {	7.7086	6.9443	6.5914	6.3883
		21.198	18.000	16.694	15.977
	5 {	6.6079	5.7861	5.4095	5.1922
		16.258	13.274	12.060	11.392
	6 {	5.9874	5.1433	4.7571	4.5337
		13.745	10.925	9.7795	9.1483
	7 {	5.5914	4.7374	4.3468	4.1203
		12.246	9.5466	8.4513	7.8467
	8 {	5.3177	4.4590	4.0662	3.8378
		11.259	8.6491	7.5910	7.0060
	9 {	5.1174	4.2565	3.8626	3.6331
		10.561	8.0215	6.9919	6.4221
	10 {	4.9646	4.1028	3.7083	3.4780
		10.044	7.5594	6.5523	5.9943
	11 {	4.8443	3.9823	3.5874	3.3567
		9.6460	7.2057	6.2167	5.6683
	12 {	4.7472	3.8853	3.4903	3.2592
		9.3302	6.9266	5.9526	5.4119
	13 {	4.6672	3.8056	3.4105	3.1791
		9.0738	6.7010	5.7394	5.2053
	14 {	4.6001	3.7389	3.3439	3.1122
		8.8616	6.5149	5.5639	5.0354
		4.5431	3.6823	3.2874	3.0556
	15 {	8.6831	6.3589	5.4170	4.8932

Table 7. Values of F_p (taken from ASTM [4])

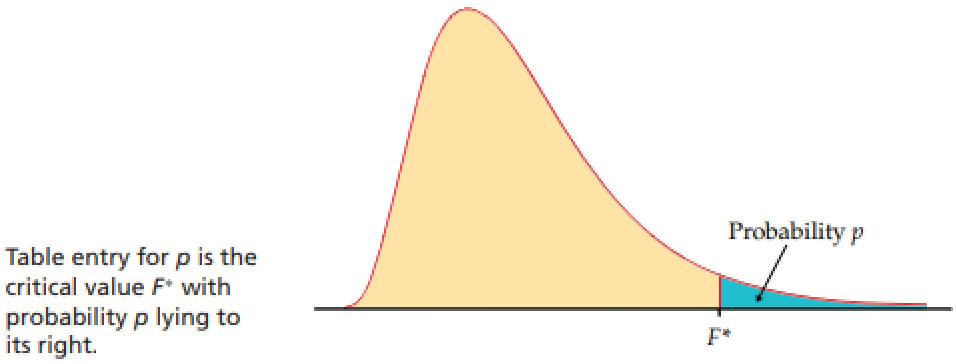

Fig. 14. F distribution [43]

Same as in section 3.3, all extracted as-welded fatigue data are analyzed with a fixed *S*-*N* slope of *m* = 3, and ground data are evaluated based on the best-fit slope with confidence interval using Eq. (15).

The results of evaluation for fatigue data from example 1 in section 3.2 are displayed in Fig.15 and Fig.16:

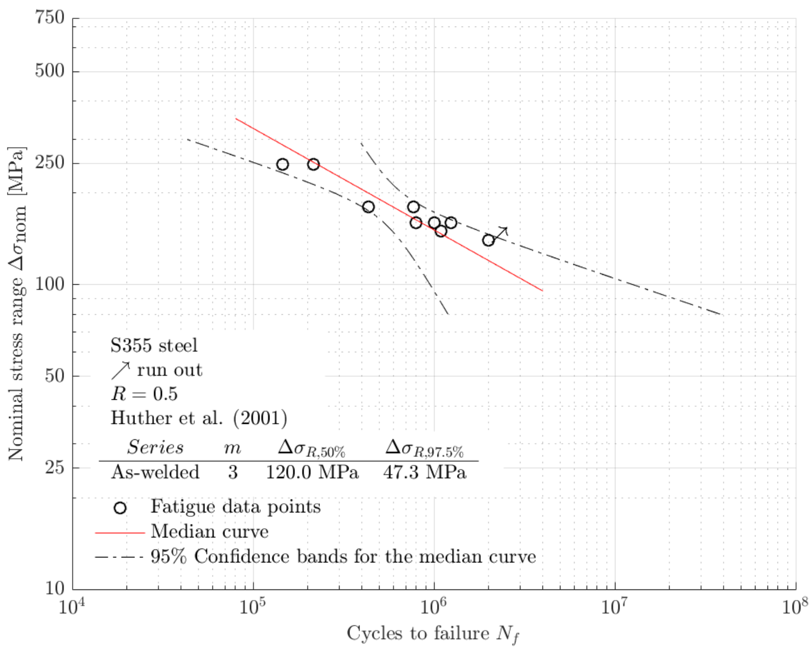

Fig. 15. Fatigue data from example 1 with ASTM practice, as-welded joints with fixed slope *m* = 3

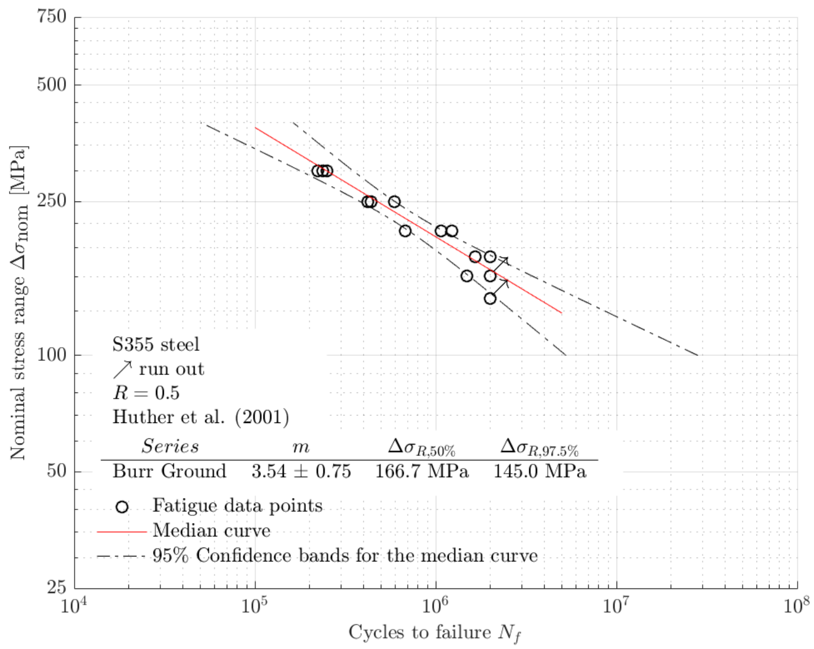

Fig. 16. Fatigue data from example 1 with ASTM practice, ground joints with best-fit slope

However, this assessment method isn't appropriate for all the extracted fatigue data. According to ASTM standard practice [4], several conditions need to be met exactly to figure out *A* and *B*: (a) the data of fatigue life are random sample (all Y_i are independent), (b) neither run-outs or paused tests can be included, (c) the relationship between S and N should be described by the linear model (Eq.(1)), (d) the fatigue life N is log-normally distributed, (e) the variance of the normal distribution $\hat{\sigma}^2$ for log N is constant. Moreover, in accordance to the assessment of all test data, more conditions are needed in this practice: (f) the required number of specimens k in testing should be greater or equal to 6, (g) replication is required in research and development applications for establishing or testing a component, where 50% can be a good replication. (h) the specimens should have more than 3 different levels and be dispersed.

To validate and emphasize the conditions above, fatigue data for example 2 from Huther et al. [2] were imported. Using Eqs.13,15 and Eq.17, the median curve and the 95% confidence band for example 2 are plotted in Figs.17-18:

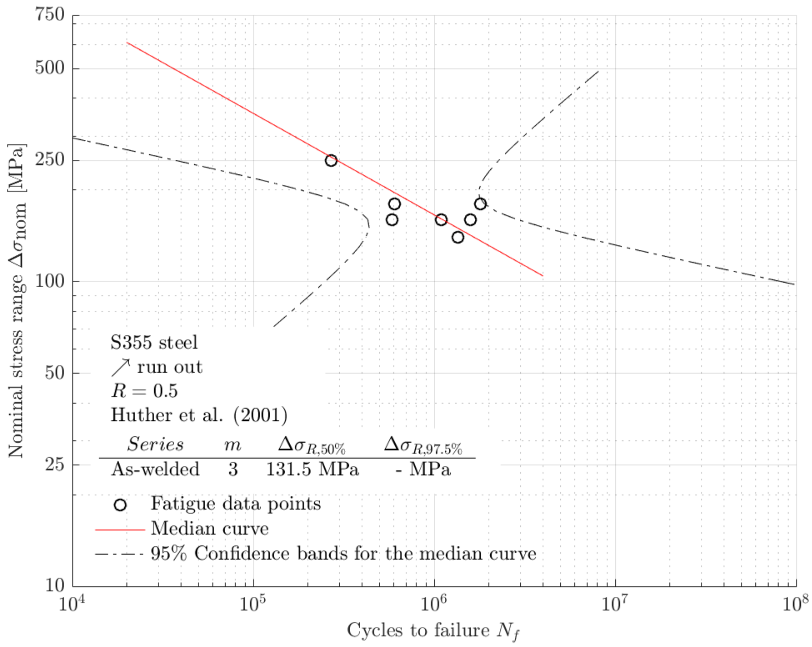

Fig. 17. Fatigue data from example 2 with ASTM practice, as-welded joints with fixed slope *m* = 3

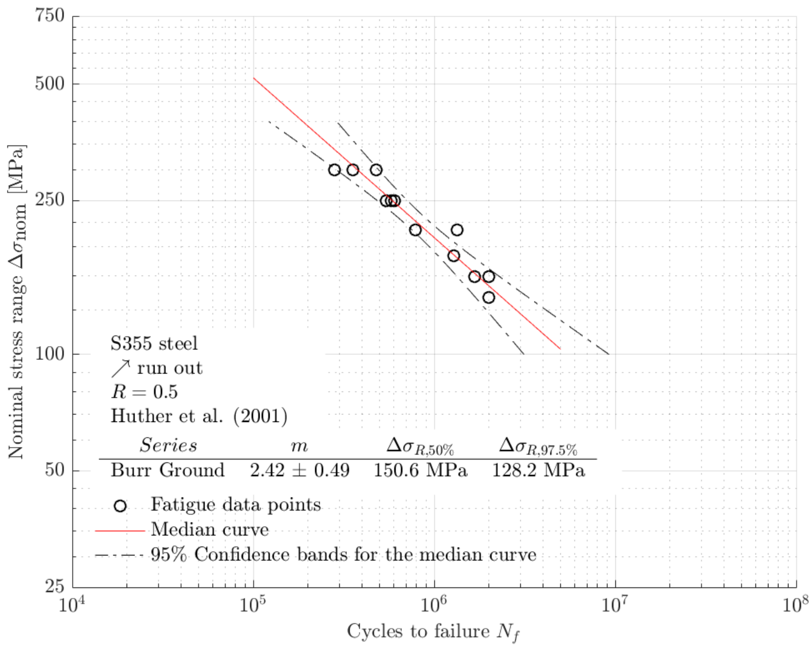

Fig. 18. Fatigue data from example 2 with ASTM practice, ground joints with best-fit slope

It is evident that there is no intersection of $N = 2 \times 10^6$ and the 97,5% curve (the bottom dotted line of the Fig. 14) for as-welded specimens with fixed *m* = 3. A narrow variation in the used stress ranges and replication of tests might be the possible explanation for the appearance of hyperbola with small curvature radius. According to Eq. (17), it is obvious that the vertex of hyperbola locates whenever $X = \bar{X}$. The lack of test replication at each of the extreme levels X_{min} and X_{max} leads to the great difference of slope between X_{min} or X_{max} and the mean value $\bar{X}$.

Therefore, the recommendation by Hobbacher [8] for International Institute of Welding (IIW) in 1996 is used to evaluate all the extracted fatigue data, especially for the data set, that cannot be analyzed by ASTM practice. More details are introduced in section 3.5.

3.5 IIW Recommendation

As explained in section 3.4, the assessment should be continued following the practice by Hobbacher [8] for International Institute of Welding (IIW) in 1996, especially for tests with small sample size and the data sets without replication or with narrow variance of stress ranges during the tests.

In this recommendation, the test results should also firstly be presented in a log-log graph with the formulae presented in Eq. (1) and run-outs may be excluded.

Then two exponents *m* and constant *log C* should be calculated. It is necessary to assess the spread of the data pairs. A fixed value of $m = 3$ should be taken for steel, if the number of specimens $k < 10$, or if the data are not sufficiently distributed enough to determine *m* exactly. In this paper, $m = 3$ will be used for as-welded data sets and best-fit slope *m* will be used for ground data, as determined in section 3.3 with recommendation from DVS, using Eq. (5) and its confidence interval with Eq. (9).

The value x_i which represents *log Ci* can be calculated from

$$x_i = logN_i - m \cdot log\Delta\sigma_i \tag{18}$$

Mean value of *log C* is given by:

$$x_m = \sum \frac{x_i}{k} = \sum \frac{logN_i}{k} + \sum \frac{m \cdot log\Delta\sigma_i}{k} \tag{19}$$

and the standard deviation *stdv_logC* can be obtained with Eq. (20):

$$stdv\_logC = \frac{\sqrt{(xm - xi)^2}}{\mathrm{k-1}} = \frac{\sqrt{(\sum dY)^2}}{\mathrm{k-1}} \tag{20}$$

in which *dY* is calculated with Eq. (7) in section 3.3.

To analyze the test results, characteristic values x_k, which represents 97.5% survival probability, should be determined using Eq. (21):

$$x_k = x_m - K \cdot stdv\_logC \tag{21}$$

where parameter *K* is obtained by using Eq. (22):

$$K = 1.645 \cdot (1 + \frac{1}{\sqrt{k}}) \tag{22}$$

Thus, the 95% confidence bands for median *S-N* curve can be computed by Eq. (23):

$$logN = (x_m \pm K \cdot stdv\_logC) - m \cdot log\Delta\sigma \tag{23}$$

The results of data sets from example 1 and 2 are indicated in Figs.19-24.

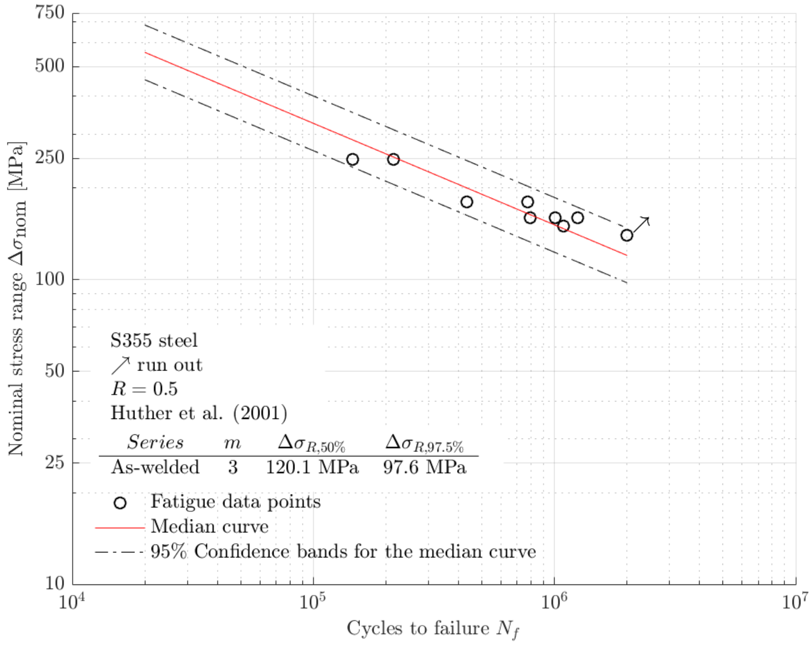

Fig. 19. Fatigue data from example 1 with IIW practice, as-welded joints with fixed slope *m* = 3

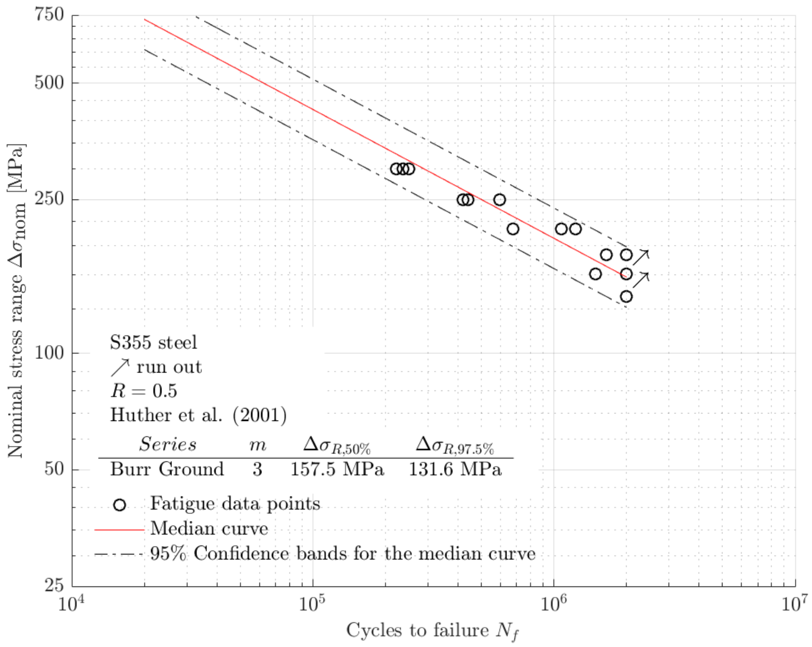

Fig. 20. Fatigue data from example 1 with IIW practice, ground joints with fixed slope *m* = 3

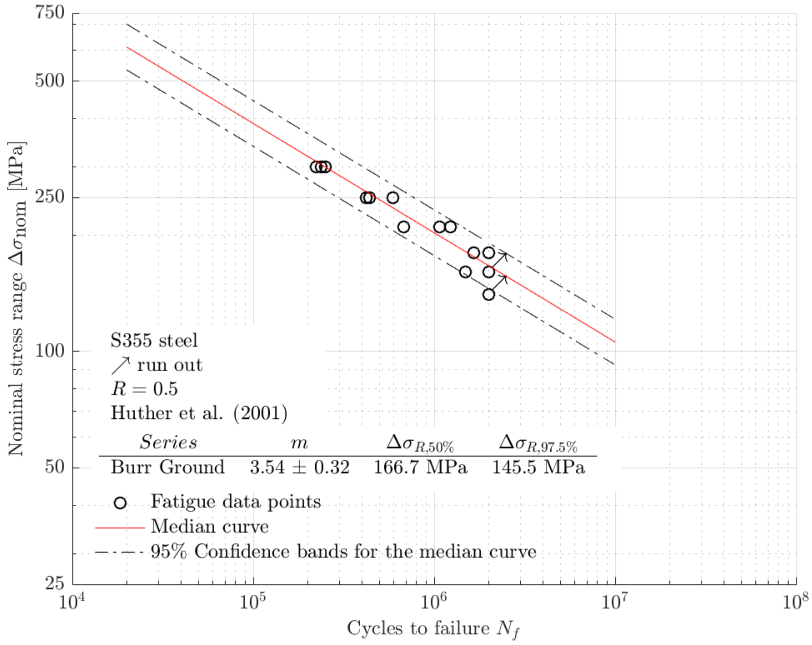

Fig. 21. Fatigue data from example 1 with IIW practice, ground joints with best-fit slope

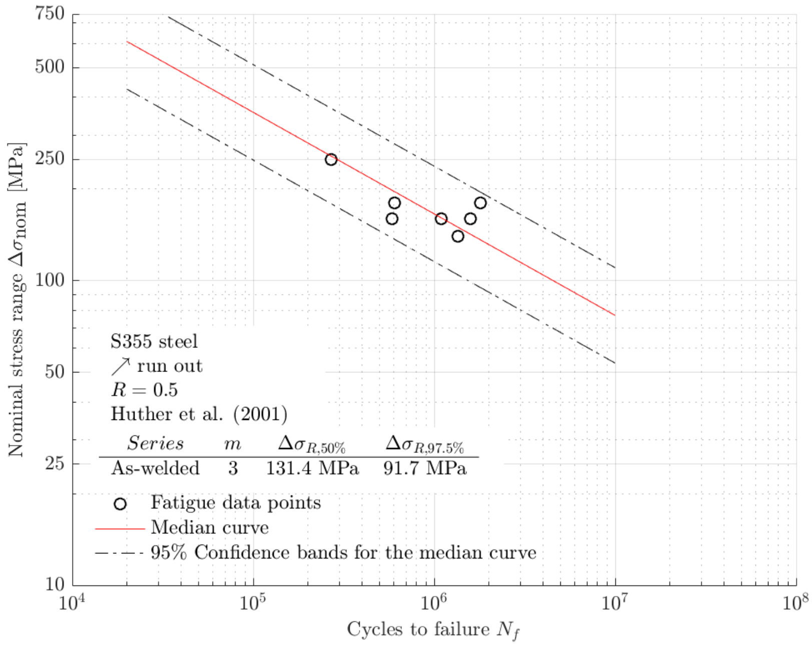

Fig. 22. Fatigue data from example 2 with IIW practice, as-welded joints with fixed slope m = 3

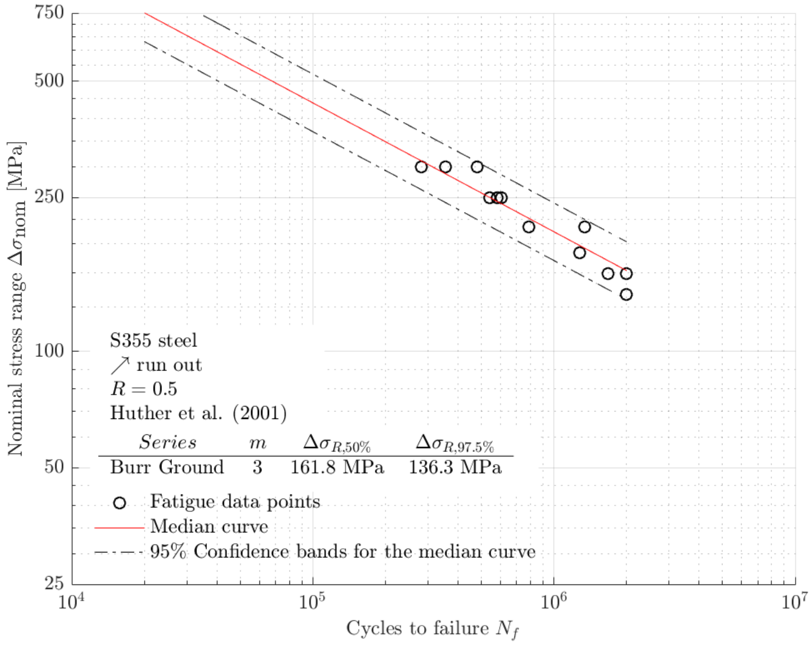

Fig. 23. Fatigue data from example 2 with IIW practice, ground joints with fixed slope *m* = 3

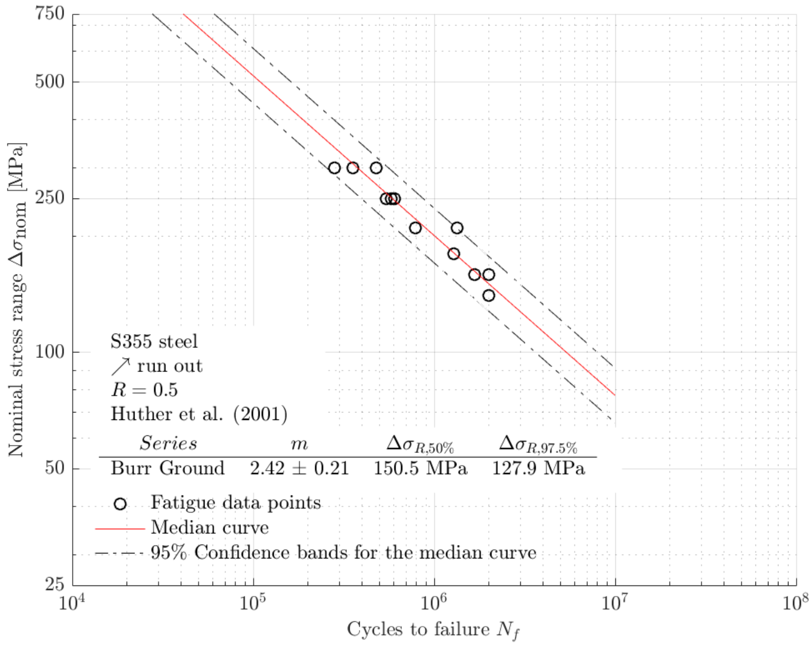

Fig. 24. Fatigue data from example 2 with IIW practice, ground joints with best-fit slope

In this paper, all the fatigue data will be analyzed using IIW recommendation:
For ground data: (1) stress range at N = 2 ×10^6 cycles of life with 50% survival probability and best-fit slope, (2) stress range at N = 2 ×10^6 cycles of life with 50% survival probability and fixed slope m = 3;
For as-welded data: (3) stress range at N =2 × 10^6 cycles of life with 50% survival probability and fixed slope m = 3, which are indicated in Tables 8-15.

4. Results

4.1 Extracted fatigue data and analysis with IIW

In total, 34 studies relative to the fatigue data points for welds improved by grinding were analyzed. These fatigue data sets include the treatment of disc, burr and weld profiling. In some of the studies, experiments were completed with different steel or welds types. Thus, totally 395 data points from 66 data sets were evaluated. Some of the data sets are listed directly in the appendix, whereas some are plotted as points in the graph. In this case, open source software like X-Y scan was used to extract fatigue data points.

In the all investigated welds types, only transverse load-carrying welds and T-joints were loading in a bending manner, whereas others were loaded with pure axial tension force. All the specimens were loaded under constant amplitude loading. The results without run-outs for butt joints, longitudinal attachments, doubling plates, transverse load-carrying welds, T-joints and transverse non-load-carrying welds, I-section with cope hole as well as out-of-plane longitudinal gusset welded to plate are summarized in Tables 8-15. The specimens have the yield strength from 175 to 1100 MPa and their thickness varies from 5 to 40 mm. In the study from Kliman et al. [9], butt joints in circular solid section with diameter of 16mm were used in the test. Only weld toe failures were taken into account.

Tables 8-15 present the steel type, plate thickness, number of specimens and stress ratio for all specimen types. The best-fit slope was calculated with linear regression recommended by the International Institute of Welding [8]. However, for some data sets, it is impossible to carry out the best-fit slope, because of the lack of specimens or the specimens were tested under the same stress range. These were noted in the tables. In some of the studies, the yield stress of the specimens was not reported. Thus, the values corresponding to the minimum value according to the steel class are taken to specify the yield stress. Moreover, some of the specimens were not identified with clear steel types. Such cases are marked with symbol '-' in Tables 8-15.

Generally, the FAT class corresponding to strength range by 97.5% survival probability for as-welded joints at $N = 2 \times 10^6$ cycles of failure are used typically for the analysis of the fatigue strength improvement [8]. However, the stress range by 50% survival probability at $N = 2 \times 10^6$ cycles of failure are used in this study. Comparing to $\Delta\sigma_{97.5\%}$, the value of $\Delta\sigma_{50\%}$ for both as-welded and ground joints can be better obtained, especially for the data sets with a few of specimens. According to study by Yıldırım et al. [44] and Fricke [42], $\Delta\sigma_{50\%}$ for as-welded specimens can be calculated with $\sigma_N = 0.206$ and $\Delta\sigma_{50\%} = \Delta\sigma_{97.5\%} \times 1.366$ as $\Delta\sigma_{50\%}$ = 123 MPa for butt joints, $\Delta\sigma_{50\%}$ = 97 MPa for longitudinal attachments with gusset length L < 150 mm and $\Delta\sigma_{50\%}$ = 86 MPa for gusset length 150 mm < L < 300 mm, $\Delta\sigma_{50\%}$ = 97 MPa for doubling plates, $\Delta\sigma_{50\%}$ = 97 MPa for transverse load-carrying welds, $\Delta\sigma_{50\%}$ = 110 MPa for T- and transverse non-load-carrying welds, $\Delta\sigma_{50\%}$ = 68 MPa for I -section with cope hole and out-of-plane longitudinal gusset welded to plate, where $\Delta\sigma_{97.5\%}$ corresponds to the FAT class for as-welded specimens, which are recommended by IIW [8]. These results are represented in Table 16.

With the results obtained in section 3.5 (indicated in Figs. 19-24), several comparisons are made to calculate the improvement of fatigue strength. As shown in Tables 8-15, 8-12 columns present (i) the value of $\Delta\sigma_{50\%}$ for ground data by best-fit slope and its fatigue strength improvement (%) compared with calculated $\Delta\sigma_{50\%}$ for as-welded data recommended by IIW [42], and (ii) the value of $\Delta\sigma_{50\%}$ for ground data by fixed slope m_1 = 3 and the increase of fatigue strength relative to the $\Delta\sigma_{50\%}$ for as-welded data by fixed slope m_1 = 3, which expresses the actual benefit of burr grinding.

The last two columns in Tables 8-15 show the results of fatigue strength and improvements (%) using assumed slope m_1 = 4.

In the Tables 8-15, the specimens from references [17]-1, [30], [31], [37]-3 and [37]-4 were improved by disc grinding, and from references [34], [37]-1 as well as [37]-6 were treated by fully burr grinding, which is normally called weld profiling. In the reference [33], specimens from 1-3 were ground with a weld toe radii r = 3 mm, 4-6 were with r = 5 mm. Additionally, it is described in studies [18]-2, [19], [27]-2 and [27]-3 that burr grinding was carried out in seawater. Moreover, specimens from same material with different plate thickness are tested in the literature [30] and [35]. The influence of steel grade of specimens was also analyzed in the studies [3], [19] and [37]. Furthermore, in the study [31], specimens were tested under different cyclic loading so that the effect of mean stress on the fatigue strength was analyzed.

It is apparent that the improvements (%) of some of the data sets were negative. That means, burr grinding has no great effect on the test welds, compared to either IIW Recommendation, or as-welded specimens. The reason for that might be following:

As the last third column in Table 8 shows, in the study from Huther et al. [3], the improvement at m_1 = 3 to as-welded has a value of -1 because the specimens were fabricated by handling-lifting builders to a defined weld quality, which can provide a better fatigue strength, and burr grinding may not be really useful when the as-welded quality is quite good. Otherwise, the effect of burr grinding is negative for applied stress range $\Delta\sigma$ > 310 MPa because of notch effect, which is described in the reference by Kliman et al. [9]. Same as the case above, the results from study by Méndez et al. [14] show a decrease of fatigue strength by burr grinding. The main cause of this observation may be the reduction of material after U-shape grinding.

Reference	Steel type	σ_{YS} (MPa)	Plate thickness(mm)	*k*	Stress ratio	Best-fit slope	$\Delta\sigma_{50\%}$ by best-fit slope (MPa)	%imp.at m_1=free to IIW [8]	$\Delta\sigma_{50\%}$ by m_1=3 (MPa)	$\Delta\sigma_{50\%}$ by m_1=3 for as-welded (MPa)	%imp.at m_1=3 to as-welded	$\Delta\sigma_{50\%}$ by m_1=4 (MPa)	%imp.at m_1=4 to IIW [8]
[28]	A515 Grade 70	320[b]	25	2	0	Same stress range			179.9	133.9	34	208.9	70
[3]	S355	355[a]	8	8	0.5	3.2	162.8	32	158.8	122.9	29	175.5	43
[3]	S355	355[a]	8	8	0.5	4	138.9	13	116.9	117.7	-1	138.9	13
[35]	HT50A	382[b]	12.7	11	0	6.12	205.6	67	113.4	95.9	18	151.9	23
[35]	HT50B	382[b]	20	2	0	17.12	311.4	153	226.6	146.7	54	249.5	103
[9]	S355	612[b]	diameter 16mm	10	-1	8.3	108.8	-12	38.7	54.1	-28	58	-53
[10]	S600	670[b]	5	10	0	7.55	436.7	255	266.7	165.1	62	327.2	166

[a] nominal σ_{YS}
[b] measured σ_{YS}

Table 8. Extracted fatigue data for butt joints improved by Burr grinding

Reference	Steel type	σ_{YS} (MPa)	Plate thickness(mm)	*k*	Stress ratio	Best-fit slope	$\Delta\sigma_{50\%}$ by best-fit slope (MPa)	%imp.at m_1=free to IIW [8]	$\Delta\sigma_{50\%}$ by m_1=3 (MPa)	$\Delta\sigma_{50\%}$ by m_1=3 for as-welded (MPa)	%imp.at m_1=3 to as-welded	$\Delta\sigma_{50\%}$ by m_1=4 (MPa)	%imp.at m_1=4 to IIW [8]
[34]	BS15	278[b]	12.7	10	-1	3.01	75.4	-12	75.5	48.4	56	83.9	-2
[34]	BS968	347[b]	12.7	5	0	2.87	120.7	40	122	87	40	129.8	51
[12]	Grade A	336[b]	10	11	-1	5.19	165.7	71	149.4	91	64	152.4	57
[16]	S500	633[b]	12	4	-1	5.05	151.2	56	129.5	70.4	84	139.8	44
[39]	S600,960,1100	600-1100[a]	8	6	0.2	2.86	98.8	2	101.2	80.6	26	114,8	18
[39]	S600,960,1100	600-1100[a]	8	6	0.2	2.1	69	-20	89.6	63.5	41	104.4	21
[15]	S690QL	819[b]	16	8	0.1	2.15	89.9	-7	106.6	91.5	17	118.7	22

[a] nominal σ_{YS}
[b] measured σ_{YS}

Table 9. Extracted fatigue data for longitudinal attachments improved by Burr grinding

Reference	Steel type	σ_{YS} (MPa)	Plate thickness(mm)	k	Stress ratio	Best-fit slope	$\Delta\sigma_{50\%}$ by best-fit slope (MPa)	%imp.at m_1=free to IIW [8]	$\Delta\sigma_{50\%}$ by m_1=3 (MPa)	$\Delta\sigma_{50\%}$ by m_1=3 for as-welded (MPa)	%imp.at m_1=3 to as-welded	$\Delta\sigma_{50\%}$ by m_1=4 (MPa)	%imp.at m_1=4 to IIW [8]
[12]	Grade A	336[b]	10	14	-1	6.07	156.9	62	127.5	102.9	24	141.3	46
[17]-1	S350	350[a]	16	9	0.1	5.44	228.4	135	157.3	130.9	20	193.6	100
[17]-2	S350	350[a]	16	8	0.1	6.37	272.9	181	196.1	130.9	50	229.2	136
[29]	-	430[b]	20	4	0.1	4.99	195.2	101	143.2	93.1	54	173.8	79
[29]	-	430[b]	20	4	0.1	Same stress range			180.1	93.1	93	201.5	108

[a] nominal σ_{YS}

[b] measured σ_{YS}

Table 10. Extracted fatigue data for doubling plates improved by Burr grinding

Reference	Steel type	σ_{YS} (MPa)	Plate thickness(mm)	k	Stress ratio	Best-fit slope	$\Delta\sigma_{50\%}$ by best-fit slope (MPa)	%imp.at m_1=free to IIW [8]	$\Delta\sigma_{50\%}$ by m_1=3 (MPa)	$\Delta\sigma_{50\%}$ by m_1=3 for as-welded (MPa)	%imp.at m_1=3 to as-welded	$\Delta\sigma_{50\%}$ by m_1=4 (MPa)	%imp.at m_1=4 to IIW [8]
[36]	SUS316L	175[b]	20	7	0.1	3.08	110.3	14	109.2	104.5	4	120.6	24
[28]	A515 Grade A	320[b]	25	4	0	1.69	69.7	-28	122.9	91.1	35	147.6	52
[19]	-	372[b]	10	5	0	3.1	129	33	126.8	79.6	59	145.3	50
[19]	-	764[b]	10	5	0	2.45	101.4	5	113.8	80.2	42	129.6	34
[18]-1	Supereiso 70	685[b]	38	5	0.1	2.95	118.1	22	119.3	99.3	20	139.3	44
[18]-2	Supereiso 70	685[b]	38	7	0.1	4.65	174.5	80	144.4	95.7	51	165	70

[a] nominal σ_{YS}

[b] measured σ_{YS}

Table 11. Extracted fatigue data for transverse load-carrying welds improved by Burr grinding

Reference	Steel type	σ_{YS} (MPa)	Plate thickness(mm)	k	Stress ratio	Best-fit slope	$\Delta\sigma_{50\%}$ by best-fit slope (MPa)	%imp.at m_1=free to IIW [8]	$\Delta\sigma_{50\%}$ by m_1=3 (MPa)	$\Delta\sigma_{50\%}$ by m_1=3 for as-welded (MPa)	%imp.at m_1=3 to as-welded]	$\Delta\sigma_{50\%}$ by m_1=4 (MPa)	%imp.at m_1=4 to IIW [8]
[14]	A36	250[b]	20	4	0	1.11	25.6	-77	196.1	232.2	-16	218.6	99
[14]	A36	250[b]	20	4	0	1.86	50.4	-54	120.1	232.2	-48	171.6	56
[12]	Grade A	336[b]	10	10	-1	3.25	114.4	4	111.5	73.9	51	121.3	10
[13]	Low carbon micro alloyed	380[b]	30	6	0.1	5.69	239.2	117	190	116.2	64	204.3	86
[32]	-	420[b]	20	5	0	4.75	232.5	111	181	115.8	56	214.4	95
[11]	S700	700[a]	6	11	0.1	5.03	353.5	221	223.9	168.9	33	297.1	170

[a] nominal σ_{YS}

[b] measured σ_{YS}

Table 12. Extracted fatigue data for T-joints improved by Burr grinding

Reference	Steel type	σ_{YS} (MPa)	Plate thickness(mm)	*k*	Stress ratio	Best-fit slope	$\Delta\sigma_{50\%}$ by best-fit slope (MPa)	%imp.at m_1=free to IIW [8]	$\Delta\sigma_{50\%}$ by m_1=3 (MPa)	$\Delta\sigma_{50\%}$ by m_1=3 for as-welded (MPa)	%imp.at m_1=3 to as-welded	$\Delta\sigma_{50\%}$ by m_1=4 (MPa)	%imp.at m_1=4 to IIW [8]
[3]	S355	355[a]	8	3	0.5	3.81	157.1	43	148.6	127.8	16	158.6	44
[3]	S355	355[a]	8	12	0.5	2.42	150.6	37	161.8	131.4	23	174.4	59
[3]	S355	355[a]	8	12	0.5	3.54	166.7	52	157.5	120.1	31	172.8	57
[3]	S235	235[a]	8	8	0.5	1.01	106.9	-3	151.2	117.2	29	158	44
[20]	S900	972[b]	10	11	0	2.01	121.4	10	185.3	77.9	138	229.7	109
[21]	Grade A	-	10	7	0.1	4.49	216.4	97	190.4	111	72	209.7	91
[21]	Grade A	-	10	3	0.1	Same stress range			146.4	98.7	48	163.9	49
[22]	S700	794[b]	8	8	0.2	3.48	205.1	86	191.4	128.3	49	216.7	97
[23]	DH36	375[b]	20	5	0.1	1.09	56.7	-48	135.1	74.5	81	152.8	39
[24]	DH36	375[b]	12.7	10	0.1	5.07	150.7	37	129.9	114.5	13	142.3	29
[25]	S355	406[b]	12.5	2	0.1	2.63	152.7	39	158.6	98.4	61	169.9	54
[26]	S275	275[a]	50	5	0	5.77	178.7	62	137.9	91.3	51	157.8	43
[27]-1	S31803	478[b]	10	11	0.1	3.76	245.7	123	225.5	118.3	91	250.7	128
[27]-2	S31803	478[b]	10	8	0.1	5.25	195.3	78	150.5	107.2	40	175.2	59
[27]-3	Austenitic 304L	256[b]	10	3	0.1	10.25	226.6	106	165	129.6	27	184.6	68
[31]	Grade 43A	260[b]	12.5	5	-1	4.41	150.2	37	126.8	106.9	19	144.7	32
[31]	Grade 43A	260[b]	12.5	4	0.5	4.57	123.8	13	107.5	94.9	13	119.1	8
[34]	BS15	278[b]	12.7	4	-1	2.54	93.3	-15	98.8	63.9	55	107.1	-3
[37]-1	S275	275[a]	12.5	5	0	6.18	198.7	81	166.4	105.3	58	181.4	65
[37]-2	S275	275[a]	12.5	6	0	3.45	143.6	31	136.7	105.3	30	150.2	37
[37]-3	S275	275[a]	12.5	9	0	5.4	153.5	40	121.7	105.3	16	138.7	26
[37]-4	HSS	685[b]	12.5	3	0	3.88	150.1	36	120.1	91.7	31	153.6	40
[37]-5	HSS	685[b]	12.5	3	0	3.91	177.8	62	142.8	91.7	56	180.9	64
[37]-6	HSS	685[b]	12.5	3	0	5.16	260.1	136	203.8	91.7	122	235.8	114
[33]-1	SM490YA	418[b]	16	6	0	4.44	124.7	13	104.3	78.3	33	119.6	9
[33]-2	SM490YA	418[b]	16	6	0	4.55	122.1	11	99.6	78.3	27	115.6	5
[33]-3	SM490YA	418[b]	16	6	0	4.42	114.5	4	92.2	78.3	18	109.1	-1
[33]-4	SM490YA	418[b]	16	5	0	3.19	104.7	-5	100.8	78.3	29	117.8	7
[33]-5	SM490YA	418[b]	16	5	0	4.03	131	19	117.2	78.3	50	130.7	19
[33]-6	SM490YA	418[b]	16	5	0	9.44	161.9	47	108.8	78.3	39	125.9	14

[a] nominal σ_{YS}

[b] measured σ_{YS}

Table 13. Extracted fatigue data for transverse non-load-carrying welds improved by Burr grinding

Reference	Steel type	σ_{YS} (MPa)	Plate thickness(mm)	k	Stress ratio	Best-fit slope	$\Delta\sigma_{50\%}$ by best-fit slope (MPa)	%imp.at m_1=free to IIW [8]	$\Delta\sigma_{50\%}$ by m_1=3 (MPa)	$\Delta\sigma_{50\%}$ by m_1=3 for as-welded (MPa)	%imp.at m_1=3 to as-welded	$\Delta\sigma_{50\%}$ by m_1=4 (MPa)	%imp.at m_1=4 to IIW [8]
[38]	-	-	19	2	0.01	Same stress range			76.9	62.7	23	81.6	20
[38]	-	-	19	5	0.01	Same stress range			89	65.3	36	97.5	43

[a] nominal σ_{YS}

[b] measured σ_{YS}

Table 14. Extracted fatigue data for I - section with cope hole improved by Burr grinding

Reference	Steel type	σ_{YS} (MPa)	Plate thickness(mm)	k	Stress ratio	Best-fit slope	$\Delta\sigma_{50\%}$ by best-fit slope (MPa)	%imp.at m_1=free to IIW [8]	$\Delta\sigma_{50\%}$ by m_1=3 (MPa)	$\Delta\sigma_{50\%}$ by m_1=3 for as-welded (MPa)	%imp.at m_1=3 to as-welded]	$\Delta\sigma_{50\%}$ by m_1=4 (MPa)	%imp.at m_1=4 to IIW [8]
[30]	S235	235[a]	10	1	-1	Lack of specimens			69.5	46.4	50	76.1	-38
[30]	S235	235[a]	18	1	-1	Lack of specimens			118.1	53.9	119	122.3	-1
[30]	S420	420[a]	10	2	-1	Lack of specimens			58.6	48.9	20	64.9	-47

[a] nominal σ_{YS}

[b] measured σ_{YS}

Table 15. Extracted fatigue data for out-of-plane longitudinal gusset welded to plate improved by Burr grinding

	Butt welds	Longitudinal attachments with l<150mm	Longitudinal attachments with l<300mm	Doubling plates	Transverse load-carrying welds	T-joints	Transverse non-load-carrying welds	I-section with cope hole	out-of-plane longitudinal gusset welded to plate
FAT class for as-welded [8]	90	71	63	71	71	80	80	50	50
FAT class for ground [8]	112	90	80	90	90	100	100	65	65
Calculated $\Delta\sigma_{50\%}$ for ground data	123	97	86	97	97	110	110	68	68

Table 16. FAT classes and calculated $\Delta\sigma_{50\%}$ for each specimen type

4.2 S-N slope calculation

All ground data sets are evaluated based on IIW recommendation [8]. The results for butt joints, longitudinal attachments, doubling plates, transverse load-carrying welds, T-joints and transverse non-load-carrying welds are shown in Fig. 25. Slopes for I-section with cope hole and out-of-plane longitudinal gusset welded to plate cannot be calculated due to a lack of fatigue data and the specimens were tested under the same stress range. The ordinates of Fig. 25 represent number of specimens *k* and the abscissas represent best-fit slopes as points and their scatter bands as error bar, assessed by Eqs. (5) and (9). Additionally, *S*-*N* slope $m_1 = 3$ and the mean value of all slopes are also represented with horizonal lines in Fig. 25. It is worth mentioning that data sets for T-joints and transverse non-load-carrying welds would be combined in one group because of their same FAT class, although they are two different types of welds.

In consideration of sufficient available fatigue data points for T-joints and transverse non-load-carrying welds, the results of their *S*-*N* slope estimates based on steel grades are shown in Fig. 26.

Most of the specimens used in the identified studies are small welded components, whereas components with large size were used in the references from Clegg et al. [17], Lotsberg et al. [29] for doubling plates and Choi et al. [38] for I-section with cope hole. Results for large doubling plates are shown in Fig. 27.

4.3 Results of analysis

All test data sets, including the extracted data for I-section with cope hole and out-of-plane longitudinal gusset welded to plate, are plotted in Fig. 30 and analyzed using assumed slope $m_1 = 4$ for 50% as well as 95% survival probability. Furthermore, the regression line, which corresponds to FAT class by IIW recommendation for as-welded joints with fixed slope $m_1 = 3$, is also presented in Fig. 30. In addition, the improvements of fatigue strength at $N = 2 \times 10^6$ cycles are noted in the figures. As shown in Fig. 30c and Fig. 30d, fatigue data for longitudinal attachments with the length of gusset L < 150 mm and 150 mm < L < 300 mm are evaluated separately, due to the difference of FAT classes recommended by IIW.

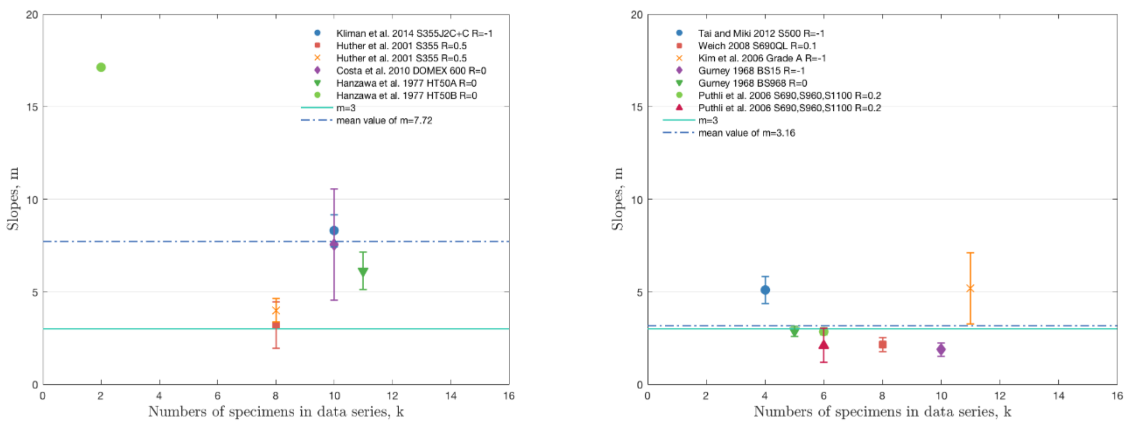

(a) Butt welds

(b) Longitudinal attachments

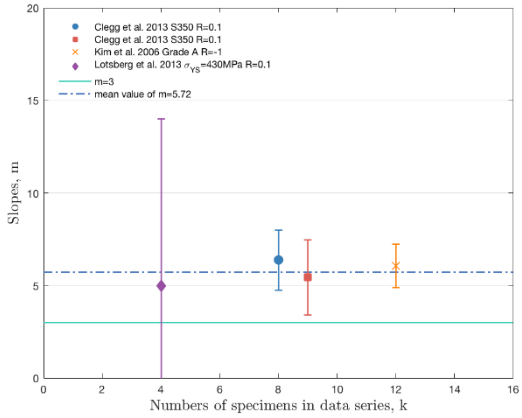

(c) Doubling plates

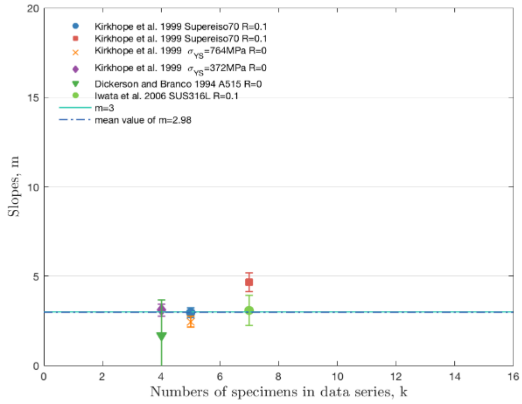

(d) Transvers load-carrying welds

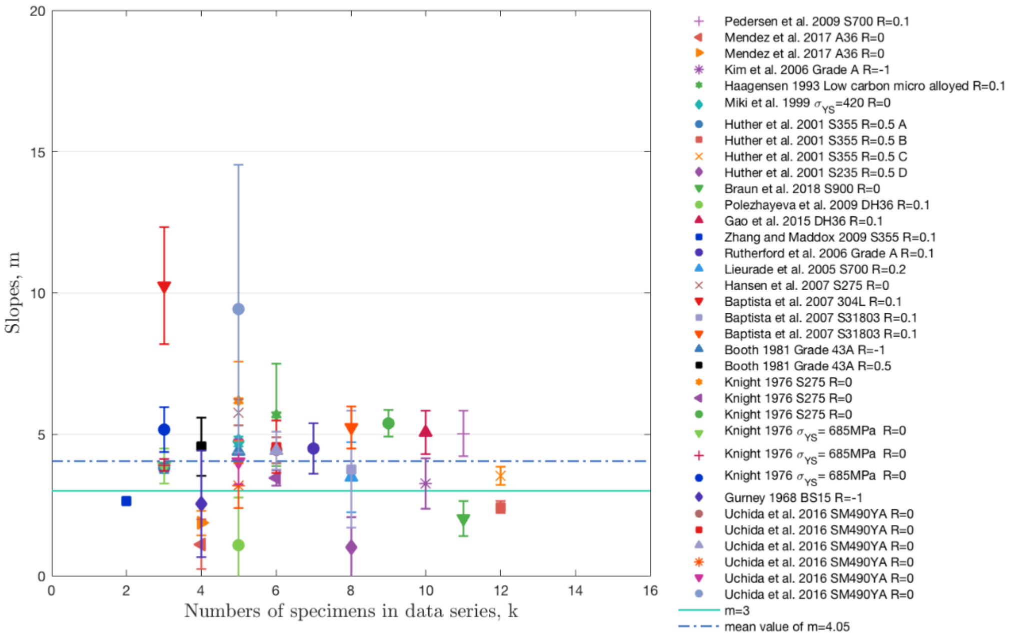

(e) T-joints and transverse non-load-carrying welds

Fig. 25. Slope calculation based on number of specimens for the extracted fatigue data improved by burr grinding

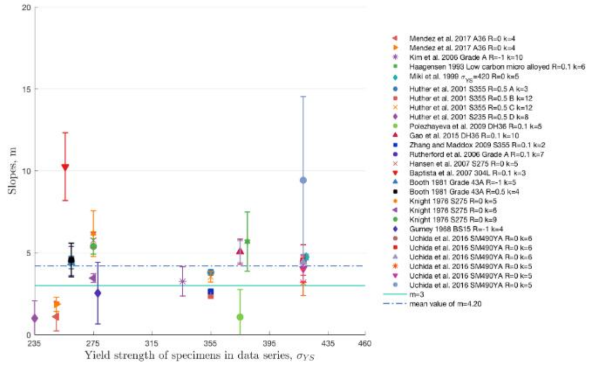

(a) 235 < σ_{YS} < 460 MPa

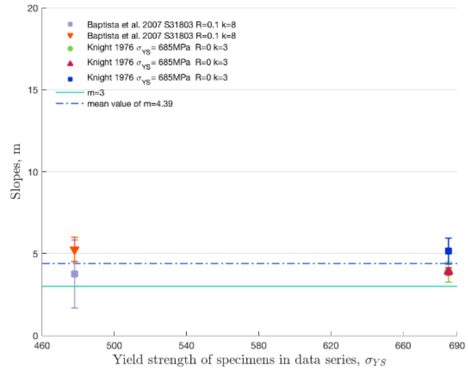

(b) 460 < σ_{YS} < 690 MPa

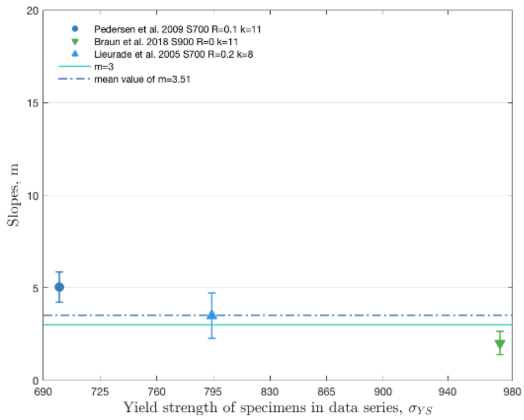

(c) 690 < σ_{YS} < 980 MPa

Fig. 26. Slope calculation based on steel grades for T-joints and transverse non-load-carrying welds improved by burr grinding

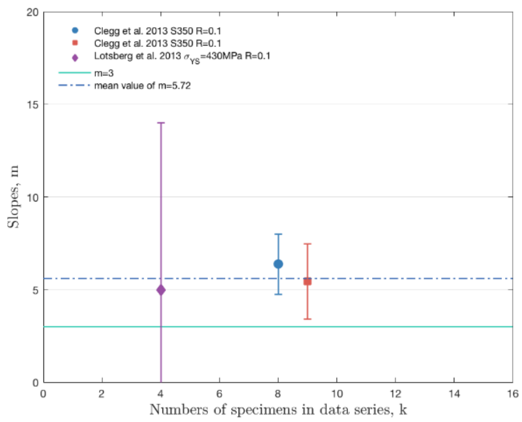

Fig. 27. Slope calculation based on number of specimens for the doubling plates in large size improved by burr grinding

5. Discussion

5.1 *S*-*N* curve slopes

As depicted in Fig. 25, m_1 = 3 is neither the best-fit slope for all test data, (doesn't passes all the scatter bands of assessed best-fit slope) nor the average value of slopes and can also not satisfy plenty of the test data sets for butt welds, doubling plates, longitudinal attachments, T-joints and non-load carrying transverse joints. In this case, an assumed value m_1 = 4 would be used for all types of welds to evaluate the improvement of burr grinding in the following discussion. [4] As shown in Figs. 28-29, ground data from example 1 and 2 are analyzed with the assumed slope m_1 = 4 following IIW Recommendation [8].

It is apparent form Fig. 25 that the best-fit slope is significantly greater than m_1 = 4, especially for butt joints and doubling plates. The mean values of m_1 for these two welds are even greater than 5. For butt welds, only 2 of them are less than m_1 = 5. The best-fit slopes of 2 out of 7 data sets for longitudinal attachments are closed to 5. Additionally, there are also slopes for doubling plates and T-joints as well as transverse non-load-carrying welds larger than 4. However, the confidence interval of the *S*-*N* slopes for doubling plates is large enough to let m_1 = 4 pass through the scatter bands. Fig. 27 shows that the assumed value of slope m_1 = 4 can be used for the large doubling plates.

The possible explanation for the large assessed values of best-fit-slopes may be a narrow variation in the stress range used in the test and a lack of specimens. If all tests were completed within the same stress range, an infinite *S*-*N* slope would be figured out. Meanwhile, if there were only two points available, the slope would be determined just by these two points and no confidence interval can be obtained. Therefore, some of the data sets are listed in Tables 8-16 without best-fit slope, but they will be included for the following analysis of the fatigue data improvements.

It can be observed from Fig. 26 that there is no increase of slope *m* regarding increased yield strength. However, the slope of specimens with higher yield strength tends to be stable in the range of 3 to 5. Certainly, more tests are needed to analyze the effect of yield strength on the slope of *S*-*N* curves.

In this study, only data with $N < 2 \times 10^6$ were evaluated. According to IIW recommendation, it is assumed that $N = 10^7$ is the 'knee point' on the *S*-*N* curve because of a fatigue limit, below which no failure will occur, or the designed *S*-*N* will be a horizontal line. However, new experimental data shows that there is no fatigue limit and the *S*-*N* curve should be continued based on a further decrease in stress range of about 10% per decade, which corresponds to a slope of m_2 = 22 for $N > 10^7$.[8]

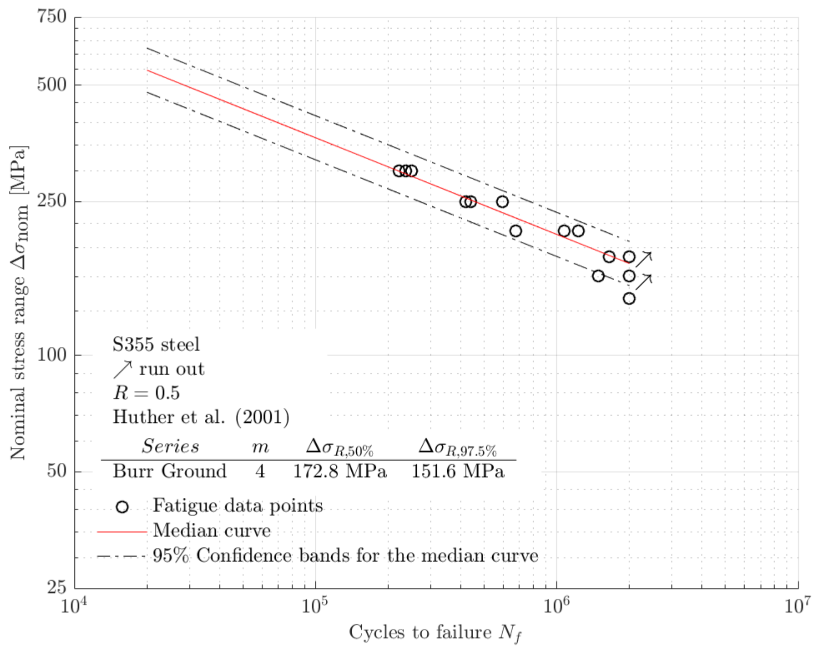

Fig. 28. Fatigue data from example 1 with IIW practice, ground joints with fixed slope $m_1 = 4$

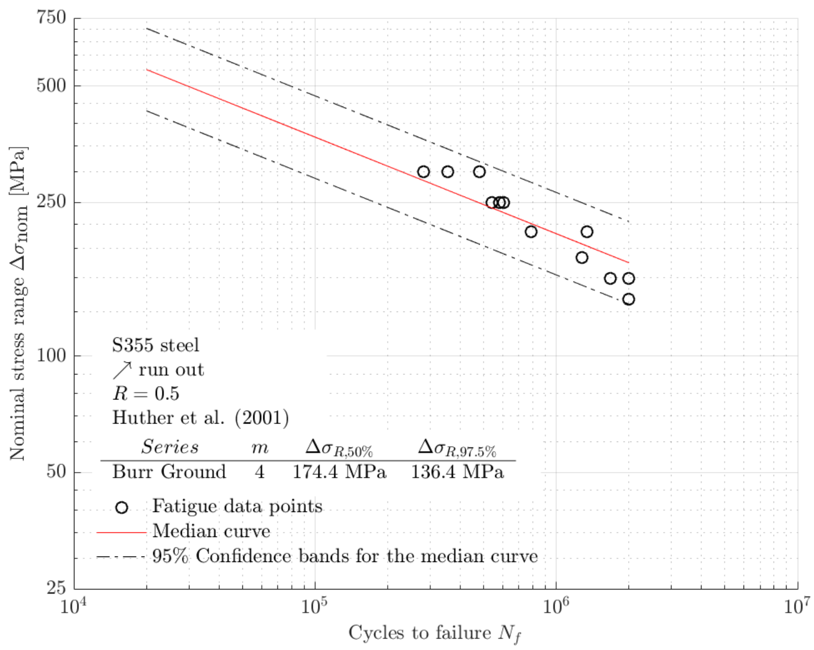

Fig. 29. Fatigue data from example 2 with IIW practice, ground joints with fixed slope $m_1 = 4$

5.2 The degree of improvements

All extracted fatigue data after burr grinding are plotted in Fig. 30, which represents also the evaluated regression lines with assumed slope m_1 = 4 for 50% and 97.5% survival probability. That is the reason that few of the data points are below the 97.5% curve, which corresponds to a 2.5% failure probability. Meanwhile, FAT classes recommended by IIW [8] with m_1 = 3 and 97.5% survival probability for as-welded joints would also be depicted in Fig. 22. The increase of stress range by $N = 2 \times 10^6$ cycles is calculated by $\Delta\sigma_{97,5\%}$ and FAT classes.

As indicated in Fig. 30b, a data set from study by Kliman et al. [9] were not analyzed, which fall below the IIW curve for FAT 90 in Fig. 30a. It is obvious that this data set has a great influence on the assessment of fatigue strength increase for the total data sets for butt welds. In the study, Kliman et.al [9] have made a conclusion that burr grinding had a positive effect on the butt welded circular solid sections only when the specimens were loaded under a low stress range at about 80 MPa. If the used stress range was above 310 MPa, the effect of burr grinding would be negative. On the other hand, a large slope was also expected. These might be the reason why the obtained $\Delta\sigma_{97,5\%}$ value for ground welds is lower than FAT class for as-welded joints, as shown in Fig. 30a.

For longitudinal attachments with gusset length L < 150 mm, an increase of 35% was obtained relative to FAT 71, while the value of improvement for the gusset length 150 mm < L< 300 mm was just 7% relative to FAT 63. For the longitudinal attachments with longer welded gusset, only 18 fatigue data points from 2 studies by Gurney [34] and Puthli et al. [39] were available for the assessment. This might be the reason for the great deviation from the increase with 30%, which was suggested by IIW.

Fig. 30e and Fig. 30f present the result for doubling plates with 68% and transverse load-carrying welds with 45% fatigue strength enhancement relative to IIW recommendation for as-welded joints. Additionally, the result for doubling plates in large size is indicated in Fig.30j with an increase of 114% in fatigue strength. It is observed that m_1 = 4 may be a conservative value predicted for doubling plates and transverse load-carrying welds.

Same as section 4.2, the fatigue data for T-joints and transverse non-load-carrying welds were plotted in one figure and their improvement would be evaluated together. It is obvious that for these two types of welds, an increase is about 28%, which is in accordance with IIW practice that the improvement by burr grinding in stress range corresponds to a factor of 1.3.

Results for I-section with cope hole with burr grinding treatment and out-of-plane longitudinal gusset welded to plate with disc grinding treatment are represented in Fig. 30h and Fig. 30i. As shown in the figures, only 6 fatigue data points are available for each weld type. Hence, the effect of burr grinding on these two types of welds cannot be investigated adequately because of the data deficiency, although the increase of fatigue strength for I-section has the value of 36%. Meanwhile, it is worth mentioning that the specimens for I-section belong to large components.

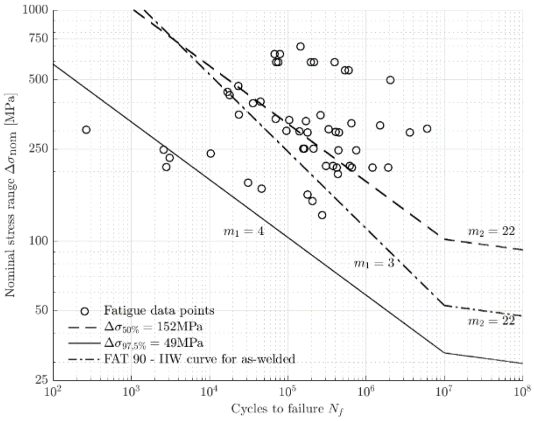

(a) Butt welds with circular solid section

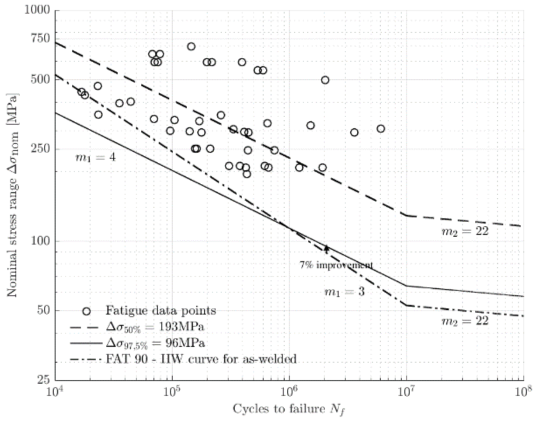

(b) Butt welds without circular solid section

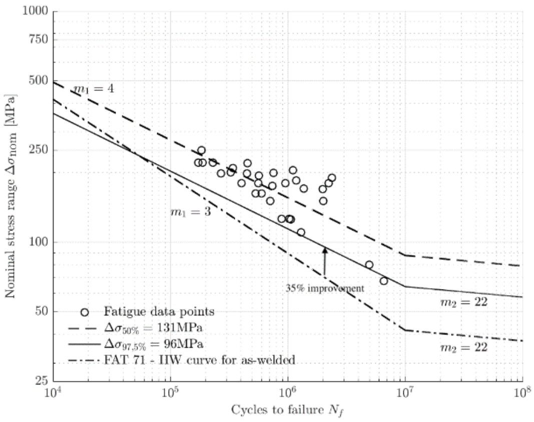

(c) Longitudinal attachments with *L* < 150 mm

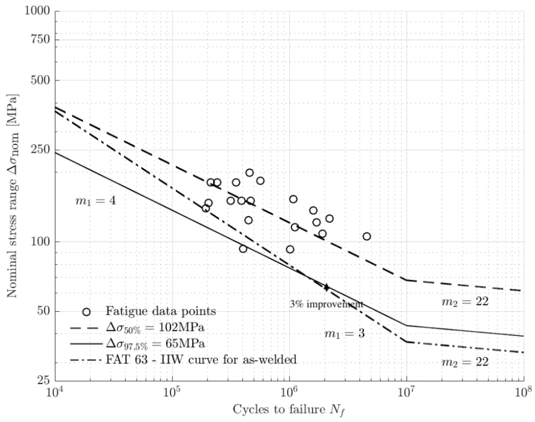

(d) Longitudinal attachments with 150 mm < *L* < 300 mm

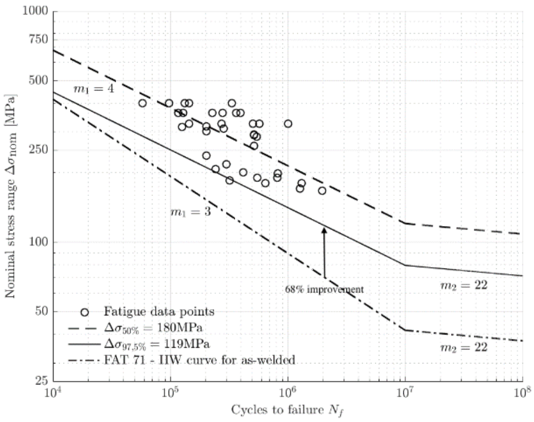

(e) Doubling plates

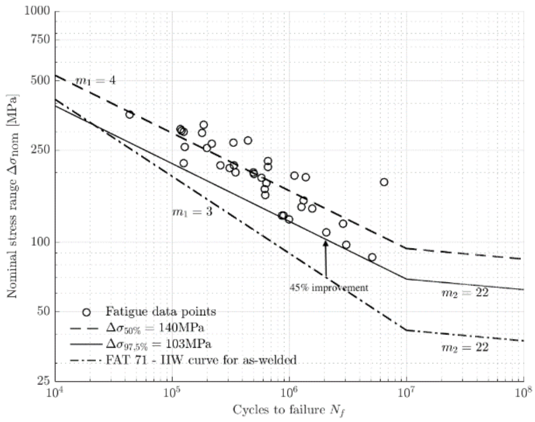

(f) Transverse load-carrying welds

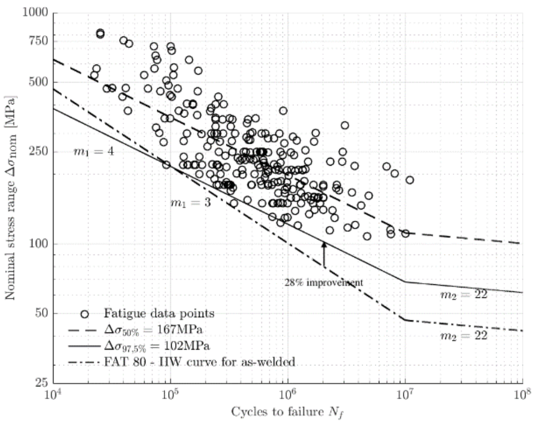

(g) Transverse non-load-carrying welds and T-joints

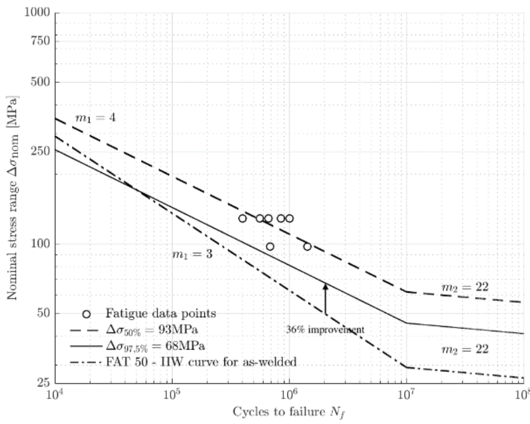

(h) I - section with cope hole

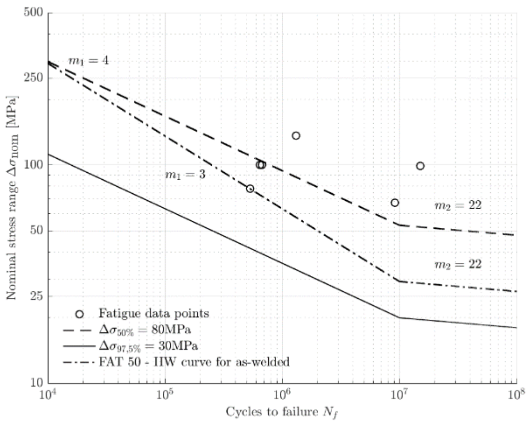

(i) Out-of-plane longitudinal gusset welded to plate

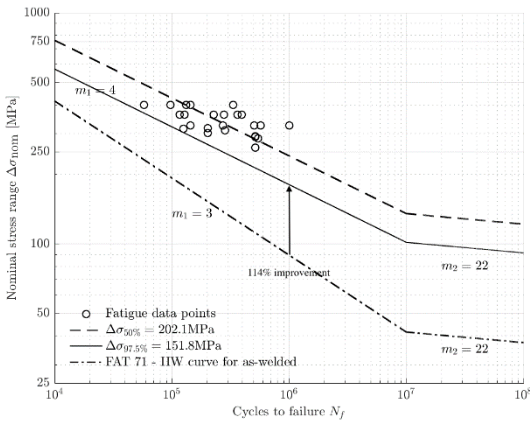

(j) Large doubling plates

Fig. 30. Analysis of fatigue data with assumed slope $m_1 = 4$

It is worth mentioning that the standard stress ratio R defined for FAT class recommended by IIW [8] has the value of 0.5. It means, for all test, which are completed with a stress ratio $R < 0.5$, a fatigue enhancement factor $f(R)$ should be multiplied to the fatigue class of details. This factor depends on the level and direction of residual stresses, which include all the stress that are not considered in the fatigue analysis. In this study, plenty of the extracted fatigue data were obtained under the loading $R < 0.5$. To determine $f(R)$, 3 cases are as follows:

1. Unwelded base material and wrought products with negligible residual stresses, stress relieved welded components, in which the effects of constraints or secondary stresses have been considered in analysis. No constraints in assembly. [8]

$f(R) = 1.6$ for $R < 1$ or completely in compression
$f(R) = -0.4 \cdot R + 1.2$ for $-1 \leq R \leq 0.5$ (24)
$f(R) = 1$ for $R > 0.5$

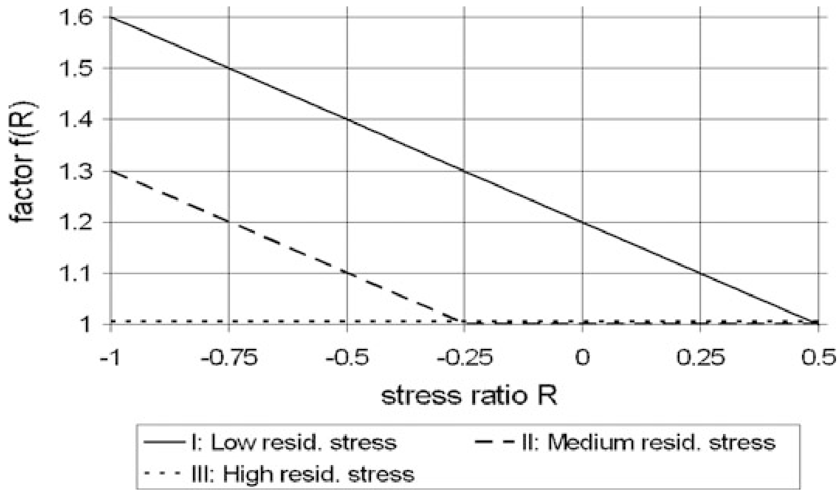

Fig. 31. Enhancement factor f(R) (taken from IIW Recommendation [8])

2. Small-scale thin-walled simple structural elements containing short welds. Parts or components containing thermally cut edges. No constraints in assembly. [8]

$f(R) = 1.3$ for $R < 1$ or completely in compression
$f(R) = -0.4 \cdot R + 0.9$ for $-1 \leq R \leq 0.25$ (25)
$f(R) = 1$ for $R > 0.25$

3. Complex two- or three-dimensional welded components, components with global residual stresses, thick-walled components. The normal case for welded components and structures. [8]

$f(R) = 1$ no enhancement (26)

However, the stress cannot be relieved completely effectively, and due to a lack of fit during assembly, displacement of abutments or other reasons, additional residual stress might be introduced. Therefore, it is recommended to use $f(R) > 1$ for welding parts only in very special cases. [8]

5.3 Proposed FAT values

All extracted fatigue data are plotted in Fig. 32, which presents the obtained $\Delta\sigma_{97.5\%}$ for ground data at N = 2 × 10^6 cycles by m_1 = 4 in solid lines and the FAT class value advised by IIW [8] in dashed lines. As mentioned before, butt welds are analyzed with and without circular solid section, as shown in Fig. 32a and Fig. 32b. Moreover, the values of $\Delta\sigma_{97.5\%}$ acquired from section 5.2 and recommended FAT classes are summarized in Table 17. It can be observed that only two of the data points fall below the proposed curve. It is possible to say that the proposed *S-N* curves might be proper to the fatigue data sets.

For longitudinal attachments with *L* < 150 mm, T-joints, transverse non-load-carrying welds and I - section with cope hole, the proposed value is same as those taken from IIW. For doubling plates and transverse-load-carrying welds, a larger FAT class value is recommended. In fact, the available data of all specimens except T- and transverse non-load-carrying welds is not enough to draw final conclusions. More testing is needed for further evaluation, especially for butt welds, longitudinal attachments with 150 mm < *L* < 300 mm, I-section and out-of-plane longitudinal attachments.

	Butt welds	Longitudinal attachments with l<150mm	Longitudinal attachments with l<300mm	Doubling plates	Transverse load-carrying welds	T-joints	Transverse non-load-carrying welds	I-section with cope hole	out-of-plane longitudinal gusset welded to plate
FAT class for ground [8]	112	90	80	90	90	100	100	65	65
$\Delta\sigma_{97.5\%}$ calculated by m_1=4	45/90	90	71	112	100	100	100	65	28

Table 17. Analysis of extracted data using a slope of m_1 = 4

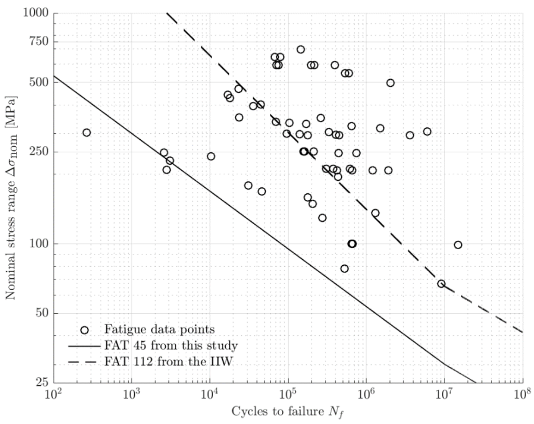

(a) Butt welds with circular solid section

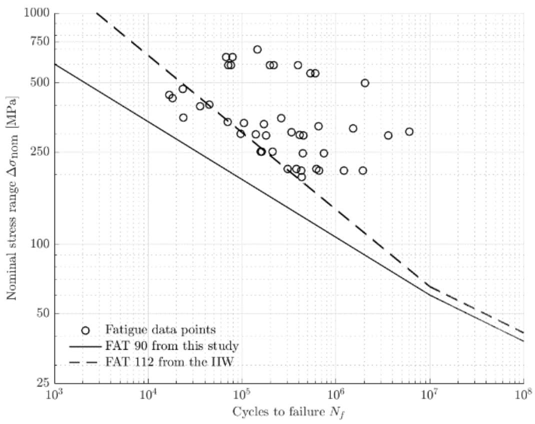

(b) Butt welds without circular solid section

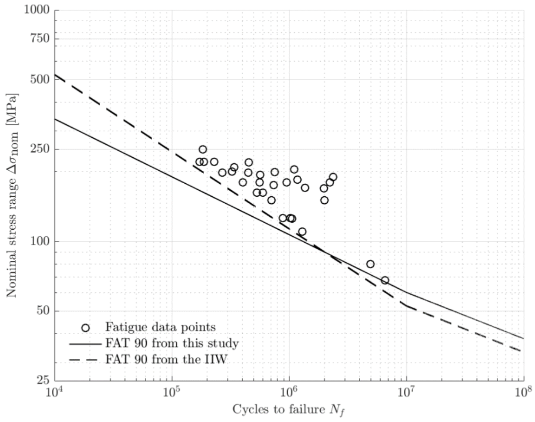

(c) Longitudinal attachments with *L*<150mm

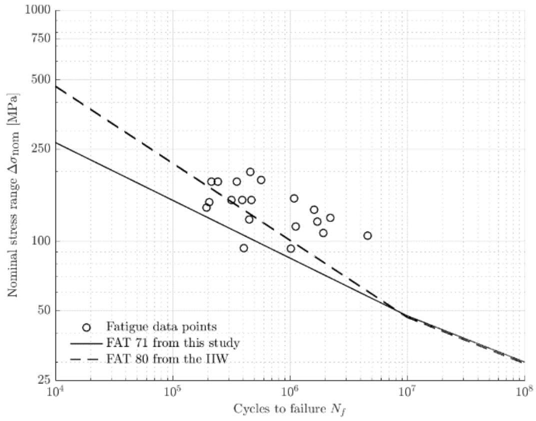

(d) Longitudinal attachments with 150mm < *L*< 300mm

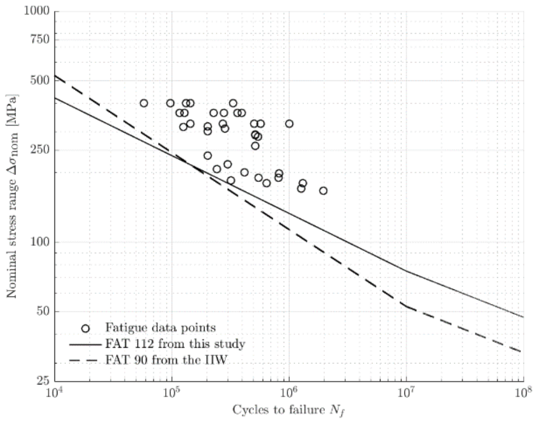

(e) Doubling plates

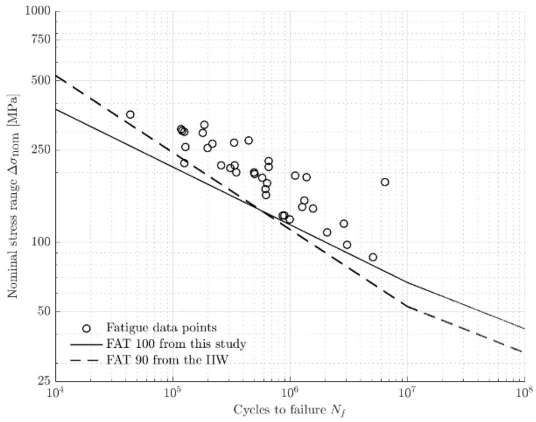

(f) Transverse load-carrying welds

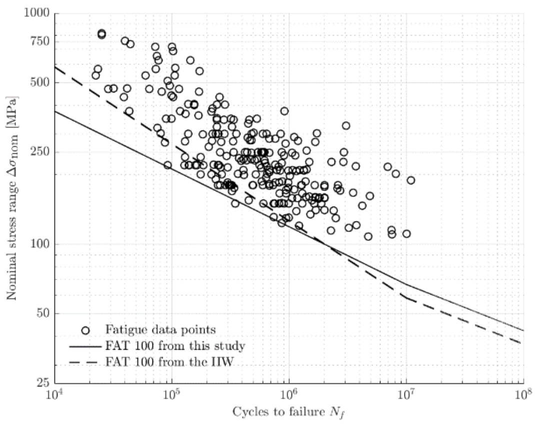

(g) T-joints and transverse non-load-carrying welds

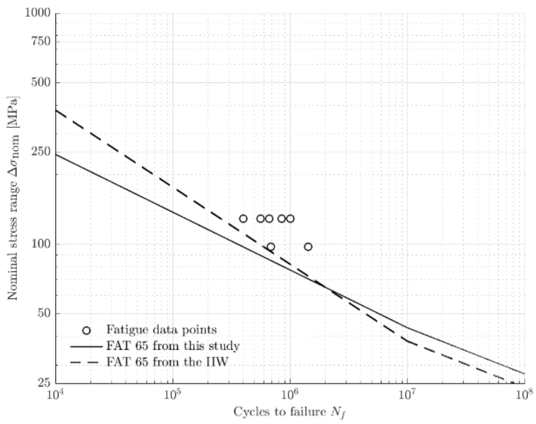

(h) I-section with cope hole

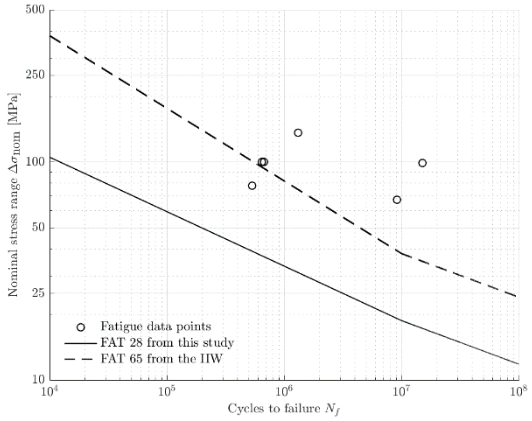

(i) Out-of-plane longitudinal gusset welded to plate

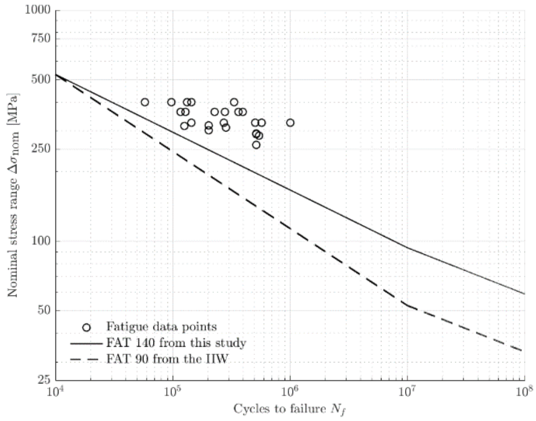

(j) Large doubling plates

Fig. 32. Improved fatigue data for each type of welds

6. Conclusion

On the basis of 395 fatigue data points extracted from 34 publications for butt joints, longitudinal attachments, doubling plates, transverse load-carrying welds, T-joints and transverse non-load-carrying welds, I-section with cope hole as well as out-of-plane longitudinal gusset welded to plate, the best-fit *S-N* curves were computed and the improvements of fatigue strength by burr grinding with a fixed slope were calculated following IIW Recommendation. The findings are summarized as follows:

- By comparing the weld toe grinding specimens with as-welded specimens, it is clear that burr grinding treatment has a great benefit on the fatigue strength of welds, unless the as-welded quality is defined and good enough or the material is reduced with U-shape grinding.
- It is also clear that weld toe grinding treatment is successful in case of seawater.
- The use of assumed *S-N* slope $m_1 = 4$ seems applicable for the evaluation of the effect of burr grinding for most of specimen types. However, based on the available data sets, for butt welds and longitudinal attachment with gusset 150 mm < L < 300 mm, a larger slope can be assumed. Hence, additional tests should be completed to validate this observation.
- An increase of the radius of groove results in a better improvement of fatigue strength at $N = 2 \times 10^6$ cycles. But more testing is needed.
- It is possible to conclude that weld profiling treatment has a greater improvement on welded specimens than burr and disc grinding.
- The assumed slope of $m_1 = 4$ and proposed FAT classes are found to be proper for the large components, such as doubling plates and I – section.
- The benefit of burr grinding on I - section with cope hole and out-of-plane longitudinal gusset welded to plate should be further validated due to a lack of specimens and levels of stress range used during the test.
- It is possible to conclude that increasing the mean stress from pulsating tension ($R = -1$) to half tensile loading ($R = 0.5$) leads to a decrease I fatigue strength.

Reference

[1] Haagensen, P. J. and Maddox, S. J. (2006). IIW Recommendations on Post Weld Improvement of Steel and Aluminium Structures, XIII-1815-00, 2006.08.18

[2] Haagensen, P. J. (2011). Fatigue Strength Improvement Methods, Norwegian University of Science and Technology (NTNU), Norway Woodhead Publishing Limited.

[3] Huther, I., Minard, V., Royer, Y. and Lieuarde, H. P., Burr Grinding Effect on the Fatigue Strength as Regard to Initial Weld Quality, IIIW - doc XIII-2038-04

[4] A. E739–10 (2015). Standard Practice for Statistical Analysis of Linear or Linearized Stress-Life and Strain-Life Fatigue Data. ASTM International, US.

[5] Fricke, W. (2010). *Betriebsfestigkeit von Schiffen und Meerestechnischen Konstruktion*, Institut für Konstruktion und Festigkeit von Schiffen Technische Universität Hamburg-Harburg

[6] Yıldırım, H. C. (2015). Review of Fatigue Data for Welds Improved by Tungsten Inert Gas Dressing, *International Journal of Fatigue* 79, 36–45.

[7] Merkblatt DVS 2403 (2019). Empfehlungen für die Durchführung, Auswertung und Dokumentation von Schwingfestigkeitsversuchen an Schweißverbindungen metallischer Werkstoffe, Deutscher Verband für Schweißen und verwandte Verfahren e. V.

[8] Hobbacher, A. (2014). Recommendations for Fatigue Design of Welded Joints and Components, IIW - doc IIW-2259-15.

[9] Kliman, V., Chmelko, V. and Margetin, M. (2015). Analysis of the notch effect of welded joint and of grinding effect. *Kovove Mater,* 53, 429-441. doi: 10.4149/km_2015_6_429. 2015.067.22

[10] Costa, J. D. M., Ferreira, J. A. M., & Abreu, L. P. M. (2010). Fatigue Behaviour of Butt Welded Joints in a High Strength Steel. *Procedia Engineering, 2*(1), 697-705. doi:10.1016/j.proeng. 2010.03.07

[11] Pedersen, M.M., Mouritsen, O.Ø., Hansen, M.R., J.G. Andersen, J.G. and Wenderby, J. (2009). Comparison of Post Weld Treatment of High Strength Steel Welded Joints in Medium Cycle Fatigue. XIII-2272-09

[12] Kim, M.H., Kang, S.W., Lee, J.M. and Kim, W.S. (2006), Evaluation of Fatigue Strength Improvement of Ship Structural Details by Weld Toe Grinding. *Key Engineering Materials* 324-325,1079-1082. http://www.scientific.net

[13] Haagensen, P. J. (1993), The effect of grinding and peening on the fatigue strength of welded T-joints. *Transactions on Engineering Sciences*, vol 2, www.witpress.com, ISSN 1743-3533

[14] Méndez, G.T., Meléndez, R.C., Hernández, A. A., Capula-Colindres, S. I., Herrera, D. A., Velázquez, J.C., Hernández, O.V. (2017). Correlation of Stress Concentration Factors for T-Welded Connections – Finite Element Simulations and Fatigue Behavior, Soldagem & Inspecao. 22(2), 194-206

[15] Weich, I.,(2008) Ermüdungsverhalten mechanisch nachbehandelter Schweißverbindungen in Abhängigkeit des Randschichtzustands.

[16] Tai, M.and Miki, C. (2012), Improvement Effects of Fatigue Strength by Burr Grinding and Hammer Peening under Variable Amplitude Loading, *Welding in the Word,* 56, 07-08

[17] Clegg, R.E., McLeod,A.J and Ruddell,W. (2013), Effect of toe treatments on the fatigue resistance of structurral steel welds.

[18] Kirkhope, K.J., Bell, R., Caron, L., Basu, R.I. and Ma, K.-T. (1999), Weld detail fatigue life improvement techniques. Part 1: review, *Marine Structures,*12, 447-474

[19] Kirkhope, K.J., Bell, R., Caron, L., Basu, R.I. and Ma, K.-T.(1999), Weld detail fatigue life improvement techniques. Part 2: application to ship structures, *Marine Structures,*12, 477-496
[20] Braun, M., Grimm, J.-H., Hoffmeister, H., Ehlers, S. and Fricke, W. (2018), Comparison of fatigue strength of post-weld improved high strength steel joints and notched base material specimens, ISSN: 1744-5302 2018.01.22, https://doi.org/10.1080/17445302.2018.1425522
[21] Rutherford, S.E. and Polezhayeva, H. (2006), Effect of Burr Grinding on the Fatigue Strength of Angled Welded Connections, *Lloyd's Register*
[22] Lieurade, H.P., Huther, I. and Lefebvre, F. (2005), Effect of Weld Quality and Postweld Improvement Techniques on the Fatigue Resistance of Extra High Strength Steels, *Welding in the World*, Doc. IIW-1863-07
[23] Polezhayeva, H., Kang, J.-K., Heo, J.-H. and Kim, K.-S. (2009), Effect of Weld Toe Burr Grinding on Fatigue Strength of Transverse Welded Specimens Made from DH36 Steel, OMAE2009-79331, May 31 - June 5, 2009
[24] Gao, W.B., Wang, D.P., Cheng, F.J., Deng, C.Y., Liu, Y. and Xu, W. (2015), Enhancement of the fatigue strength of underwater wet welds by grinding and ultrasonic impact treatment, *Journal of Materials Processing Technology*, http://dx.doi.org/10.1016/j.jmatprotec.2015.04.013
[25] Zhang, Y.H. and Maddox, S.J. (2009), Fatigue life prediction for toe ground welded joints, *International Journal of Fatigue,* doi:10.1016/j.ijfatigue.2009.01.03
[26] Hansen, A.V., Agerskov, H. and Bjørnbak-Hansen, J. (2007), Improvement of Fatigue Life of Welded Structural Components by Grinding, *Welding in the World*, Vol. 51, 3-4. Doc. IIW-1779-06
[27] Baptiata, R., Infante, V. and Branco, C.M. (2007), Study of the fatigue behavior in welded joints of stainless steels treated by weld toe grinding and subjected to saltwater corrosion.
[28] Dickerson, T. and Branco, C. M. (1994), Weld Improvement Methods for Low Cycle Fatigue Applications, European Commission EUR 17823.
[29] Lotsberg, I., Fjeldstad, A., Helsem, M. R. and Oma, N. (2013), Fatigue life improvement of welded doubling plates by grinding and ultrasonic peening. *Weld World,* DOI 10.1007/s40194-014-0161-8.
[30] Mecséri, B. J. and Kövesdi, B. (2020), Assessment of grinding weld treatment methods using effective notch stresses.
[31] Booth, G.S., The fatigue life of ground or peened fillet welded steel joints - the effect of mean stress, Metal Construction, February 1981
[32] Miki, C., Anami, K., Tani, H. and Sugimoto, I. (1999), Methods for fatigue strength improvement by weld toe treatment, *Welding International,* https://doi.org/10.1080/09507119909449006, 2010.01.05
[33] Uchida, D., Mori, T. and Sasaki, Y. (2016), Influence of Grinding Depth on Fatigue Strength of Out-Of-Plane Gusset Joints with Finished Weld Toes, 鋼構造論文集,23,89
[34] Gurney, T. R. (1968), Effect of Peening and Grinding on the Fatigue Strength of Fillet Welded Joints, British Welding Journal, December, British Welding Journal, 601-609
[35] Hanzawa, M., Yokota, H., Ishiguro, T., Takashima, H., Kado, S., Tanigaki, T. and Hashida, Y. 1977, Improvement of Fatigue Strength in Welded High Tensile Strength Steel by Toe Treatment, IIW DOC. XIII-829-77.
[36] Iwata, T., Matsuoka, K. and Kobayashi, Y. (2006), Fatigue Strength of Welded Joints of SUS316L for Chemical Tankers, *Welding In the World*. 50. 9-10. Doc. IIW-1743-06
[37] Knight, J.W. (1976), Improving the Fatigue Strength of Fillet Welded Joints by Grinding and Peening, *The Welding Institute*, XIII-851-77.

[38] Choi, S.M., Tateishi, K. and Hanji, T. (2013). Fatigue Strength Improvement of Weld Joints with Cope Hole, *International Journal of Steel Structures*, Vol 13, No 4, 683-690, doi: 10.1007/s13296-013-4009-7, December 2013
[39] Puthli, R., Herion, S. and Bergers, J. (2006), Influence of Longitudinal Attachments on the Fatigue Behaviour of High strength Steels, *International Offshore and Polar Engineering Conference*, ISBN 1-880653-66-4 May 28-June 2.
[40] Tec-science, Fatigue Test, 2018, https://www.tec-science.com/material-science/material-testing/fatigue-test/
[41] Quadco Engineering, Certainty of Survival, (2020) https://www.quadco.engineering/en/know-how/fatigue-certainty-of-survival.htm
[42] Fricke W. (2012) IIW recommendations for the fatigue assessment of welded structures by notch stress analysis. Cambridge: Woodhead Publishing Ltd.;
[43] Purdue Department of Statistics, 250 N. Universität St.,West Lafayette, IN 47907.https://www.stat.purdue.edu/~jtroisi/STAT350Spring2015/tables/FTable.pdf
[44] Yıldırım, H.C. (2012). Marquis GB. Overview of fatigue data for high frequency mechanical impact treated welded joints. *Weld World 2012*; 56(7–8):82–96. http://dx.doi.org/10.1007/BF03321368.

Appendix

A. Slope calculation based on number of specimens for the extracted fatigue data improved by burr grinding

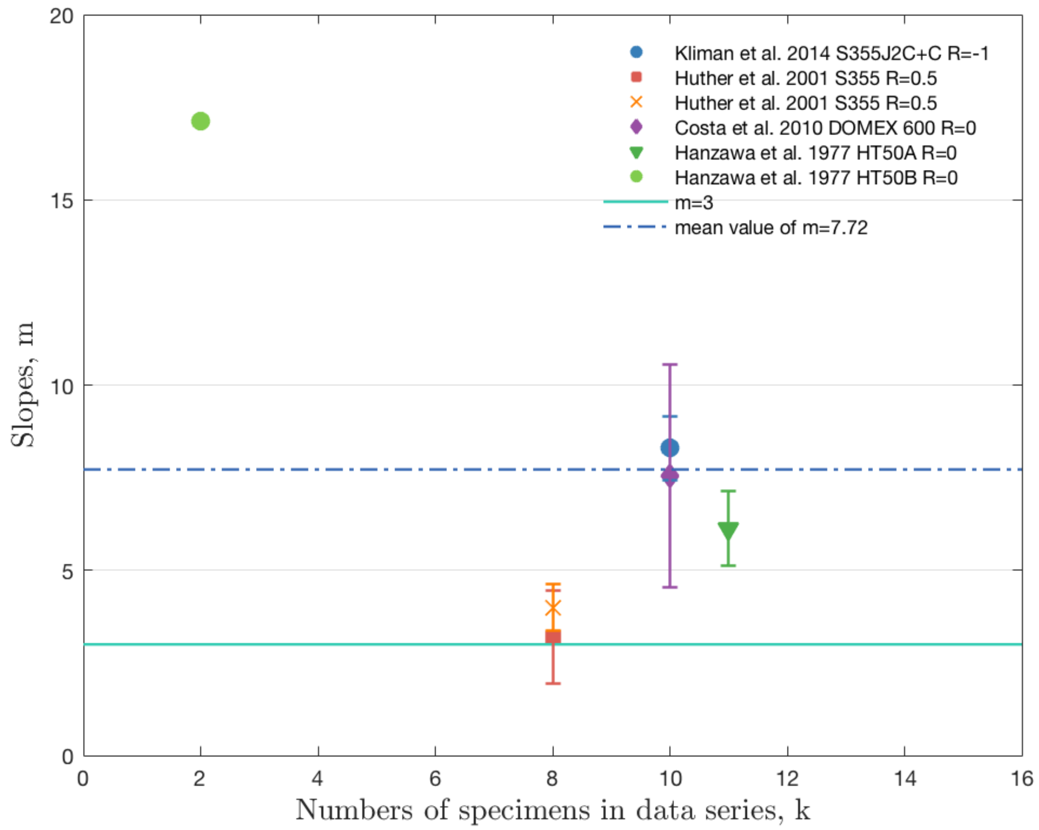

(a) Butt welds

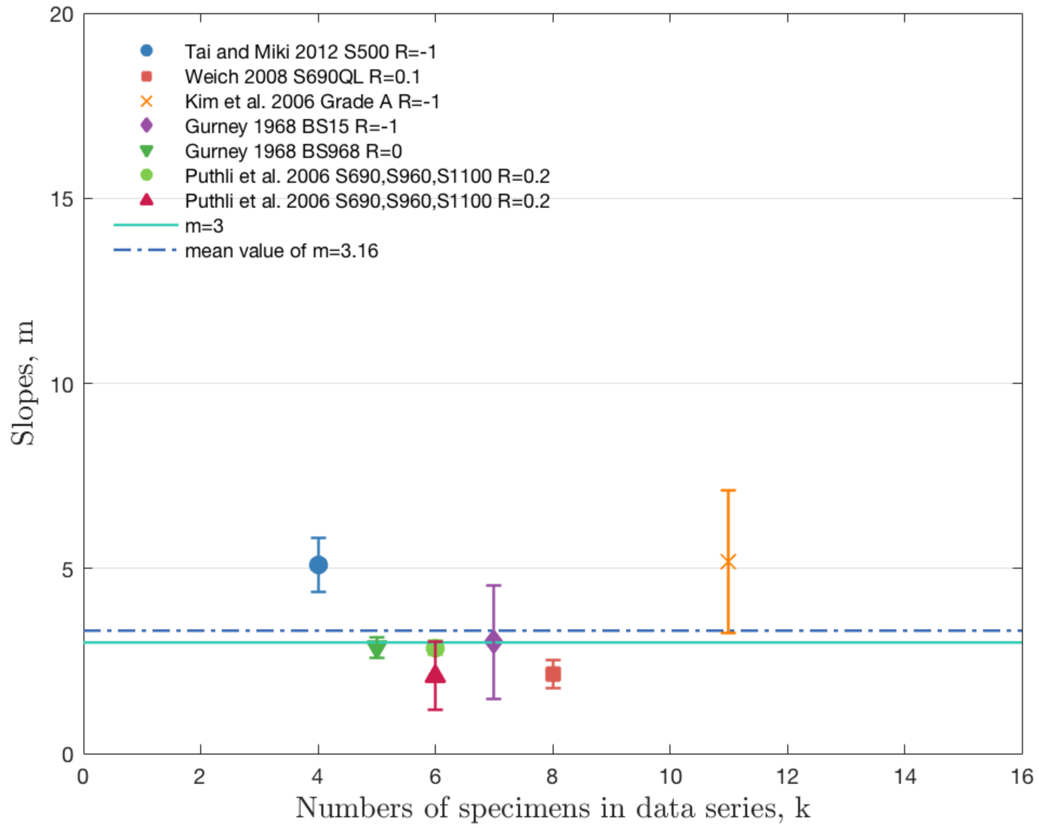

(b) Longitudinal attachments

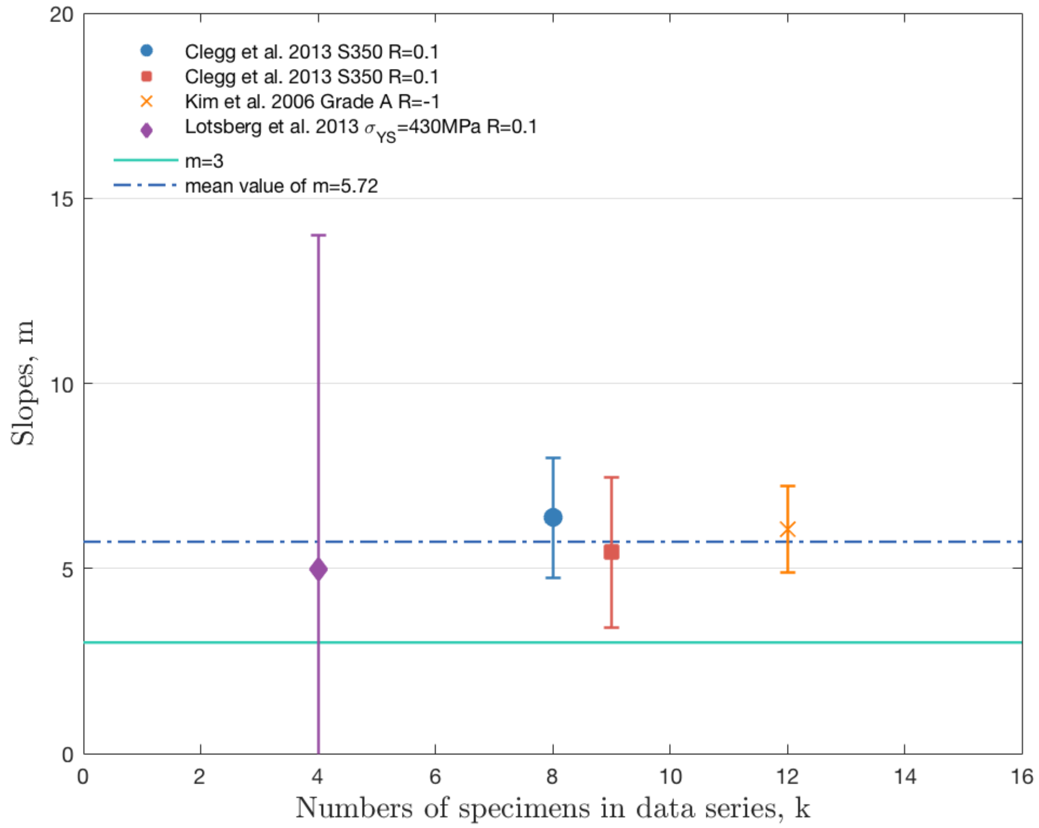

(c) Doubling plates

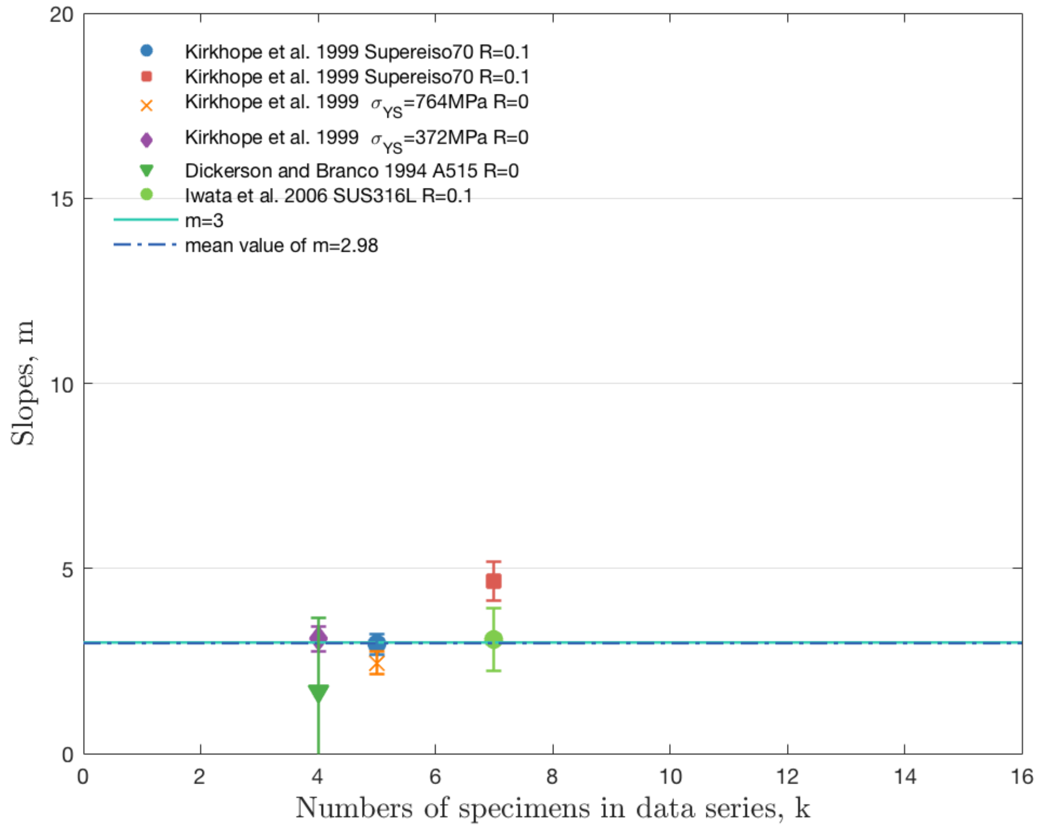

(d) Transverse load-carrying welds

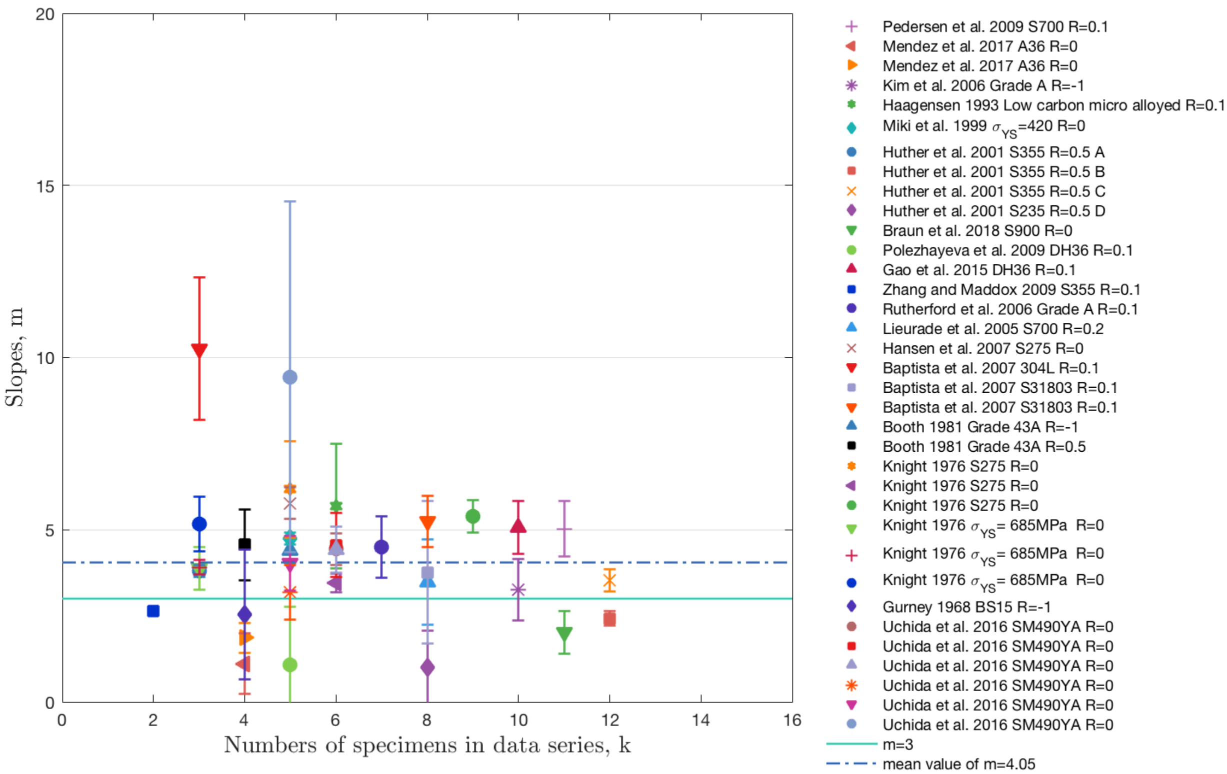

(e) T-joints and transverse non-load-carrying welds

B. Slope calculation based on steel grades for T-joints and transverse non-load-carrying welds improved by burr grinding

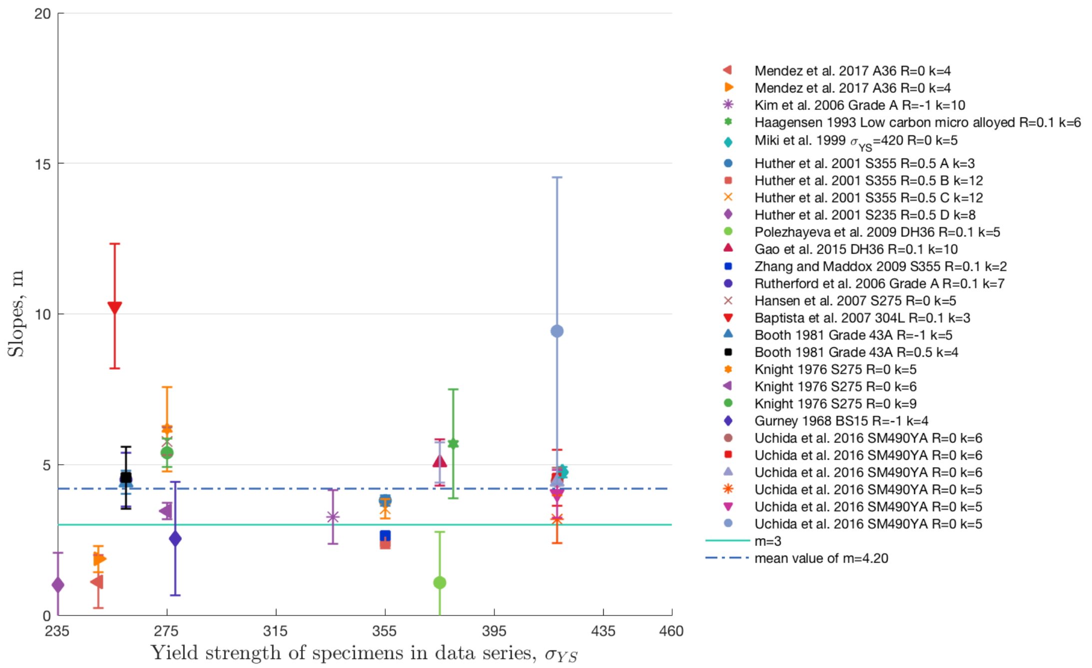

(a) $235 < \sigma_{\mathrm{YS}} < 460\ MPa$

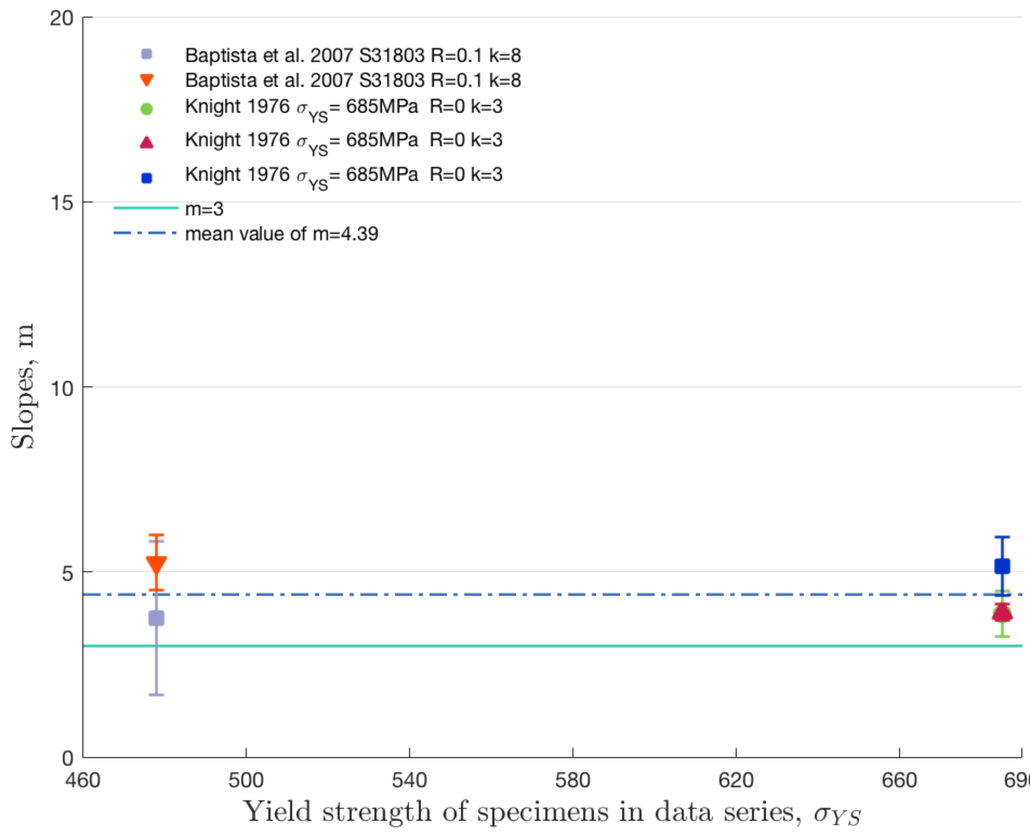

(b) $460 < \sigma_{\mathrm{YS}} < 690$ MPa

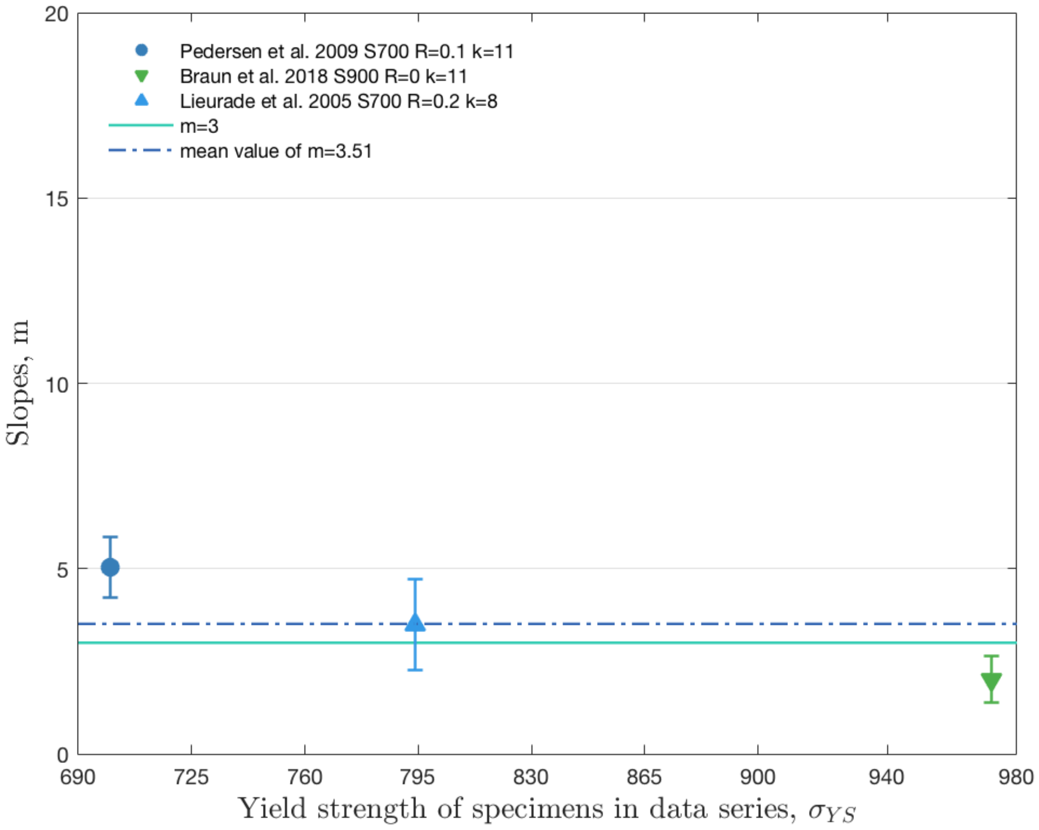

(c) $690 < \sigma_{\mathrm{YS}} < 980$ MPa

C. Slope calculation based on number of specimens for the doubling plates in large size improved by burr grinding

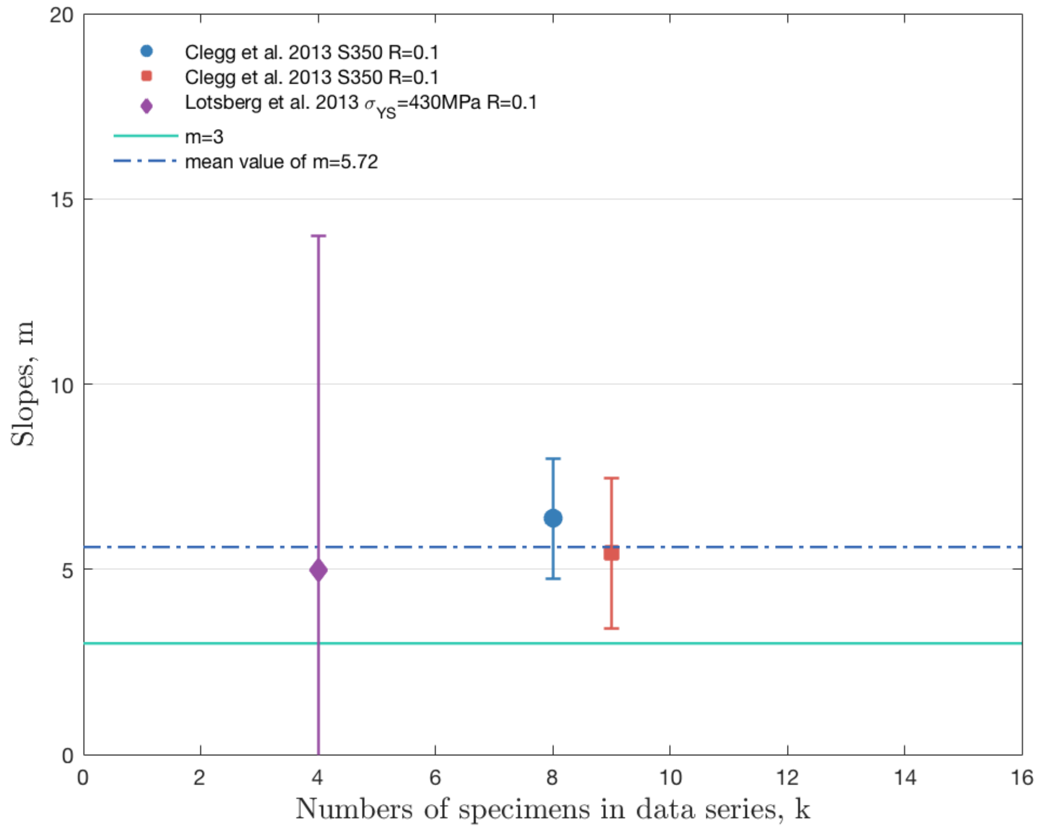

D. Analysis of fatigue data with assumed slope m_1=4

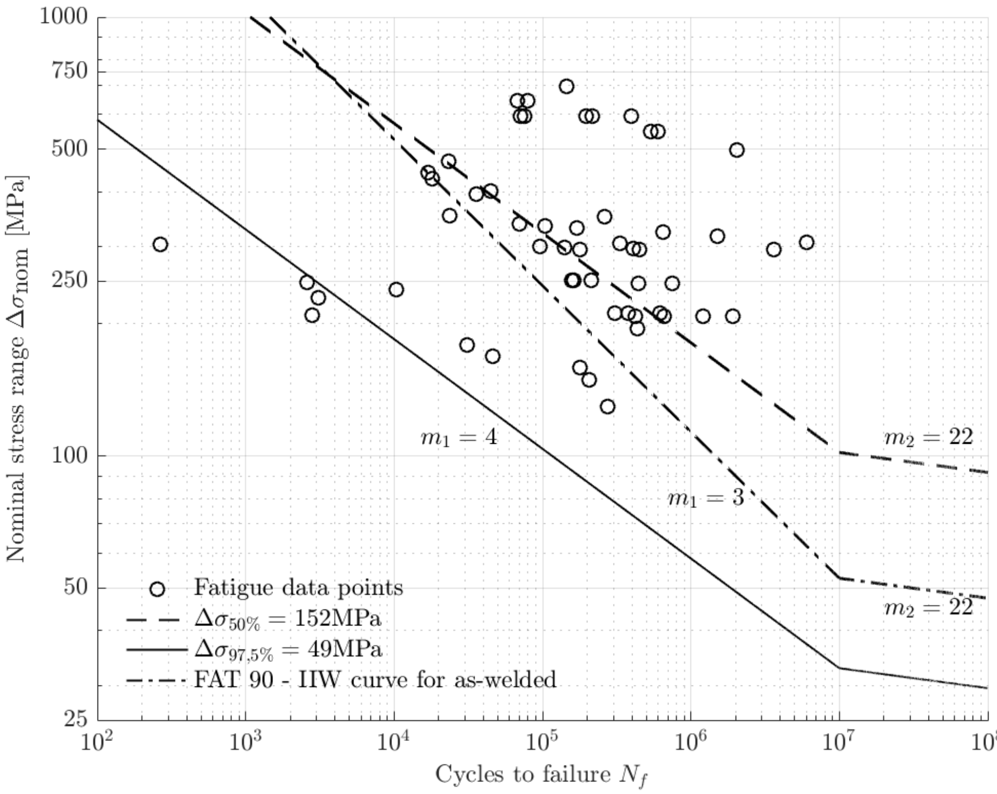

(a) Butt welds with circular section

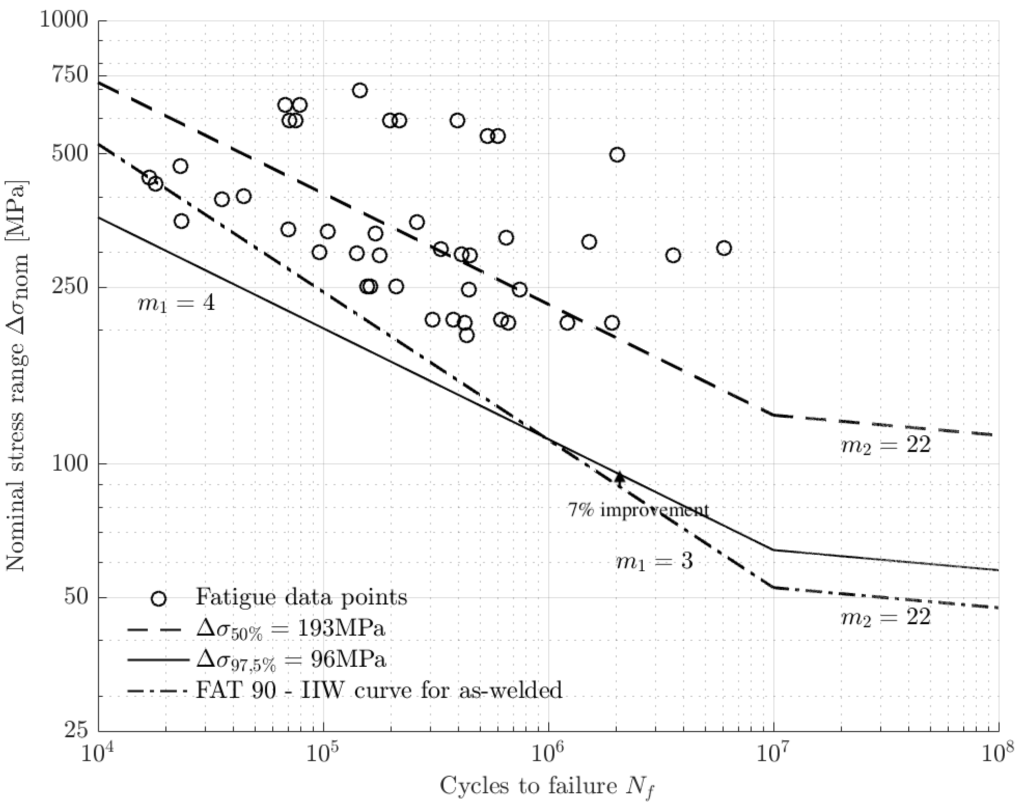

(b) Butt welds without circular section

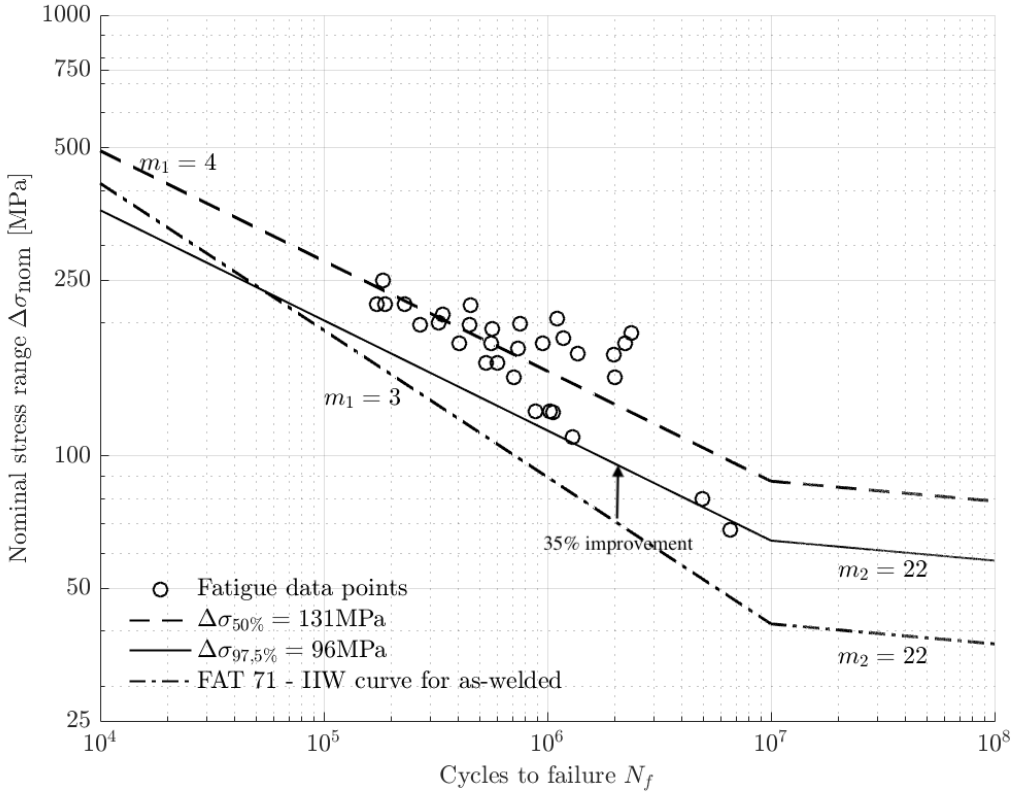

(c) Longitudinal attachments with *L* < 150 mm

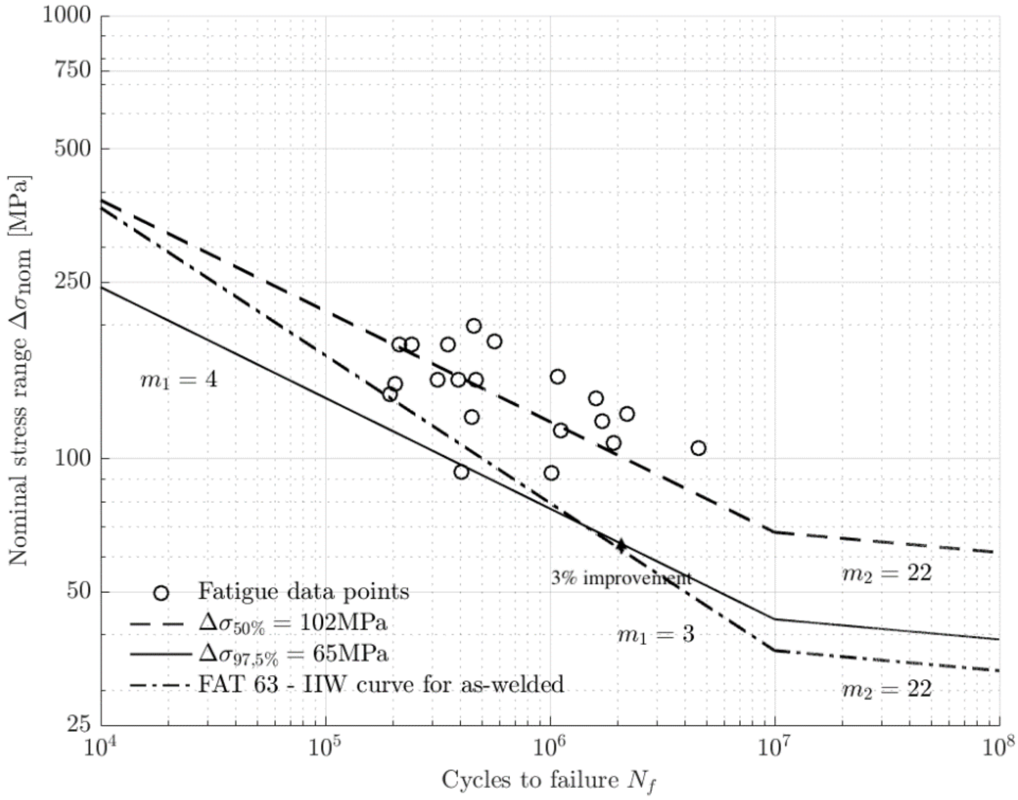

(d) Longitudinal attachments with 150 mm < *L* < 300mm

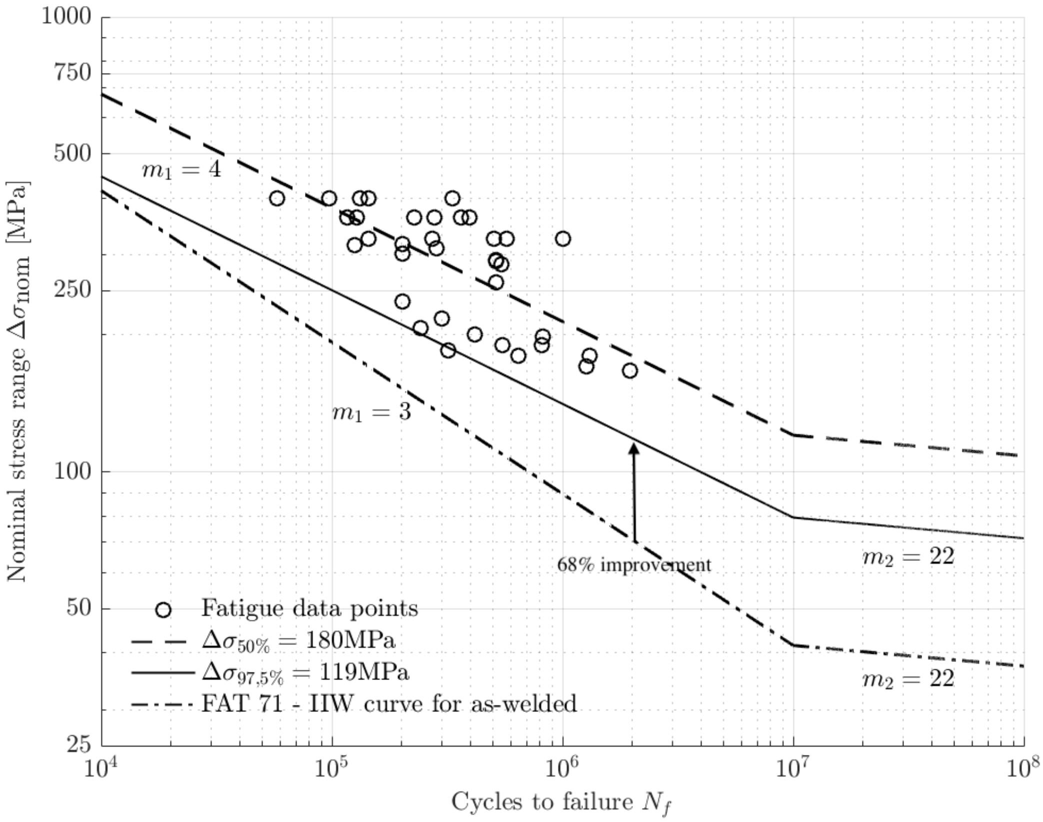

(e) Doubling plates

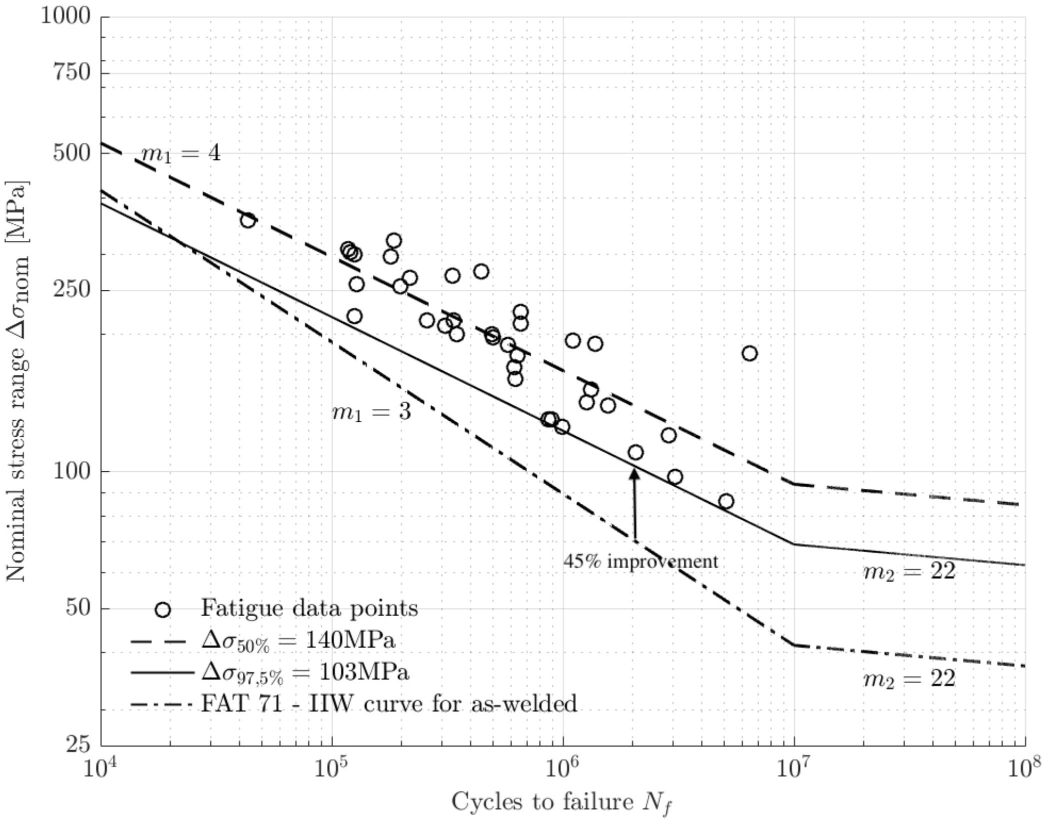

(f) Transverse load-carrying welds

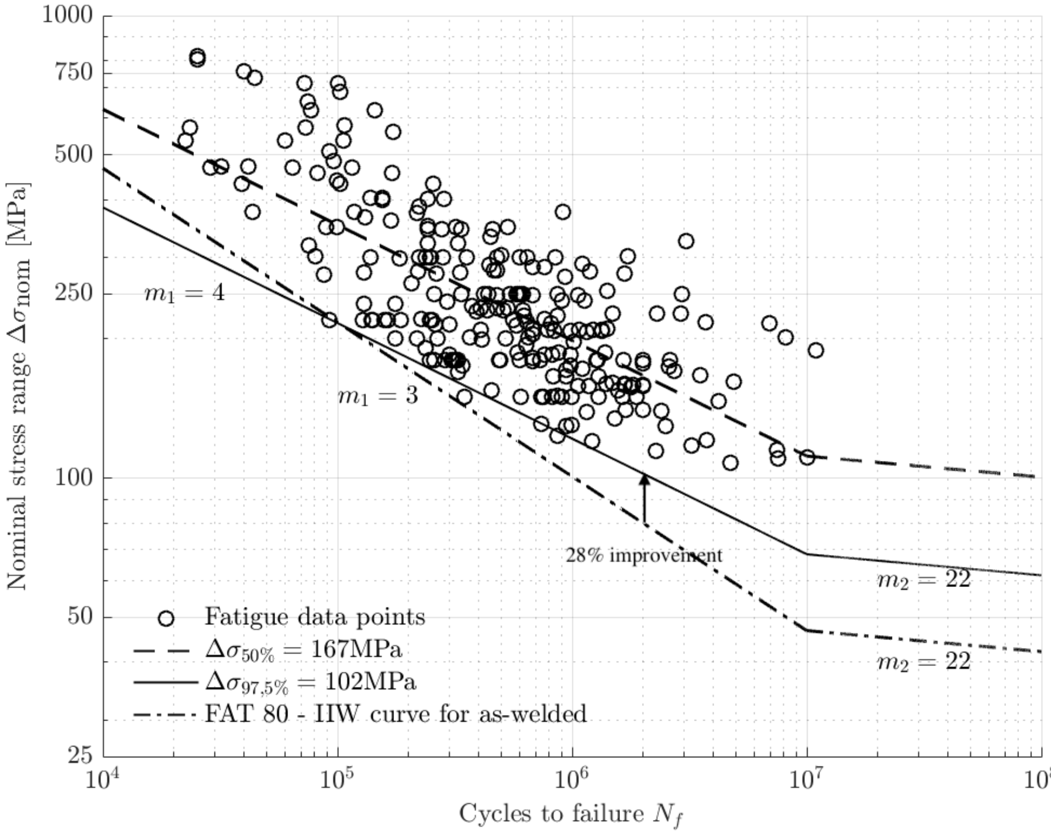

(g) Transverse non-load-carrying welds and T-joints

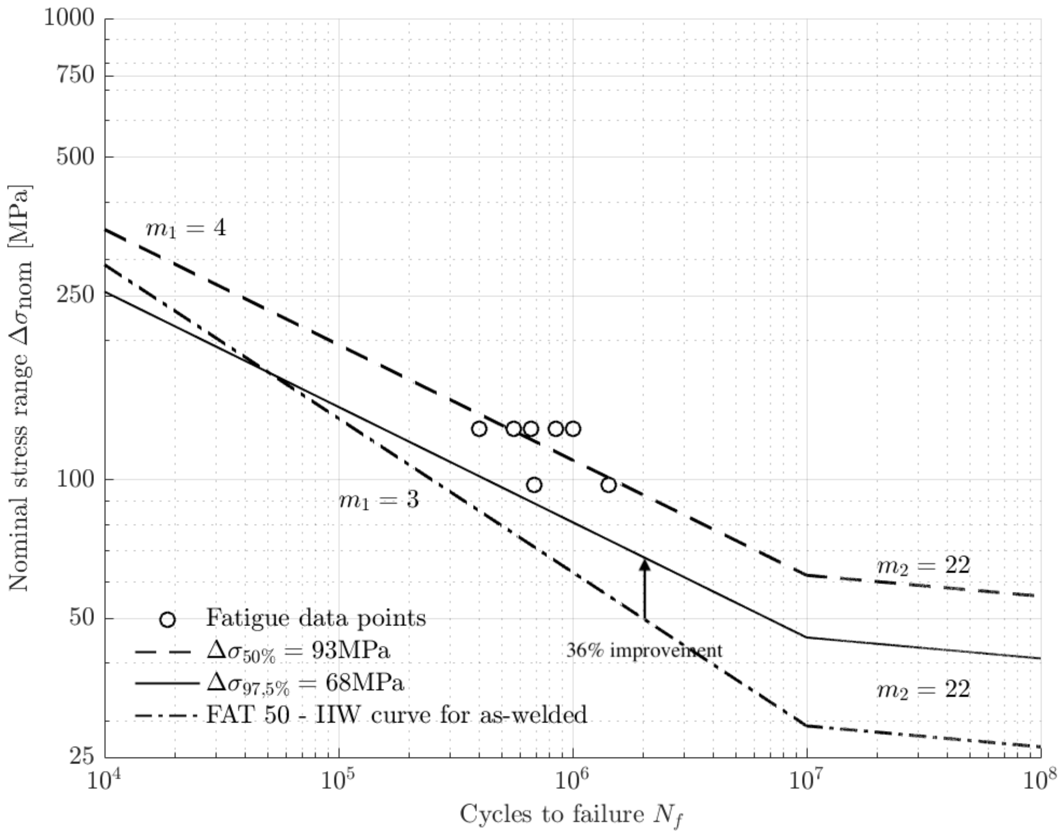

(h) I - section with cope hole

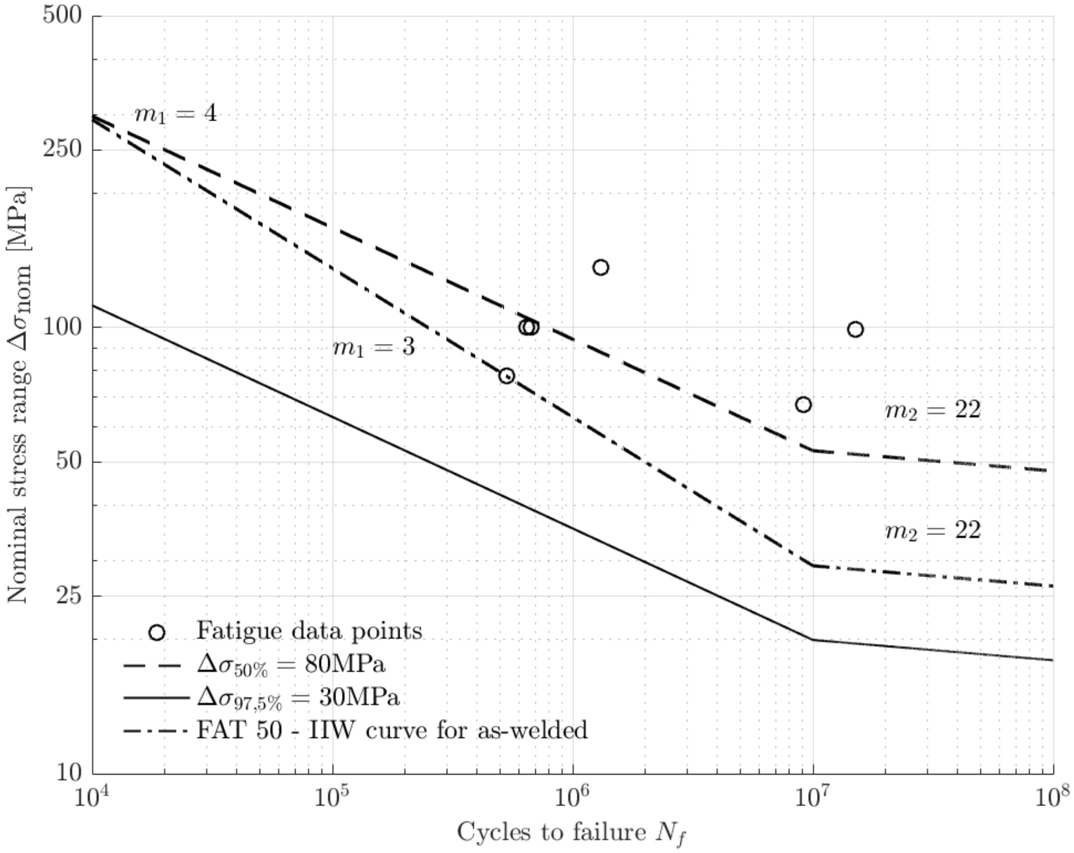

(i) Out-of-plane longitudinal welded gusset on plate

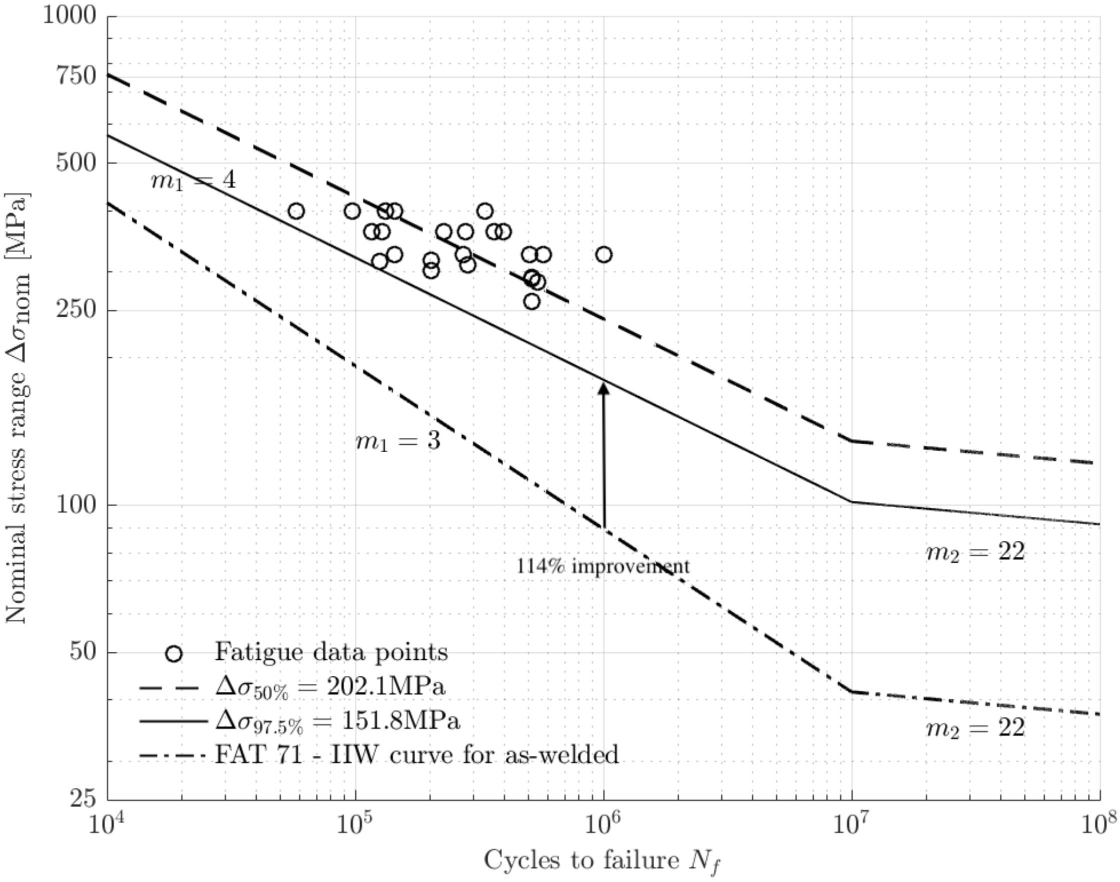

(j) Large doubling plates

E. Improved fatigue data for each type of welds

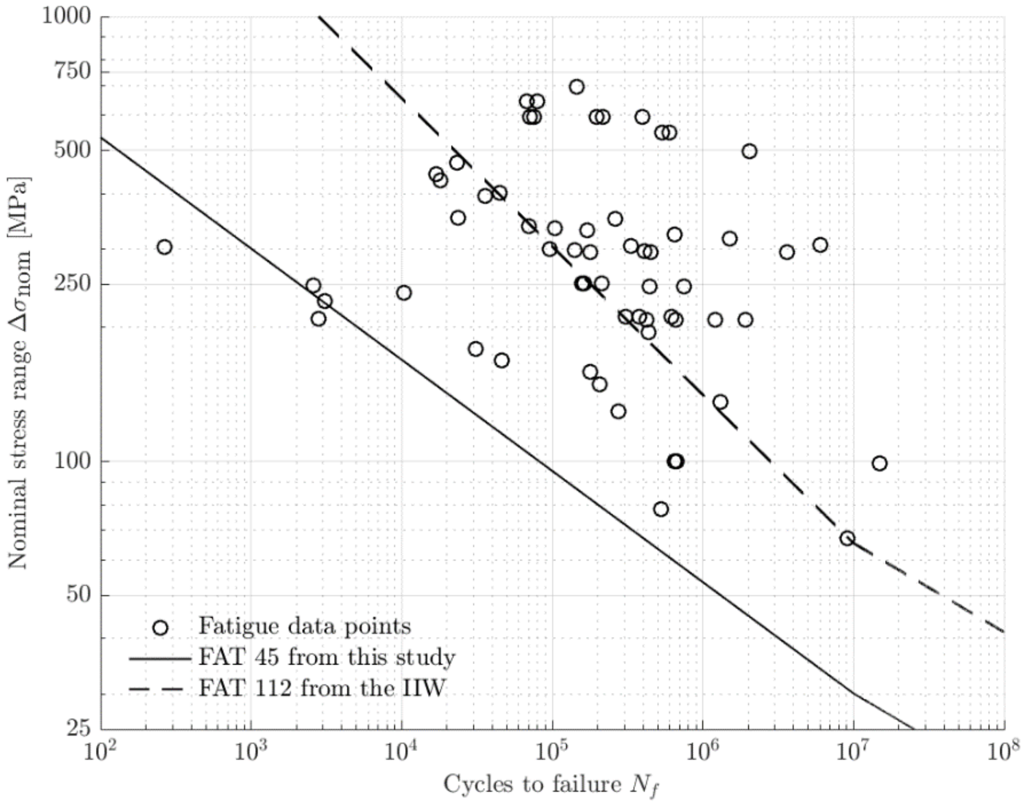

(a) Butt welds with circular solid section

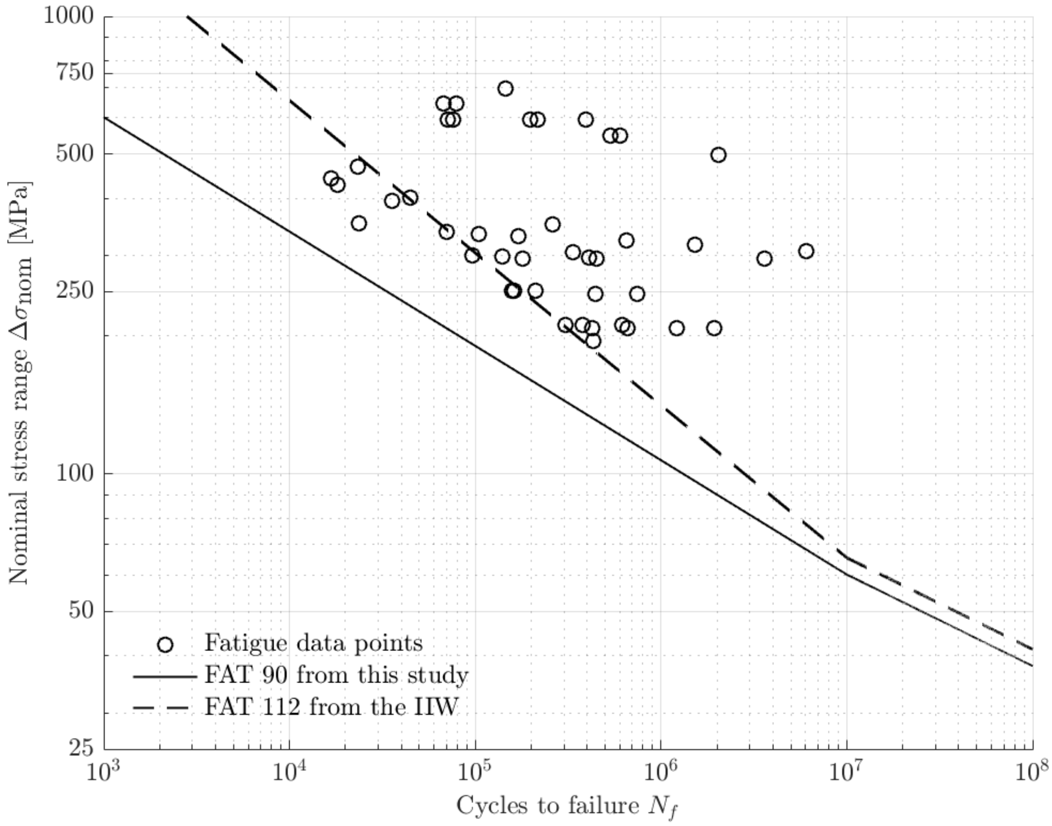

(b) Butt welds without circular solid section

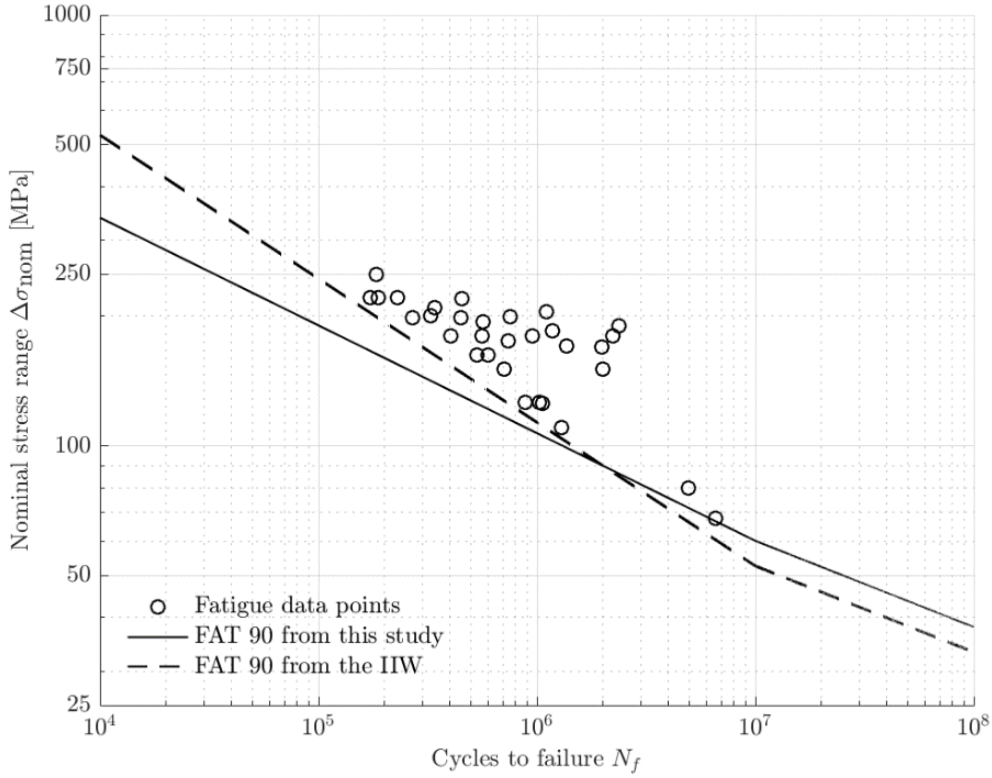

(c) Longitudinal attachments with *L* < 150 mm

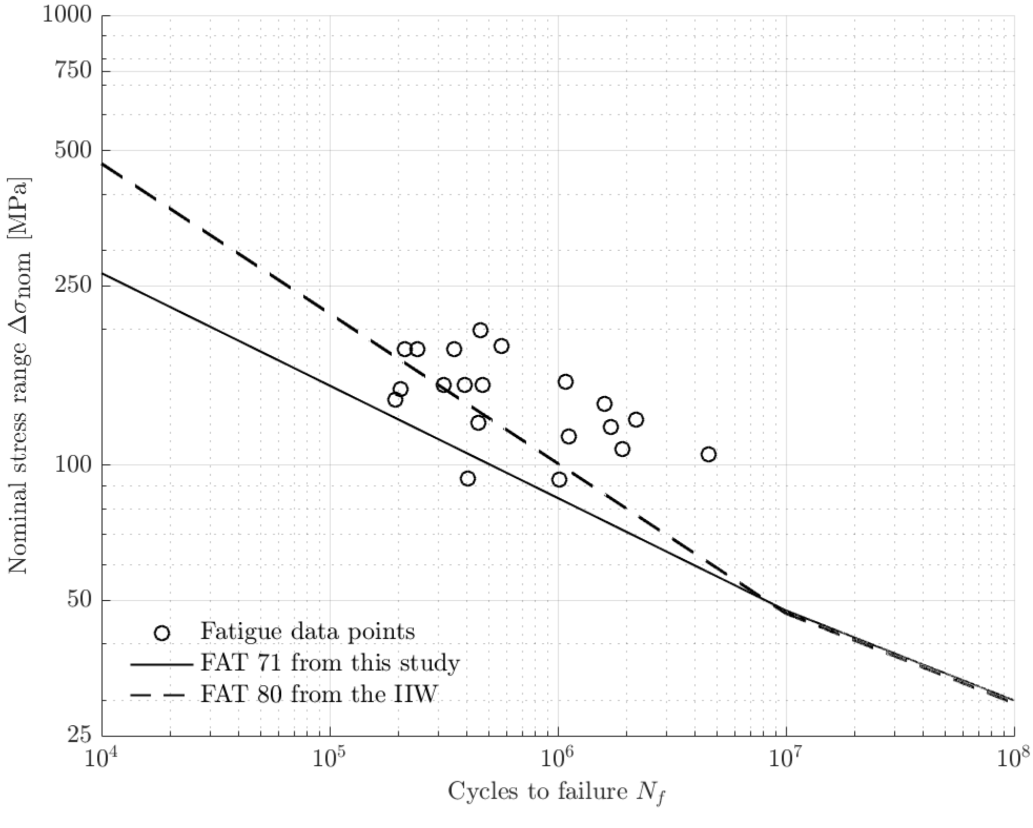

(d) Longitudinal attachments with 150 mm < *L* < 300 mm

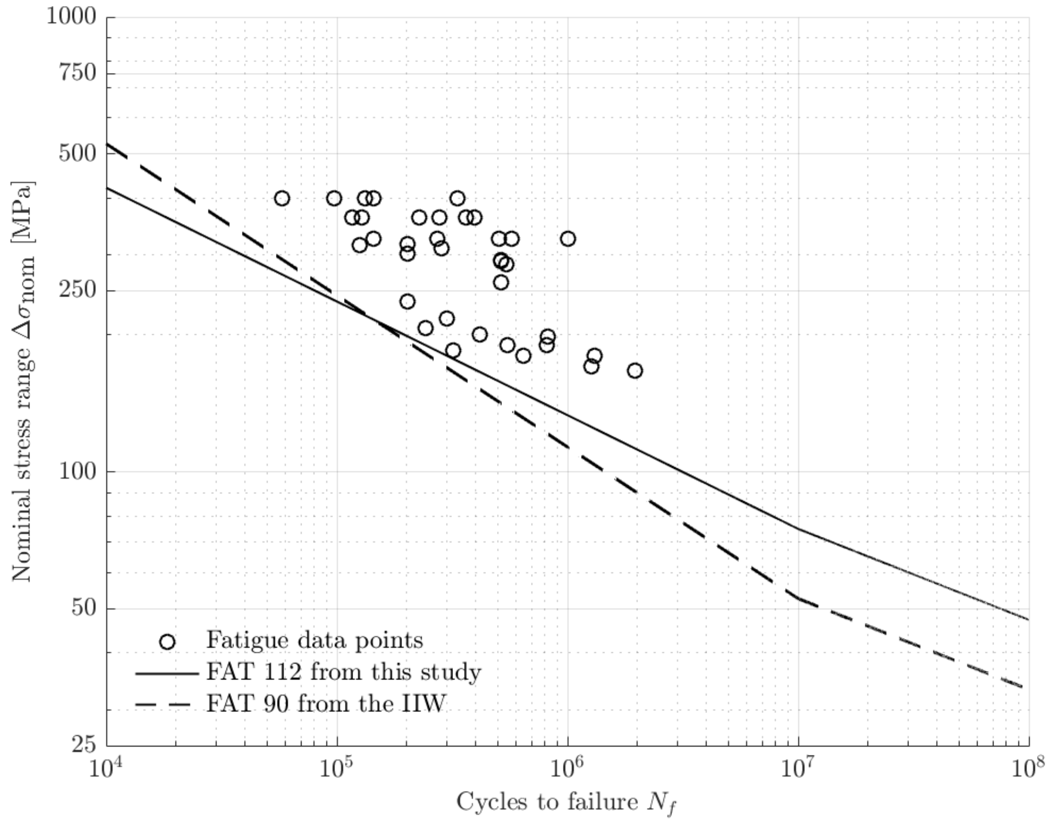

(e) Doubling plates

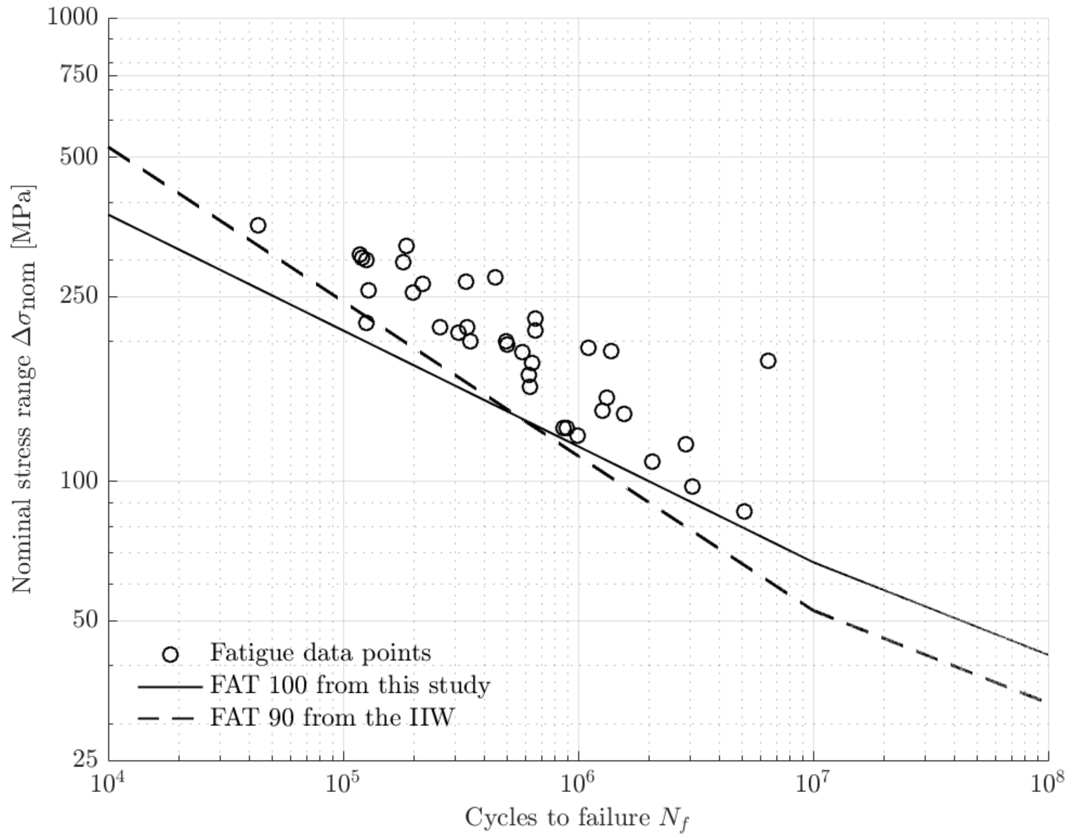

(f)Transverse load-carrying welds

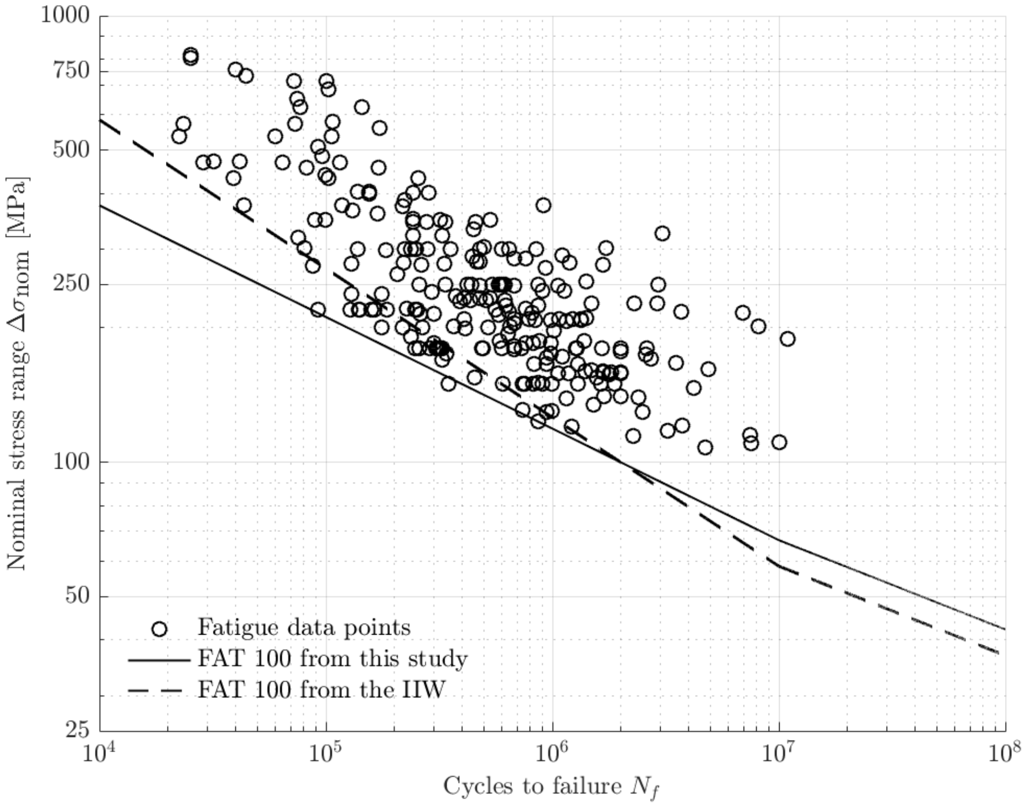

(g) T-joints and transverse non-load-carrying welds

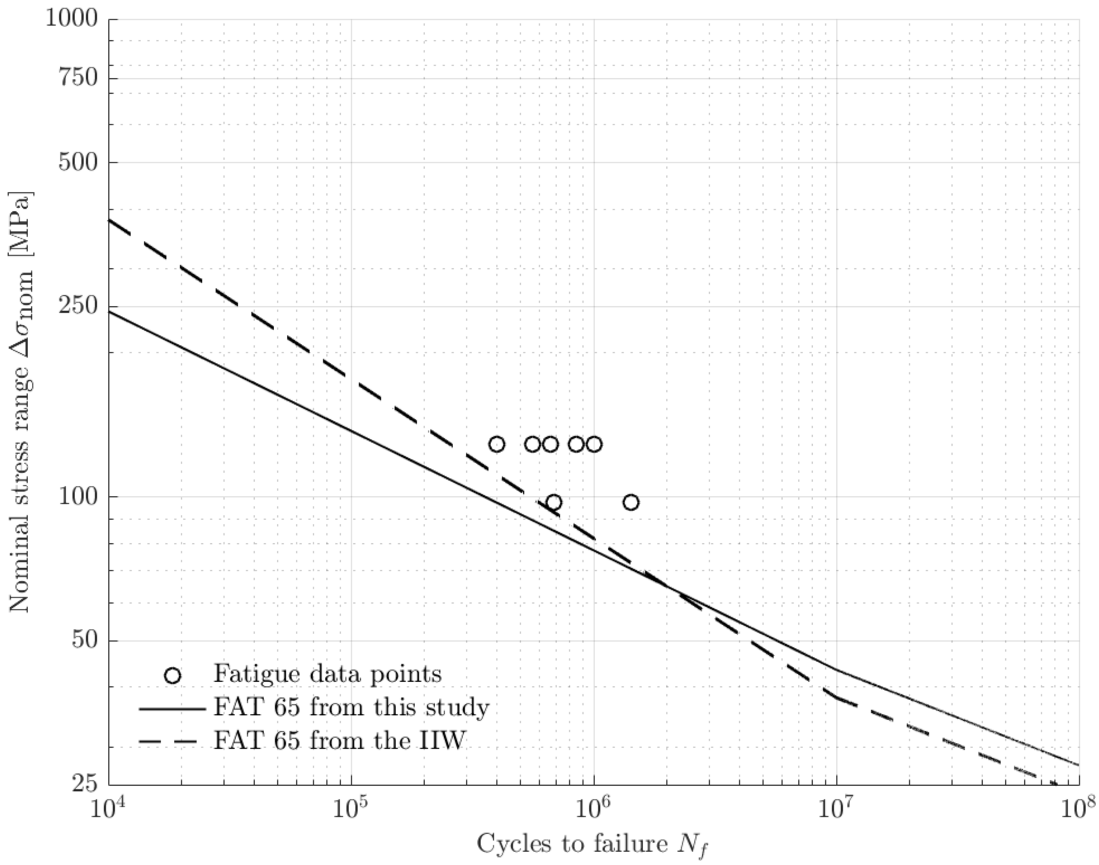

(h) I-section with cope hole

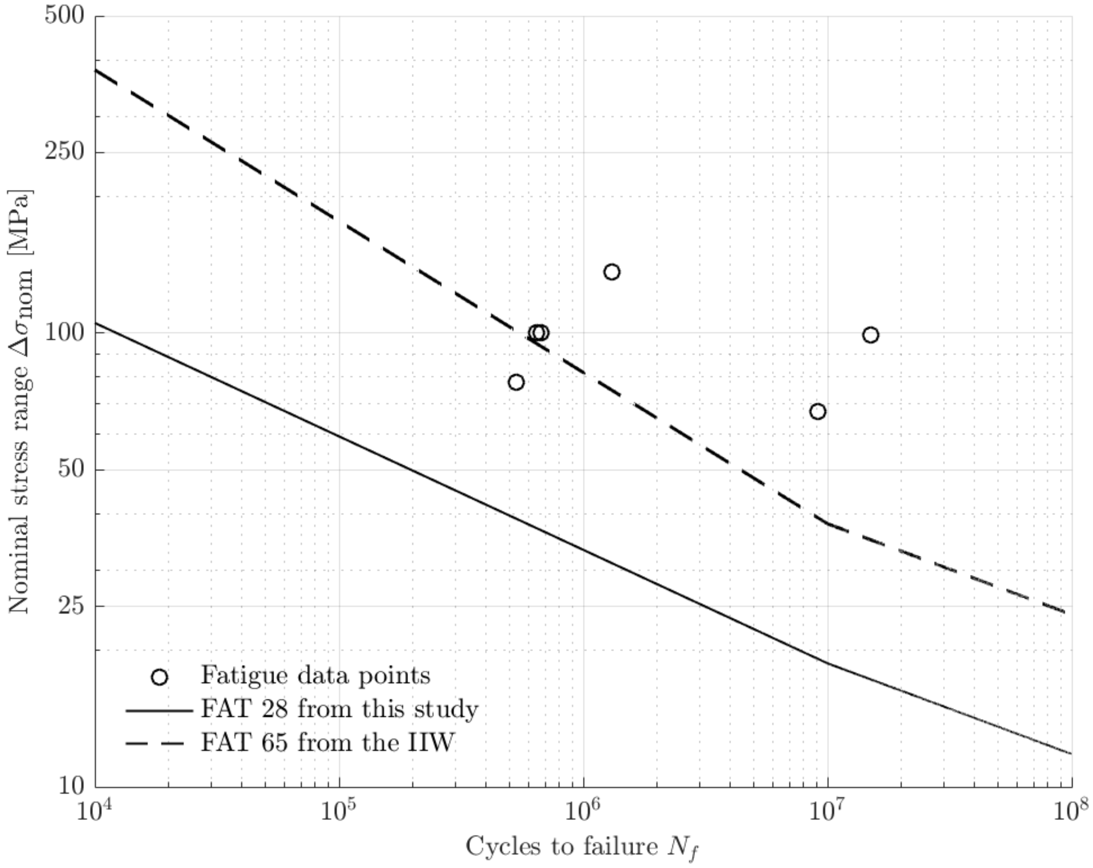

(i) Out-of-plane longitudinal gusset welded on plate

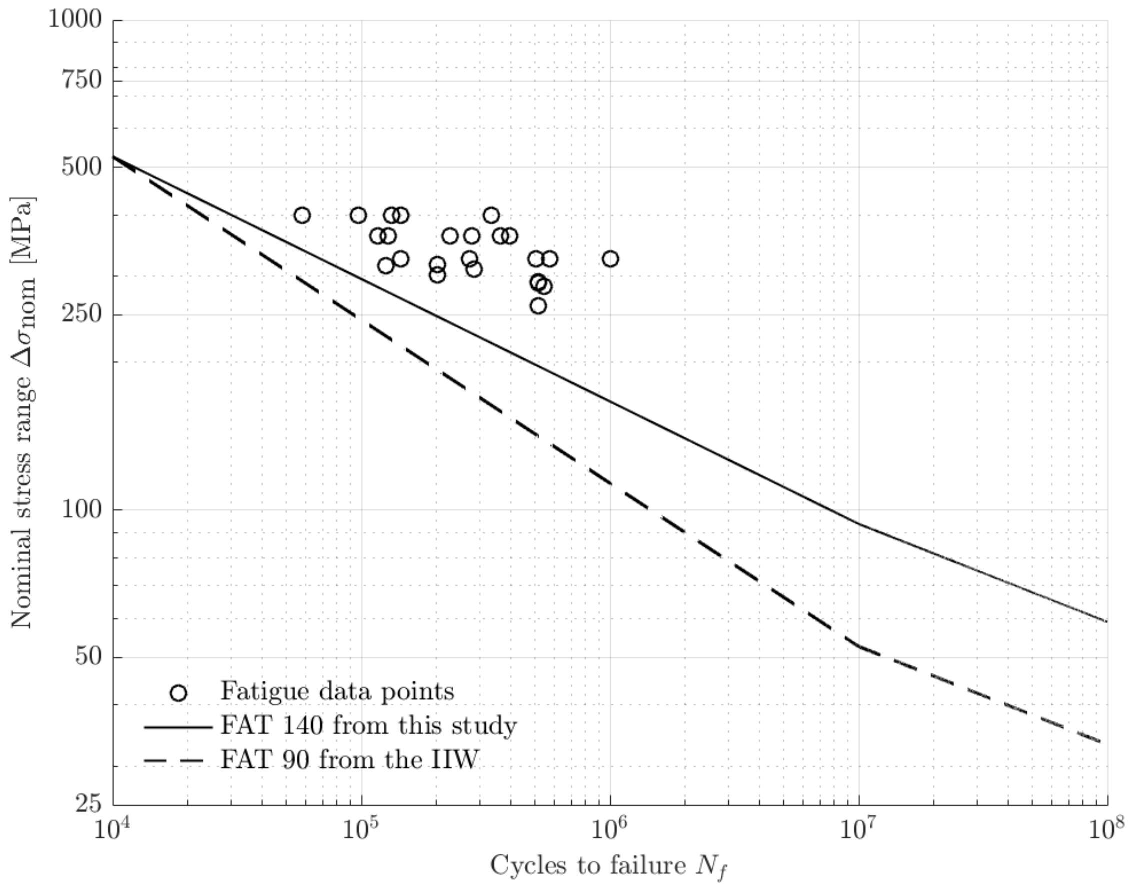

(j) Large doubling plates